Geometry II
Discrete Differential Geometry

Alexander I. Bobenko

December 3, 2015

Preliminary version. Partially extended and partially incomplete. Based on the lecture notes of Geometry 2 (Summer Semester 2014 TU Berlin).

- Typed by Jan Techter.

Contents

1 Introduction

Aim

DDG aims to develop discrete equivalents of the geometric notions and methods of classical differential geometry. The latter appears then as a limit of refinement of the the discretization.

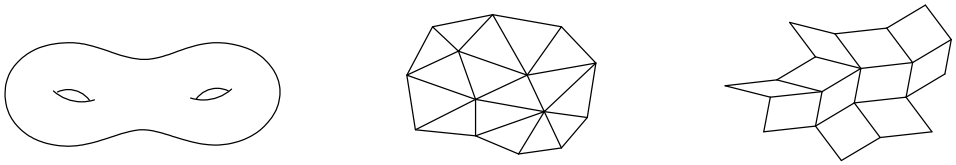

smooth surface simplicial surface quad-surface

Figure 1.1. Different kinds of surfaces.

One might suggest many different reasonable discretizations (with the same smooth limit). Among these, which one is the best? DDG initially arose from the observation that when a notion from smooth geometry (such as the notion of a minimal surface) is discretized "properly", the discrete objects are not merely approximations of the smooth ones, but have special properties of their own, which make them form a coherent entity by themselves.

DDG versus Differential Geometry

In general

- DDG is more *fundamental*: The smooth theory can always be recovered as a limit of the discrete theory, while it is a nontrivial problem to find out which discretization has the desired properties.
- DDG is *richer*: The discrete theory uses some structures (such as combinatorics of the mesh) which are missing in the smooth theory.
- DDG is *clarifying*: Often a discretization clarifies the structures of the smooth theory (for example unifies surfaces and their transformations, cp. Fig. 1.2).

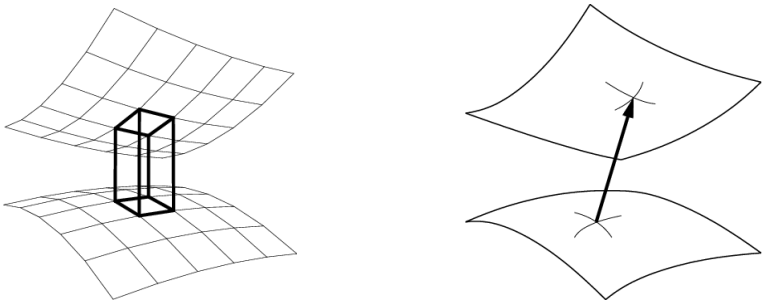

Figure 1.2. From the discrete master theory to the classical theory: surfaces and their transformations appear by refining two of three net directions.

- DDG is *simpler*: It uses difference equations and elementary geometry instead of calculus and analysis.
- DDG has (unexpected) *connections* to projective geometry and its subgeometries. In particular some theorems of differential geometry follow from incidence theorems of projective geometry.

Applications

Current interest in DDG derives not only from its importance in pure mathematics, but also from its applications in other fields including:

- *Computer graphics.* CG deals with discrete objects (surfaces and curves for instance) only.

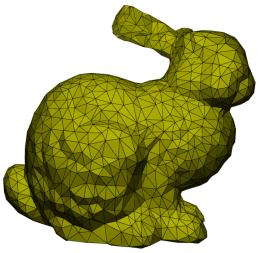

Figure 1.3. A simplicial rabbit.

- *Architecture.* Freeform architecture buildings have non-standard (curved) geometry but are made out of planar pieces. Common examples are glass an steel constructions.

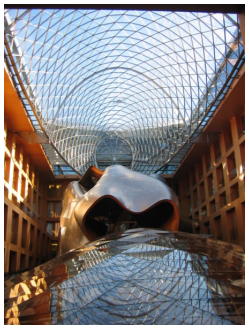

Figure 1.4. Two examples from Berlin: The "Philologische Bibliothek der FU Berlin" and an inside view of the DZ Bank at Pariser Platz.

- *Numerics.* "Proper" discretizations of differential equations are often geometric in order to preserve some important properties. There are many examples and also recent progress in hydrodynamics, electrodynamics, elasticity and so on.
- *Mathematical physics.* Discrete models are popular. DDG helps for example to clarify the phenomenon of integrability.

History

Three big names in (different branches of) DDG are:

- *R. Sauer* (starting 1930's)
  Theory of quad-surfaces (build from quadrilateral) as an analogue of parametrized surfaces. Important difference equations (related to integrable systems), special classes of surfaces.
- *A.D. Alexandrov* (starting 1950's)
  Metric geometry of discrete surfaces. Approximation of smooth surfaces by polyhedral surfaces.
- *W. Thurston* (1980's)
  Developed Koebe's ideas of discrete complex analysis based on circle patterns. Further development of this theory led in particular to construction of surfaces from circles.

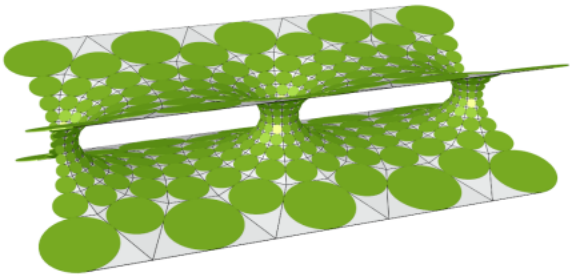

Figure 1.5. A discrete version of the Sherk tower, made out of touching discs.

Discretization principles

Which discretization ist the best?

- *Theoretical point of view.* The one which preserves all the fundamental properties of the smooth theory.
- *Practical point of view* (from Applications). The one which possesses good convergence properties and represents a smooth shape by a discrete shape with just a few elements very well.

Fortunately it turns out that in many cases a "natural" theoretical approximation possesses remarkable approximation properties.

Two principles of geometric discretization

- *Transformation group principle*: Smooth geometric objects and their transformations should belong to the same geometry. In particular discretizations should be invariant with respect to the same transformation group as the smooth objects are (projective, hyperbolic, Möbius etc.). For example a

discretization of a notion which belongs to Riemannian geometry should be given in metric terms only.

Another discretization principle is more special, deals with parametrized objects, and generalizes the observation from Fig. 1.2:

- *Consistency principle*: Discretizations of surfaces, coordinate systems, and other smooth parametrized objects should allow to be extended to multidimensional consistent nets. All directions of such nets are indistinguishable.

Part I
Discrete Curves

2 Curves and curvature

2.1 Basic definitions

Definition 2.1 (smooth curves)**.** Let $I \subset \mathbb{R}$ be a finite or infinite interval. Then a *smooth curve* in $\mathbb{R}^N$ is a map

$$\gamma : I \to \mathbb{R}^N$$

such that all derivatives γ', γ'',... exist.
The *length* of a smooth curve γ is defined by

$$L(\gamma) \coloneqq \int_I \|\gamma'(x)\| \, \mathrm{d}x.$$

γ is called *regular* if $\|\gamma'(x)\| > 0$ for all $x \in I$.
For a regular curve γ the (unit) *tangent vector* at $x \in I$ is defined by

$$T(x) \coloneqq \frac{\gamma'(x)}{\|\gamma'(x)\|}.$$

γ is called *arc length parametrized* if $\|\gamma'(x)\| = 1$ for all $x \in I$.

Remark 2.1.

- Any arc length parametrized curve is regular and any regular curve can be parametrized by arc length. We usually denote the arc length parameter of a curve by s.
- The length of an arc length parametrized curve is given by $L(\gamma) = |I|$.
- We defined curves as 'parametrized curves'. But we are also interested in quantities that are invariant under reparametrization and Euclidean transformations, i.e. well-defined on equivalence classes representing the 'shape of a curve'.

Definition 2.2 (discrete curves)**.** Let $I \subset \mathbb{Z}$ be a finite or infinite interval. Then a *discrete curve* in $\mathbb{R}^N$ is a map

$$\gamma : I \to \mathbb{R}^N.$$

For a discrete curve γ we define the *vertex difference vector* at the edge $(k, k+1)$ with $k, k+1 \in I$ by

$$\Delta\gamma_k \coloneqq \gamma_{k+1} - \gamma_k,$$

and its *length* by

$$L(\gamma) \coloneqq \sum_{k,k+1 \in I} \|\gamma_{k+1} - \gamma_k\| .$$

If any two successive points of γ are different, i.e. $\|\Delta\gamma_k\| > 0$ we can define the (unit) *tangent vector* at the edge $(k, k+1)$ with $k, k+1 \in I$ by

$$T_k \coloneqq \frac{\gamma_{k+1} - \gamma_k}{\|\gamma_{k+1} - \gamma_k\|}.$$

We further define

$$\begin{aligned} \gamma \textit{ regular} \quad &:\Leftrightarrow \quad \text{any three successive points } \gamma_{k-1}, \gamma_k, \gamma_{k+1} \\ &\qquad\quad \text{are different for all } k-1, k, k+1 \in I \\ \gamma \textit{ arc length parametrized} \quad &:\Leftrightarrow \quad \|\gamma_{k+1} - \gamma_k\| = 1 \text{ for all } k \in I \end{aligned}$$

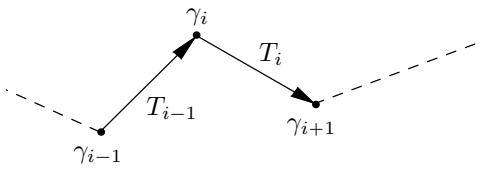

Figure 2.1. Part of a discrete arc length parametrized curve.

Remark 2.2.

- The vertex difference vectors $\Delta\gamma_k$ and tangent vectors T_k are naturally defined on edges rather than vertices despite the notation.
- For a discrete arc length parametrized curve γ the tangent and vertex difference vectors coincide

  $$T_k = \Delta\gamma_k = \gamma_{k+1} - \gamma_k.$$

  It is regular if and only if two successive tangent vectors T_{k-1} and T_k are not anti-parallel.
- The definition of regularity is more than is needed to define edge tangent vectors. But we will see that it allows to have a well defined discrete tangent flow at vertices as well.
- For plane curves it will be sometimes convenient to identify $\mathbb{R}^2 \cong \mathbb{C}$ and for space curves $\mathbb{R}^3 \cong \mathrm{Im}\mathbb{H}$

2.2 On the smooth limit

Consider a discrete curve $\gamma : \mathbb{Z} \to \mathbb{R}^N$. To obtain a continuous limit we introduce a small parameter $\varepsilon > 0$ and replace the lattice $\mathbb{Z}$ by

$$\mathcal{B}^\varepsilon \coloneqq \varepsilon\mathbb{Z}$$

for $\varepsilon > 0$ and $\mathcal{B}^0 \coloneqq \mathbb{R}$. So the discrete curve is replaced by a family

$$\gamma^\varepsilon : \mathcal{B}^\varepsilon \to \mathbb{R}^N.$$

In the limit $\varepsilon \to 0$ the vertices $\varepsilon k \in \varepsilon\mathbb{Z}$ become points $x \in \mathbb{R}$.[1]

We will not concern ourselves with the question of convergence of the curve itself but are more interested whether we can recover the smooth quantities –like tangent vectors and arc length– from the corresponding discrete definitions. Suppose that γ^ε possesses a smooth limit

$$\gamma^\varepsilon \to \gamma \quad (\varepsilon \to 0).$$

or alternatively start with the smooth curve and define the family of discrete curves by sampling. Then we can investigate how properties from the discrete case transfer to the smooth case in the following way:

- Take some local discrete quantity depending on some vertex $k \in \mathbb{Z}$ and its neighbors.
- Replace $k \in \mathbb{Z}$ by a point $x \in \mathbb{R}$, $k-1$ by $x-\varepsilon$, $k+1$ by $x+\varepsilon$, ...
- Investigate the limit $\varepsilon \to 0$, e.g. by applying Taylor's theorem at $\varepsilon = 0$.

The discrete unit tangent vectors $T_k = \frac{\gamma_{k+1}-\gamma_k}{\|\gamma_{k+1}-\gamma_k\|}$ become smooth unit tangent vectors $T = \frac{\gamma'(x)}{\|\gamma'(x)\|}$:

$$\begin{aligned} T_k &= \frac{\gamma(x+\varepsilon)-\gamma(x)}{\|\gamma(x+\varepsilon)-\gamma(x)\|} = \frac{\gamma'(x)\varepsilon + o(\varepsilon)}{\|\gamma'(x)\varepsilon + o(\varepsilon)\|} \\ &= \frac{\gamma'(x)+o(1)}{\|\gamma'(x)\|+o(1)} \to \frac{\gamma'(x)}{\|\gamma'(x)\|}. \end{aligned}$$

If we consider the (non-unit) vertex differences $\Delta\gamma_k = \gamma_{k+1} - \gamma_k$ we have to scale appropriately to obtain the tangent vector $\gamma'(x)$ in the limit. Indeed

$$\frac{1}{\varepsilon}(\gamma_{k+1}-\gamma_k) = \frac{1}{\varepsilon}(\gamma'(x)\varepsilon + o(\varepsilon)) \to \gamma'(x).$$

Starting with a discrete arc length parametrized curve for $\varepsilon = 1$, i.e. $\|\Delta\gamma_k\| = 1$, we take all curves of the family γ^ε to have vertex differences of constant length, i.e. $\|\Delta\gamma^\varepsilon_{\varepsilon k}\| = \varepsilon$ for all $\varepsilon > 0$, $k \in \mathbb{Z}$. Then the smooth limit is also arc length parametrized:

$$\|\gamma'(x)\| \leftarrow \frac{1}{\varepsilon}\|\gamma_{k+1}-\gamma_k\| = \frac{\varepsilon}{\varepsilon} = 1.$$

In the arc length parametrized case the tangent vectors T_k are equal to the vertex differences $\Delta\gamma_k$. But while scaling down the lattice size by ε we get

$$T_k = \frac{\Delta\gamma_k}{\varepsilon},$$

due to the normalization of T_k.

[1] Depending on the situation it might be more convenient to consider a refinement of the lattice, like $\frac{1}{2^k}\mathbb{Z}$. The procedure described above is convenient for the investigation of local properties around 0.

Let us investigate sum and difference of two neighboring tangent vectors T_k and T_{k-1} in the smooth limit. In this limit the angle between the vectors tends to 0.

$$\begin{aligned}
T_k + T_{k-1} &= \frac{1}{\varepsilon}(\Delta\gamma_k + \Delta\gamma_{k-1}) \\
&= \frac{1}{\varepsilon}(\gamma(x+\varepsilon) - \gamma(x-\varepsilon)) \\
&= \frac{1}{\varepsilon}(\gamma(x) + \varepsilon\gamma'(x) - \gamma(x) + \varepsilon\gamma'(x) + o(\varepsilon)) \\
&= 2\gamma'(x) + o(1). \\
T_k - T_{k-1} &= \frac{1}{\varepsilon}(\Delta\gamma_k - \Delta\gamma_{k-1}) \\
&= \frac{1}{\varepsilon}(\gamma(x+\varepsilon) - 2\gamma(x) + \gamma(x-\varepsilon)) \\
&= \frac{1}{\varepsilon}\left(\varepsilon\gamma'(x) + \frac{1}{2}\varepsilon^2\gamma''(x) - \varepsilon\gamma'(x) + \frac{1}{2}\varepsilon^2\gamma''(x) + o(\varepsilon^2)\right) \\
&= \varepsilon\gamma''(x) + o(\varepsilon).
\end{aligned}$$

So to approximate the second derivative of the curve we have to scale the difference of the tangent vectors by $\frac{1}{\varepsilon}$.

2.3 Discrete curvature from osculating circles

Definition 2.3 (curvature of smooth curves)**.** Let $\gamma : I \to \mathbb{R}^N$ be a smooth curve parametrized by arc length. Then the curvature of γ at $s \in I$ is

$$\kappa(s) \coloneqq \left\|\gamma''(s)\right\|.$$

This definition extends to any smooth regular curve upon reparametrization by arc length.

Remark 2.3.

- The *osculating circle* at $s \in I$ is the unique circle best approximating γ at $\gamma(s)$. It can for example be obtained
  - as the arc length parametrized circle through $\gamma(s)$ agreeing with γ up to second order.
  - by a limiting procedure of circles through three distinct points on γ going to $\gamma(s)$.
  - as the circle among all tangent circles at $\gamma(s)$ for which the distance to γ in normal direction decays the least.

  Let $R(s) > 0$ be the radius of the osculating circle. Then the curvature of γ at $s \in I$ is the reciprocal
  $$\kappa(s) = \frac{1}{R(s)}.$$
- If $\gamma''(s) \neq 0$ the osculating circle lies in the *osculating plane* which is the plane spanned by $\gamma'(s)$ and $\gamma''(s)$.
  If $\gamma''(s) = 0$ it degenerates to a line and $\kappa(s) = 0$.

- Let $\gamma : I \to \mathbb{R}^2$ be a plane curve parametrized by arc length. Then we can define a signed curvature $\kappa_\pm(s)$ of γ at $s \in I$ by

$$T'(s) = \kappa_\pm(s)N(s),$$

where $T(s) = \gamma'(s)$ and $N(s) \coloneqq iT(s)$ is $T(s)$ rotated by $\frac{\pi}{2}$.

We consider three possibilities of defining osculating circles in the discrete case leading to different notions of discrete curvature. Let $\gamma : I \to \mathbb{R}^N$ be a discrete curve. We define

$$\varphi_k \coloneqq \measuredangle(\Delta\gamma_k, \Delta\gamma_{k-1}) = \measuredangle(T_k, T_{k-1}) \in [0, \pi].$$

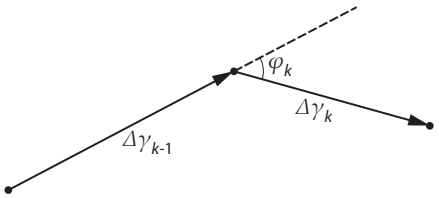

Figure 2.2. Turning angle at a vertex of a discrete curve.

For planar curves $\gamma : I \to \mathbb{R}^2$ we can define the angle φ_k to be in $[-\pi, \pi]$.

2.3.1 Vertex osculating circle

Definition 2.4 (vertex osculating circle)**.** The *vertex osculating circle* at a vertex k is the circle through γ_k and its two neighbors γ_{k-1} and γ_{k+1}.

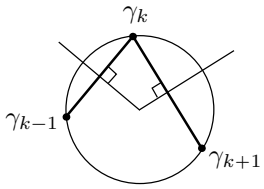

Figure 2.3. Vertex osculating circle as the circle through three neighboring vertices.

Its center is given by the intersection of the two bisecting lines of the adjacent difference vectors $\Delta\gamma_k$ and $\Delta\gamma_{k-1}$. The radius is given by $\|\gamma_{k+1} - \gamma_{k-1}\| = 2R_k \sin\varphi_k$ which leads to the curvature

$$\kappa_k = \frac{2\sin\varphi_k}{\|\gamma_{k+1} - \gamma_{k-1}\|}.$$

Note that for planar curves with $\varphi_k \in [-\pi, \pi]$ this leads to a signed curvature where the sign corresponds to the expected behavior from the smooth case.

Remark 2.4. For discrete arc length parametrized curves we find

- $T_k - T_{k-1}$ is perpendicular to the circle at γ_k. So $T_k + T_{k-1}$ is tangent to the vertex osculating circle.
- The curvature is bounded from above by 2 since the radius of the vertex osculating circle is always greater than $\frac{1}{2}$ in this case.

2.3.2 Edge osculating circle

The edge osculating circle can only be defined for planar curves since we need any three consecutive edges to be planar.

Definition 2.5 (edge osculating circle)**.** Let γ be a planar discrete curve. Then the *edge osculating circle* of γ at the edge $(k, k+1)$ is the oriented circle which touches the lines through the three successive edges $\Delta\gamma_{k-1}$, $\Delta\gamma_k$ and $\Delta\gamma_{k+1}$ such that the orientation of the circle at the touching points matches the orientation of the lines (which are oriented by the direction of the corresponding edges).

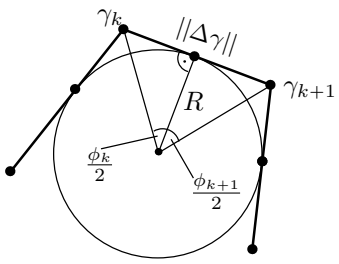

Figure 2.4. Edge osculating circle as the circle touching three consecutive edges.

The edge osculating circle is uniquely determined as long as the three consecutive edges are of different directions. Even if the curve is non-convex.

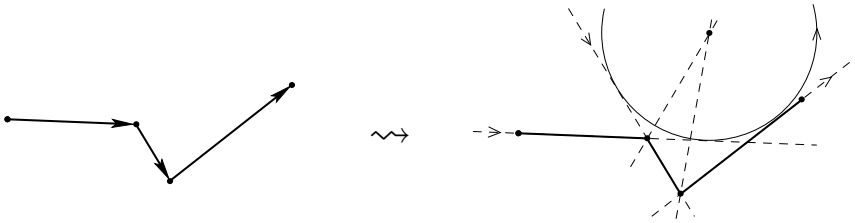

Figure 2.5. Edge osculating circle for a non-convex discrete curve.

Its center is the intersection of the two angular bisectors of the three consecutive edges. The radius is given by $\|\Delta\gamma_k\| = R_k(\tan\frac{\varphi_k}{2} + \tan\frac{\varphi_{k+1}}{2})$. This leads to the curvature

$$\kappa_k = \frac{\tan\frac{\varphi_k}{2} + \tan\frac{\varphi_{k+1}}{2}}{\|\Delta\gamma_k\|}.$$

It is unbounded from above even for arc length parametrized curves but has the disadvantages of being not as local as the previous definition,[2] while only being applicable to planar curves.

2.3.3 Osculating circle for arc length parametrized curves

For arc length parametrized discrete curves we can achieve the locality of the first and the unboundedness of the second definition by taking the circle touching two consecutive edges in their midpoints. This works in any dimension.

Definition 2.6 (osculating circle for arclength parametrized curves)**.** Let $\gamma : I \to \mathbb{R}^N$ be a discrete arc length parametrized curve. Then we define the *osculating circle* at vertex k to be the circle touching the two edges T_{k-1} and T_k in its midpoints.

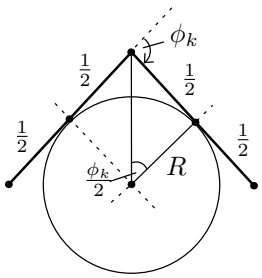

Figure 2.6. Osculating circle for a discrete arc length parametrized curve.

The center is given by the intersection of the bisecting lines of the two edges while we find for the radius $2R_k \tan \frac{\varphi_k}{2} = 1$ which leads to the following definition of curvature

$$\kappa_k = 2 \tan \frac{\varphi_k}{2}. \tag{2.1}$$

Note that it is zero at straight vertices and goes to infinity at non-regular vertices.

[2] It is defined at edges while depending on the neighboring edges which makes it involve a total of four consecutive points.

3 Flows on curves

3.1 Flows on smooth curves

3.1.1 Local geometric flows

We want to describe the motion of a curve $\gamma : I \to \mathbb{R}^N$ in space by applying some vector field v. In general v might depend on the whole curve, i.e. be some vector field on some domain in the space of curves. If v depends only locally on γ, i.e. only on a small neighborhood at each point of the curve, we call the generated flow a *local flow*. This is the case if the evolution process of γ under the flow generated by v can be described by a differential equation

$$\partial_t \gamma = v\left(\gamma, \gamma', \gamma'', \dots\right). \tag{3.1}$$

A one-parameter family of curves

$$\gamma : I \times J \to \mathbb{R}^N$$

which is a solution of (3.1) in the sense that

$$\partial_t \gamma(s,t) = v\left(\gamma(s,t), \gamma'(s,t), \gamma''(s,t), \dots\right) =: v(s,t)$$

for all $(s,t) \in I \times J$ is called the *evolution of the curve* $\gamma_0(s) = \gamma(s,0)$ under the flow given by v.
For this particular initial curve γ_0 the vector field v becomes a one-parameter family of vector fields along the parametrization

$$v : I \times J \to \mathbb{R}^N$$

and (3.1) becomes

$$\partial_t \gamma(s,t) = v(s,t).$$

The map

$$\Phi : (t, \gamma) \mapsto \Phi_t \gamma,$$

where $\Phi_t \gamma(s) \coloneqq \gamma(s,t)$ is the evolution of γ is called the *curve flow* given by v. Note that in general Φ might not be well defined due to lack of existence and uniqueness of solutions of (3.1) for arbitrary γ_0.

Additionally one might want the flow to be *geometric*, i.e. only depend on the shape of the curve. For this it should be invariant with respect to

- Euclidean motions,[3]
- reparametrization of the curve.

The flow is then well defined on the corresponding equivalence classes of parametrized curves.

Example 3.1 (planar geometric flow)**.** For planar curves these two conditions can be realized by the ansatz:

$$v = v(\kappa, \kappa', \kappa'', \dots) = \alpha(\kappa, \kappa', \kappa'', \dots)T + \beta(\kappa, \kappa', \kappa'', \dots)N. \tag{3.2}$$

[3] Or more general, invariant with respect to the action of some other Lie group.

3.1.2 Arc length preserving flows

Now we restrict our attention to flows that preserve the arc length parametrization, i.e.

$$\partial_t \left\|\gamma'\right\| = 0. \tag{3.3}$$

If we think of the curve as a one-dimensional distribution of mass, (3.3) means that the density along the curve does not change under the action of the flow. In particular the length of the curve is preserved.

Example 3.2 (planar geometric flow preserving arc length)**.** Using the ansatz (3.2) for a planar geometric flow and starting out with an arc length parametrization we obtain

$$\partial_t \gamma' = \alpha' T + \alpha T' + \beta' N + \beta N' = (\alpha' - \kappa\beta)T + (\kappa\alpha + \beta')N,$$

where we used $T' = \kappa N$ and $N' = -\kappa T$. Under this condition (3.3) becomes

$$0 = \frac{1}{2}\partial_t \langle \gamma', \gamma' \rangle = \langle \partial_t \gamma', \gamma' \rangle = \alpha' - \kappa\beta.$$

The solution $\alpha = 1$, $\beta = 0$ leads to the *tangent flow*

$$\partial_t \gamma = T,$$

while $\alpha = \frac{1}{2}\kappa^2$, $\beta = \kappa'$ leads to the *modified Korteweg-deVries flow* (mKdV flow)

$$\partial_t \gamma = \frac{1}{2}\kappa^2 T + \kappa' N.$$

The curvature κ of curves evolving under the mKdV flow changes as

$$\begin{aligned} \partial_t \kappa &= \partial_t \langle T', N \rangle = \langle \partial_t T', N \rangle = (\kappa\alpha + \beta')' \\ &= \frac{3}{2}\kappa^2 \kappa' + \kappa''', \end{aligned}$$

which is the *mKdV equation*.

Example 3.3 (arc length preserving tangent flow)**.** Consider a curve flow on curves in $\mathbb{R}^N$ in tangent direction

$$\partial_t \gamma = \alpha T.$$

Closed curves and infinite curves are invariant with respect to such a flow. In general the flow just induces a reparametrization of the curve. It is arc length preserving if and only if α is constant along the curve at any time, i.e. $\alpha = \alpha(t)$. The normalized version $\alpha = 1$ acts as

$$\Phi_t \gamma(s) = \gamma(t, s) = \gamma(0, s + t) = \gamma(s + t).$$

Example 3.4 (Heisenberg flow)**.** For arc length parametrized curves in $\mathbb{R}^3$ consider the *Heisenberg flow*[4]

$$\partial_t \gamma = \gamma'' \times \gamma'. \tag{3.4}$$

[4]The Heisenberg flow is also known as the *smoke ring flow* or *Hashimoto flow*.

Using a Frenet frame T, N, B we obtain

$$\partial_t \gamma = T' \times T = \kappa N \times T = -\kappa B.$$

So the Heisenberg flow is always acting in binormal direction and is therefore arc length preserving.
The tangent vector evolves under the Heisenberg flow as

$$\partial_t T = (\gamma'' \times \gamma')' = \gamma''' \times \gamma' = T'' \times T.$$

3.2 Flows on discrete arc length parametrized curves

For $I \coloneqq [0, \dots, n] \subset \mathbb{Z}$ finite interval, $I = \mathbb{Z}_n \coloneqq \mathbb{Z}/n\mathbb{Z}$ and $I = \mathbb{Z}$ we define the space

$$\mathcal{C}_I \coloneqq \{\gamma : I \to \mathbb{R}^N\}$$

of finite, finite closed and infinite curves respectively. Note that in the finite case $\mathcal{C}_I \cong (\mathbb{R}^N)^n$. By $\mathcal{C}_I^{\text{reg}}$ and $\mathcal{C}_I^{\text{arc}}$ we denote the corresponding submanifolds of regular and arc length parametrized curves.

A *flow of discrete curves* is given by a vector field

$$v : \mathcal{C}_I \to \mathrm{T}\mathcal{C}_I, \quad \gamma \mapsto v[\gamma] \in \mathrm{T}_\gamma \mathcal{C}_I,$$

or on some submanifold $U \subset \mathcal{C}_I$. In the finite case we have $\mathrm{T}_\gamma \mathcal{C}_I = (\mathbb{R}^N)^n$. So v gives a direction in $\mathbb{R}^N$ at every vertex k which possibly depends on the whole curve γ. We state this relation as

$$v_k[\gamma] \in \mathbb{R}^N.$$

For a given initial curve $\gamma : I \to \mathbb{R}^N$ the vector field v on $\mathcal{C}_I$ becomes a one-parameter family of vector fields along the parametrization of the curve

$$v : I \times J \to \mathbb{R}^N,$$

where $J \subset \mathbb{R}$ is an open interval. The action of the flow leads to a continuous deformation of the curve $\gamma_k = \gamma_k(0)$

$$\gamma : I \times J \to \mathbb{R}^N$$

satisfying

$$\partial_t \gamma_k(t) = v_k(t).$$

In the following we restrict our attention to inner vertices only. The advantage is that we have to define vector fields only on inner vertices. This restriction is realized by examining closed and infinite curves, i.e. $I = \mathbb{Z}_n$ or $I = \mathbb{Z}$.
As in the smooth case we focus on local geometric flows on $\mathcal{C}_I^{\text{arc}}$. In the discrete case we interpret these conditions as follows.

arc length preserving To preserve arc length parametrization, i.e. make γ stay in $\mathcal{C}_I^{\text{arc}}$ the flow must satisfy[5]

$$\begin{aligned} & 0 = \partial_t \left\| \Delta \gamma_k \right\| \\ \Leftrightarrow \; & 0 = \langle \partial_t \Delta \gamma_k, T_k \rangle = \langle \partial_t \gamma_{k+1} - \partial_t \gamma_k, T_k \rangle = \langle v_{k+1} - v_k, T_k \rangle. \end{aligned} \tag{3.5}$$

[5]This means we want the vector field v to be defined on the submanifold $\mathcal{C}_I^{\text{arc}}$ of $\mathcal{C}_I$, i.e. make sure that $v[\gamma] \in \mathrm{T}_\gamma \mathcal{C}_I^{\text{arc}} \subset \mathrm{T}_\gamma \mathcal{C}_I$.

Decomposing the vector field at the vertex k into its parts along the tangent plane $\operatorname{span}\{T_k, T_{k-1}\}$ and its orthogonal complement we see that this only imposes constraints on the former.

local flow By a *local flow* we mean a flow which at every vertex k only depends on the curve at the adjacent vertices[6], i.e. γ_{k-1}, γ_k, γ_{k+1}:

$$v_k[\gamma] = v(\gamma_{k-1}, \gamma_k, \gamma_{k+1}).$$

geometric Since we do not consider reparametrizations in the discrete case a *geometric flow* is a flow which is just invariant with respect to Euclidean transformations, i.e. translations and rotations.
On the level of the vector field this means that for $R \in \mathrm{SO}(N)$, $a \in \mathbb{R}^N$

$$v_k[R\gamma + a] = Rv_k[\gamma].$$

Let us break down these conditions a little bit further in the case of local flows on $\mathcal{C}_I^{\mathrm{arc}}$.

translation invariance For a local flow given by the vector field v translation invariance means that for any $a \in \mathbb{R}^N$

$$v(\gamma_{k-1} + a, \gamma_k + a, \gamma_{k+1} + a) = v(\gamma_{k-1}, \gamma_k, \gamma_{k+1}),$$

which can also be expressed the following way: For any given direction $b \in \mathbb{S}^{N-1}$

$$\left.\frac{\mathrm{d}}{\mathrm{d}\varepsilon}\right|_{\varepsilon=0} v(\gamma_{k-1} + \varepsilon b, \gamma_k + \varepsilon b, \gamma_{k+1} + \varepsilon b) = 0.$$

For a flow on $\mathcal{C}_I^{\mathrm{arc}}$ we can rewrite a local vector field to be a function of the form $v_k = v_k(\gamma_k, T_k, T_{k-1})$. For this we get

$$0 = \left.\frac{\mathrm{d}}{\mathrm{d}\varepsilon}\right|_{\varepsilon=0} v(\gamma_k + \varepsilon b, T_k, T_{k-1}) = \frac{\partial v_k}{\partial \gamma_k} \cdot b$$

for all $b \in \mathbb{S}^{N-1}$, i.e. v must not explicitly depend on γ_k and therefore be of the form

$$v_k = v(T_k, T_{k-1}). \tag{3.6}$$

rotation invariance For a local translation invariant vector field (3.6) on $\mathcal{C}_I^{\mathrm{arc}}$ this means that for any rotation $R \in \mathrm{SO}(N)$

$$v(RT_k, RT_{k-1}) = Rv(T_k, T_{k-1}).$$

We consider this further in the three dimensional case. At every vertex[7] k we can take $T_k, T_{k-1}, T_k \times T_{k-1}$ as a rotation invariant basis.[8]

[6] By this we mean in particular that v depends on the adjacent vertices "equally" at every vertex.

[7] At least at regular, non-straight vertices.

[8] In this context T_k, T_{k-1} have to be interpreted as vector fields on $\mathcal{C}_I$. The cross product of two rotation invariant vector fields is rotation invariant. So we get three rotation invariant vector fields which define a basis of $\mathrm{T}_\gamma \mathcal{C}_I = (\mathbb{R}^3)^n$ for any curve γ, i.e. a basis of $\mathbb{R}^3$ at every vertex k.
Note that this in general is not an orthonormal basis. Such a basis could be obtained by taking $\frac{T_k + T_{k-1}}{\|T_k + T_{k-1}\|}, \frac{T_k - T_{k-1}}{\|T_k - T_{k-1}\|}, \frac{T_k \times T_{k-1}}{\|T_k \times T_{k-1}\|}$.

Expressing v in this basis we get

$$v_k(T_k, T_{k-1}) = \alpha_1(T_k, T_{k-1})T_k + \alpha_2(T_k, T_{k-1})T_{k-1} + \alpha_3(T_k, T_{k-1})T_k \times T_{k-1}, \tag{3.7}$$

and see that rotation invariance is equivalent to the invariance of the scalar components α_i:

$$\alpha_i(RT_k, RT_{k-1}) = \alpha_i(T_k, T_{k-1}). \tag{3.8}$$

3.2.1 Tangent flow

Since tangent vectors of a discrete arc length parametrized curve γ live on edges it is not instantly clear what the tangent direction at a vertex k should be. If we want it to depend only on the neighboring tangent vectors an obvious symmetric choice would be[9]

$$T_k + T_{k-1}.$$

If we set a local flow on $\mathcal{C}_I^{\text{arc}}$ to be parallel to $T_k + T_{k+1}$ it is already uniquely determined –up to a constant– and turns out to be geometric.

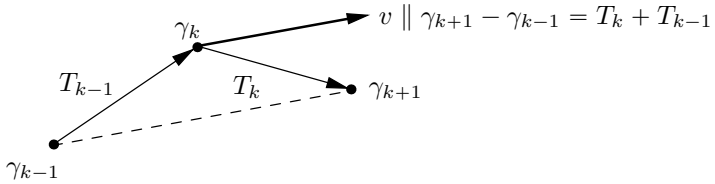

Figure 3.1. Tangent flow on a discrete arc length parametrized curve.

Proposition 3.1 (discrete tangent flow)**.** *The* discrete tangent flow[10]

$$\partial_x \gamma_k = v_k \coloneqq \frac{T_k + T_{k-1}}{1 + \langle T_k, T_{k-1} \rangle}$$

is up to a multiplicative constant the only discrete local curve flow in tangent direction $T_k + T_{k-1}$ which preserves arc length parametrization.
It is geometric.

Proof. Let us start with a general flow in tangent direction

$$v_k = \alpha_k(T_k + T_{k-1}),$$

where $\alpha_k = \alpha_k[\gamma]$ might depend on the curve in any way.
Now we impose arc length preservation. From (3.5) we know that

$$\begin{aligned}
& 0 = \partial_t \|\Delta\gamma_k\| \\
\Leftrightarrow \quad & 0 = \langle v_{k+1} - v_k, T_k \rangle \\
& = \langle \alpha_{k+1}(T_{k+1} + T_k) - \alpha_k(T_k + T_{k-1}), T_k \rangle \\
& = \alpha_{k+1}(\langle T_{k+1}, T_k \rangle + 1) - \underbrace{\alpha_k(\langle T_k, T_{k-1} \rangle + 1)}_{=: c_k} \\
\Leftrightarrow \quad & c_{k+1} = c_k
\end{aligned}$$

[9] Note that this is only a well-defined direction on regular vertices.
[10] Note that x is the flow parameter of the tangent flow here.

for all $k \in I$. So $c_k = c_k[\gamma] =: c[\gamma]$ is constant in k and therefore

$$\alpha_k[\gamma] = \frac{c[\gamma]}{1 + \langle T_k, T_{k-1} \rangle},$$

where this constant might still depend on γ.
Now the locality of the flow ensures that c is the same for any curve γ.[11]
The flow is geometric since it is of the translation invariant form

$$v_k[\gamma] = \alpha(T_k, T_{k-1})(T_k + T_{k-1}),$$

where $\alpha(T_k, T_{k-1}) = \frac{1}{1+\langle T_k, T_{k-1} \rangle}$ is rotation invariant. □

Remark 3.1.

- Since $1 + \langle T_k, T_{k-1} \rangle \to \infty$ as $T_k \to -T_{k-1}$ it is only well-defined at regular vertices.
- Comparing with the smooth tangent flow on arc length parametrized curves which is $\partial_x \gamma = \gamma'$ gives rise to the definition of the *vertex tangent vector* at the vertex k of an arc length parametrized curve[12] to be

  $$\frac{T_k + T_{k-1}}{1 + \langle T_k, T_{k-1} \rangle}.$$

  Note that

  $$1 + \langle T_k, T_{k-1} \rangle = \frac{1}{2} \|T_k + T_{k-1}\|^2.$$

  So the vertex tangent vectors are not of constant length

  $$\left\| \frac{T_k + T_{k-1}}{1 + \langle T_k, T_{k-1} \rangle} \right\| = \frac{2}{\|T_k + T_{k-1}\|}.$$

- For the discrete tangent-flow v

$v[\gamma]$ is a translation	$\Leftrightarrow$	γ is a straight zig-zag curve
$v[\gamma]$ is a rotation	$\Leftrightarrow$	γ is a circular zig-zag curve.

  Note that the first case includes straight lines and the second regular polygons as special cases.

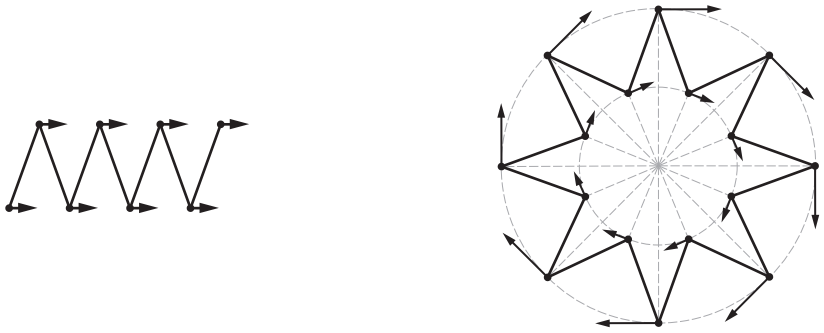

Figure 3.2. Discrete tangent flow. Straight zig-zag curves evolve by a translation. Circular zig-zag curves evolve by a rotation.

[11] ∂_x local $\Rightarrow c[\gamma] = c(\gamma_{k-1}, \gamma_k, \gamma_{k+1})$ with the same value for every k.
[12] This can be generalized to general discrete curves as can be seen in [**ddg-script-hoffmann**].

- We investigate the smooth limit where we refine the lattice $\varepsilon\mathbb{Z} \to \mathbb{R}$ as $\varepsilon \to 0$ as discussed in Section 2.2. We set $\|\Delta\gamma_k\| = \varepsilon$ and therefore $T_k = \frac{\Delta\gamma_k}{\varepsilon}$. Replacing $k \in \mathbb{Z}$ by $x = \varepsilon k \in \mathbb{R}$ we have

$$T_k + T_{k-1} = 2\gamma'(x) + o(1)$$

and

$$1 + \langle T_k, T_{k-1}\rangle = \frac{1}{2}\|T_k + T_{k-1}\|^2 = 2\|\gamma'(x)\| + o(1) = 2 + o(1)$$

since the smooth limit is arc length parametrized, i.e. $\|\gamma'(x)\| = 1$. So

$$\frac{T_k + T_{k+1}}{1 + \langle T_k, T_{k-1}\rangle} = \frac{2\gamma'(x) + o(1)}{2 + o(1)} \to \gamma'(x),$$

which is the smooth tangent flow of an arc length parametrized curve as introduced in Section 3.1.

3.2.2 Heisenberg flow

We now consider curves in $\mathbb{R}^3$ and a flow in binormal direction $T_k \times T_{k-1}$. Any flow in binormal direction is arc length preserving.[13] So this property does not distinguish any of these flows as for the flows in tangent direction. But there is only one that commutes with the tangent flow.

Proposition 3.2 (discrete Heisenberg flow)**.** *The* discrete Heisenberg flow

$$\partial_t\gamma_k = w_k \coloneqq \frac{T_k \times T_{k-1}}{1 + \langle T_k, T_{k-1}\rangle} \tag{3.9}$$

is up to a multiplicative constant the only discrete local curve flow in binormal direction $T_k \times T_{k-1}$ which commutes with the tangent flow.
It is geometric and preserves arc length parametrization.

Remark 3.2.

- Commuting flows (infinitely many) is a characteristic feature of integrable systems.
- Two flows given by v and w commute if they can be integrated simultaneously. This means for some initial curve γ there is some local two-parameter variation

$$\begin{aligned}\gamma\colon (-\varepsilon,\varepsilon)\times(-\varepsilon,\varepsilon) &\to \mathcal{C}_I^{\text{arc}}\\ (x,t) &\mapsto \gamma(x,t)\end{aligned}$$

satisfying

$$\begin{cases}\partial_x\gamma_k &= v_k\\ \partial_t\gamma_k &= w_k.\end{cases}$$

A necessary and sufficient condition for this is

$$\partial_x\partial_t\gamma_k = \partial_t\partial_x\gamma_k,$$

[13] See for example (3.5).

formally meaning that the derivatives ∂_x, $\partial_t \in \mathrm{T}_\gamma \mathcal{C}_I^{\mathrm{arc}}$ on $\mathcal{C}_I^{\mathrm{arc}}$ identified with the vector fields v, w at the point γ commute, i.e.

$$0 = [\partial_x, \partial_t] \in \mathrm{T}_\gamma \mathcal{C}_I^{\mathrm{arc}}.$$

Proof. We start with a general flow in binormal direction

$$\partial_t \gamma = w_k = \beta_k (T_k \times T_{k-1}),$$

where $\beta_k = \beta_k[\gamma]$.

($\Rightarrow$) We have to show that, if w commutes with the tangent flow

$$\partial_x \gamma = v_k = \frac{T_k + T_{k-1}}{1 + \langle T_k, T_{k-1} \rangle},$$

it has to be the Heisenberg flow, where x is the flow parameter of the tangent flow and t is the flow parameter of our ansatz.

$$\begin{aligned}
\partial_x \partial_t \gamma &= \partial_x w_k \\
&= \partial_x \left(\beta_k T_k \times T_{k-1} \right) \\
&= \beta_k \left(\partial_x T_k \times T_{k-1} + T_k \times \partial_x T_{k-1} \right) \\
&\qquad + \left(\partial_x \beta_k \right) T_k \times T_{k-1} \\
&= \beta_k \left[(v_{k+1} - v_k) \times T_{k-1} + T_k \times (v_k - v_{k-1}) \right] \\
&\qquad + \left(\partial_x \beta_k \right) T_k \times T_{k-1} \\
&= \beta_k \Bigg[\left(\frac{T_{k+1} + T_k}{1 + \langle T_{k+1}, T_k \rangle} - \frac{T_k + T_{k-1}}{1 + \langle T_k, T_{k-1} \rangle} \right) \times T_{k-1} \\
&\qquad + T_k \times \left(\frac{T_k + T_{k-1}}{1 + \langle T_k, T_{k-1} \rangle} - \frac{T_{k-1} + T_{k-2}}{1 + \langle T_{k-1}, T_{k-2} \rangle} \right) \Bigg] \\
&\qquad + \left(\partial_x \beta_k \right) T_k \times T_{k-1}.
\end{aligned}$$

So in particular

$$\langle \partial_x \partial_t \gamma, T_k \rangle = \beta_k \frac{\langle T_{k+1} \times T_{k-1}, T_k \rangle}{1 + \langle T_{k+1}, T_k \rangle}. \tag{3.10}$$

On the other hand

$$\begin{aligned}
\partial_t\partial_x\gamma &= \partial_t v_k \\
&= \partial_t\left(\frac{T_k + T_{k-1}}{1+\langle T_k, T_{k-1}\rangle}\right) \\
&= \frac{1}{1+\langle T_k, T_{k-1}\rangle}\partial_t\left(T_k + T_{k+1}\right) + \partial_t\left(\frac{1}{1+\langle T_k, T_{k-1}\rangle}\right)(T_k + T_{k+1}) \\
&= \frac{1}{1+\langle T_k, T_{k-1}\rangle}\left(w_{k+1} - w_{k-1}\right) \\
&\quad - \frac{1}{(1+\langle T_k, T_{k-1}\rangle)^2}\Big(\langle w_{k+1} - w_k, T_{k-1}\rangle + \langle T_k, w_k - w_{k-1}\rangle\Big)(T_k + T_{k-1}) \\
&= \frac{1}{1+\langle T_k, T_{k-1}\rangle}\Big(\beta_{k+1}T_{k+1}\times T_k - \beta_{k-1}T_{k-1}\times T_{k-2}\Big) \\
&\quad - \frac{1}{(1+\langle T_k, T_{k-1}\rangle)^2}\Big(\beta_{k+1}\langle T_{k+1}\times T_k, T_{k-1}\rangle \\
&\quad - \beta_{k-1}\langle T_k, T_{k-1}\times T_{k-2}\rangle\Big)(T_k + T_{k-1}).
\end{aligned}$$

In particular

$$\langle \partial_t\partial_x\gamma, T_k\rangle = -\beta_{k+1}\frac{\langle T_{k+1}\times T_k, T_{k-1}\rangle}{1+\langle T_k, T_{k-1}\rangle}. \tag{3.11}$$

Comparing (3.10) and (3.11) we get

$$\begin{aligned}
&\frac{\beta_k}{1+\langle T_{k+1}, T_k\rangle} = \frac{\beta_{k+1}}{1+\langle T_k, T_{k-1}\rangle} \\
\Leftrightarrow\quad &\beta_k(1+\langle T_k, T_{k-1}\rangle) = \beta_{k+1}(1+\langle T_{k+1}, T_k\rangle)
\end{aligned}$$

for all $k \in I$ which is equivalent to

$$\beta_k[\gamma] = \frac{c[\gamma]}{1+\langle T_k, T_{k-1}\rangle},$$

where c is some constant depending on the curve γ. Imposing the locality of w eliminates this dependence.

($\Leftarrow$) A similar –but even longer– calculation shows that the obtained Heisenberg flow actually does commute with the tangent flow. After calculating $\partial_x\partial_t\gamma$ and $\partial_t\partial_x\gamma$ one can compare the scalar products with T_k, T_{k-1} and $T_k \times T_{k-1}$ respectively.

We still have to show that the Heisenberg flow is geometric and arc length preserving.
Similar to the tangent flow it is of the translation invariant form

$$w_k[\gamma] = \beta(T_k, T_{k-1})T_k \times T_{k-1},$$

where β is rotation invariant. Since $T_k \times T_{k-1}$ is a rotation invariant vector field the Heisenberg flow is geometric.
It always lies in the orthogonal complement of $\operatorname{span}\{T_k, T_{k-1}\}$ and therefore is arc length preserving. □

Remark 3.3. We investigate the smooth limit using the method described in Section 2.2. Setting $x = \varepsilon k$ we have[14]

$$\begin{aligned} T_k \times T_{k-1} &= T(x) \times T(x-\varepsilon) \\ &= T(x) \times (T(x) - \varepsilon T'(x) + o(\varepsilon)) \\ &= \varepsilon T'(x) \times T(x) + o(\varepsilon) \end{aligned}$$

and

$$1 + \langle T_k, T_{k-1} \rangle = 2 + o(1).$$

Rescaling the time by replacing $t \to \frac{\varepsilon t}{2}$ we obtain the smooth limit

$$\partial_\tau \gamma = T' \times T. \tag{3.12}$$

This results in the following equation of motion for T

$$\partial_t T(x) = T'' \times T, \tag{3.13}$$

which is the continuous Heisenberg magnetic chain as described in Section A. This is an integrable system as is the discretization obtained from (3.9) which yields

$$\begin{aligned} \partial_t T_k &= \frac{T_{k+1} \times T_k}{1 + \langle T_{k+1}, T_k \rangle} - \frac{T_k \times T_{k-1}}{1 + \langle T_k, T_{k-1} \rangle} \\ &= \left(\frac{T_{k+1}}{1 + \langle T_{k+1}, T_k \rangle} + \frac{T_{k-1}}{1 + \langle T_k, T_{k-1} \rangle} \right) \times T_k. \end{aligned} \tag{3.14}$$

[14] Which might be seen immediately from $T_k \times T_{k-1} = (T_k - T_{k-1}) \times T_{k-1}$.

4 Elastica

4.1 Smooth elastic curves

We consider variations of curves γ in $\mathbb{R}^3$ with fixed endpoints, fixed end directions and fixed length.

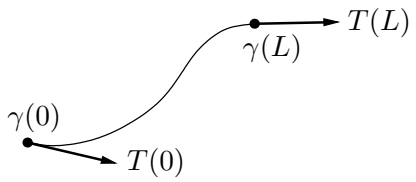

Figure 4.1. Curve with fixed endpoints and fixed end tangent vectors.

We represent each curve by its arc length parametrization $\gamma : [0, L] \to \mathbb{R}^3$ with $T \coloneqq \gamma' : [0, L] \to \mathbb{S}^2$. Then admissible variations have to

- fix $\gamma(0)$, $\gamma(L) \in \mathbb{R}^3$,
- fix $T(0)$, $T(L) \in \mathbb{S}^2$,
- preserve the arc length parametrization, i.e. $\|T(s)\| = 1$,
  in particular this implies that the length of γ is preserved.

We define the bending energy of γ to be

$$\mathcal{E}[\gamma] \coloneqq \int_0^L \kappa(s)^2 \mathrm{d}s = \int_0^L \langle T', T' \rangle \mathrm{d}s = \mathcal{E}[T],$$

where $\kappa = \|\gamma''\|^2 = \|T'\|^2$ is the curvature of γ.

Remark 4.1. Note that the bending energy is invariant w.r.t. Euclidean motions.

Definition 4.1 (Bernoulli's elastica)**.** An *elastic curve* is a critical point γ of the bending energy $\mathcal{E}$ under the described admissible variations.

The tangent vector $T : [0, L] \to \mathbb{S}^2$ uniquely determines the curve γ up to translations. We note that fixed $\gamma(0)$, $\gamma(L) \in \mathbb{R}^3$ implies

$$\int_0^L T(s) \mathrm{d}s = \gamma(L) - \gamma(0).$$

So if we reformulate the problem of finding critical points of the bending energy $\mathcal{E}[T]$ only in terms of $T : [0, L] \to \mathbb{S}^2$, we have to impose this additional constraint. Admissible variations of T have to

- fix $T(0)$, $T(L) \in \mathbb{S}^2$,
- satisfy $\int_0^L T(s) \mathrm{d}s = const. \in \mathbb{R}^3$,
- preserve $\|T(s)\| = 1$ for all $s \in [0, L]$.

Basic fact from the calculus of variations: Lagrange-multipliers. *The critical points of the functional*

$$\mathcal{S}[q] = \int_0^L \mathcal{L}(q(s), q'(s))\mathrm{d}s$$

on the space of smooth functions $q : [0, L] \to \mathbb{R}^3$ *under the variations preserving the constraints*

$$F_i = \int_0^L f_i(q, q')\mathrm{d}s = c_i \in \mathbb{R}, \qquad i = 1, \dots, N$$

are the critical points of the functional

$$\mathcal{S}_\lambda \coloneqq \mathcal{S} + \sum_{i=1}^{N} \lambda_i F_i$$

with some constants λ_i *(*Lagrange-Multipliers*).*
These constants are determined from the conditions $F_i = c_i,\ i = 1, \dots, N$.

Basic fact from Lagrangian mechanics: Hamilton's principle of least action. *The trajectory* $q(t)$ *of a mechanical system with potential energy* $\mathcal{U}$ *and kinetic energy* $\mathcal{T}$ *is critical for the* action functional

$$\mathcal{S}[q] \coloneqq \int_{t_1}^{t_2} \mathcal{L}(q(t), q'(t))\mathrm{d}t$$

with the Lagrangian $\mathcal{L} \coloneqq \mathcal{T} - \mathcal{U}$.

Implementing the constraint $\int_0^L T(s)\mathrm{d}s = const. \in \mathbb{R}^3$ into the functional via Lagrange-multiplicators, we obtain the following physical interpretation.

Theorem 4.1 (Kirchhoff analogy for elastic curves)**.** *An arc length parametrized curve* $\gamma : [0, L] \to \mathbb{R}^3$ *is an elastic curve if and only if its tangent vector* $T \coloneqq \gamma' : [0, L] \to \mathbb{S}^2$ *describes the evolution of the axis of a spherical pendulum.*
The arc length parameter of the curve coincides with the time parameter of the pendulum.

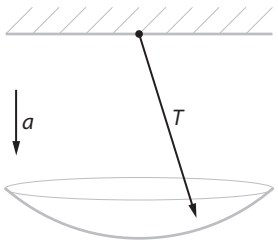

Figure 4.2. Spherical pendulum T with gravitational vector a.

Proof. The extrema of the functional

$$\mathcal{E}_a[T] \coloneqq \int_0^L \left(\langle T', T'\rangle + 2\langle a, T\rangle\right) \mathrm{d}s,$$

where $a \in \mathbb{R}^3$ and $T : [0, L] \to \mathbb{S}^2$ can be interpreted in two different ways:

(1) Extrema of the bending energy

$$\mathcal{E} = \int_0^L \kappa^2 \mathrm{d}s = \int_0^L \langle T', T' \rangle \mathrm{d}s$$

for variations with fixed endpoints under the constraint $\int_0^L T \mathrm{d}s = const. \in \mathbb{R}^3$. Here $a = (a_1, a_2, a_3)$ are treated as Lagrange-multipliers

$$\sum_{i=1}^3 \lambda_i F_i = \sum_{i=1}^3 a_i \int_0^L T_i(s) \mathrm{d}s = \int_0^L \langle a, T \rangle \mathrm{d}s.$$

(2) Extrema of the action functional with Lagrangian $\mathcal{L} = \mathcal{T} - \mathcal{U}$ where $\mathcal{T} = \langle T', T' \rangle, \mathcal{U} = -\langle a, T \rangle$ are the kinetic and potential energy of the spherical pendulum.
Here $a \in \mathbb{R}^3$ is the gravitational vector.

□

Remark 4.2.

- Planar elastica were first classified by Euler.
  The tangent vector describes the motion of a planar pendulum. The only closed elastica in the plane are the circle and Euler's elastic eight.

Figure 4.3. Some planar elastic curves.

- Elastica in $\mathbb{R}^N$ are reduced to elastica in $\mathbb{R}^3$.
  They always lie in the 3-dimensional space

$$\mathrm{span}\{\gamma(L) - \gamma(0), T(0), T(L)\}.$$

  Similarly the spherical pendulum in $\mathbb{S}^{N-1}$ always lies in the 2-dimensional space

$$\mathbb{S}^{N-1} \cap \mathrm{span}\{a, T(0), T'(0)\}.$$

Basic fact from calculus of variations: Euler-Lagrange equations. *$q : [0, L] \to \mathbb{R}^3$ is a critical point of the functional $\mathcal{S}[q] = \int_0^L \mathcal{L}(q(s), q'(s)) \mathrm{d}s$ under variations with fixed endpoints $q(0)$, $q(L)$ if and only if*

$$\frac{\mathrm{d}}{\mathrm{d}s} \nabla_{q'} \mathcal{L} - \nabla_q \mathcal{L} = 0.$$

We can implement the remaining constraint $\|T\| = 1$ into the functional using a "continuous Lagrange-multiplier":

$$\mathcal{E}_{(a,c)}[T] \coloneqq \int_0^L \left(\langle T', T' \rangle + c(s)(\langle T, T \rangle - 1) + 2\langle a, T \rangle \right) \mathrm{d}s.$$

From this we obtain the Euler-Lagrange equations for elastic curves.

Theorem 4.2 (Euler-Lagrange equations for elastic curves)**.** *An arc length parametrized curve $\gamma : [0, L] \to \mathbb{R}^3$ is an elastic curve if and only if*

$$\gamma'' \times \gamma' = a \times \gamma + b$$

for some $a, b \in \mathbb{R}^3$,
or equivalently if and only if its tangent vector $T : [0, L] \to \mathbb{S}^2$ satisfies

$$T'' \times T = a \times T$$

for some $a \in \mathbb{R}^3$.

Proof. The equation for γ can be obtained from the equation for T by integration, using $(\gamma'' \times \gamma')' = T'' \times T$.
With

$$\mathcal{L}(T, T') \coloneqq \frac{1}{2}\langle T', T' \rangle + \frac{1}{2}c(s)(\langle T, T \rangle - 1) + \langle a, T \rangle$$

we obtain

$$\begin{aligned} \frac{\mathrm{d}}{\mathrm{d}s}\nabla_{T'}\mathcal{L} = \nabla_T \mathcal{L} \;&\Leftrightarrow\; T'' = c(s)T + a \\ &\Leftrightarrow T'' \times T = a \times T, \end{aligned}$$

where we applied the cross-product with T. □

Remark 4.3. We recognize the left-hand side of the Euler-Lagrange equations as the Heisenberg flow (3.4) (acting on γ and T respectively) while the right-hand side describes an infinitesimal Euclidean motion.

Corollary 4.3. *A curve γ is an elastic curve if and only if the Heisenberg flow preserves its form, i.e. under the action of the Heisenberg flow the curve evolves by an Euclidean motion.*

Proof. That $v \mapsto a \times v + b$ is the infinitesimal generator of an Euclidean motion is best be seen using the quaternionic description of Euclidean motions, which is described in the following section. □

4.2 Quaternions and Euclidean Motions

The *quaternionic algebra* $\mathbb{H}$ is a 4-dimensional generalization of the complex numbers. It can be constructed the following way.

Let $\mathbb{H}$ be a real 4-dimensional vector space $\mathbb{R}^4$ where we denote the standard basis by $\{\mathbb{1}, \mathbb{i}, \mathbb{j}, \mathbb{k}\}$. So a general quaternion $q \in \mathbb{H}$ can be written as

$$q = q_0\mathbb{1} + q_1\mathbb{i} + q_2\mathbb{j} + q_3\mathbb{k}$$

with $q_i \in \mathbb{R}$.

We define a multiplication on $\mathbb{H}$ by prescribing it on the basis vectors. By distributivity it uniquely extends to all quaternions. For this the following relations are sufficient:

$$\mathbb{i}^2 = \mathbb{j}^2 = \mathbb{k}^2 = \mathbb{ijk} = -\mathbb{1}. \tag{4.1}$$

Associativity then fixes the multiplication for all combinations of basis vectors.

$$\begin{aligned}\mathbb{i}\mathbb{j} &= -\mathbb{j}\mathbb{i} = \mathbb{k}\\ \mathbb{j}\mathbb{k} &= -\mathbb{k}\mathbb{j} = \mathbb{i}\\ \mathbb{k}\mathbb{i} &= -\mathbb{i}\mathbb{k} = \mathbb{j}\end{aligned}$$

This also implies skew symmetry and therefore *non-commutativity* of the quaternionic multiplication. On the other hand we see that $\mathbb{1}$ commutes with everything, which is why we can identify the first component of the quaternions with the real numbers where $\mathbb{1} = 1$. Eventually we write

$$q = q_0 + q_1\mathbb{i} + q_2\mathbb{j} + q_3\mathbb{k}$$

with $q_i \in \mathbb{R}$.
The quaternionic multiplication extends the scalar multiplication of the vector space.

We denote the *real and imaginary part*[15] of $q \in \mathbb{H}$ by

$$\begin{aligned}\mathrm{Re}q &\coloneqq q_0 = q_0 1 = q_0\mathbb{1}\\ \mathrm{Im}q &\coloneqq q_1\mathbb{i} + q_2\mathbb{j} + q_3\mathbb{k}\end{aligned}$$

and the *conjugated quaternion* by

$$\overline{q} \coloneqq \mathrm{Re}q - \mathrm{Im}q.$$

Like in the complex case we define the absolute value of an quaternion $q \in \mathbb{H}$ by

$$|q|^2 \coloneqq q\overline{q} = \overline{q}q = q_0^2 + q_1^2 + q_2^2 + q_3^2$$

which turns out to be the same as the Euclidean distance in $\mathbb{R}^4$.

Quaternionic conjugation and absolute value give us means to define an inverse[16] for $q \in \mathbb{H}$, $q \neq 0$:

$$q^{-1} \coloneqq \frac{\overline{q}}{|q|^2}.$$

We see that the quaternionic multiplication induces a group structure on the following subsets of $\mathbb{H}$:

$$\begin{aligned}\mathbb{H}_* &\coloneqq \mathbb{H}\backslash\{0\}\\ \mathbb{H}_1 &\coloneqq \{q \in \mathbb{H} \mid |q| = 1\} \ \textit{unitary quaternions}\end{aligned}$$

4.2.1 Euclidean motions in $\mathbb{R}^3$

The set

$$\mathrm{Im}\mathbb{H} \coloneqq \{q \in \mathbb{H} \mid \mathrm{Re}q = 0\}$$

of *imaginary quaternions* is a 3-dimensional vector space which we identify with $\mathbb{R}^3$:

$$v_1\mathbb{i} + v_2\mathbb{j} + v_3\mathbb{k} \in \mathrm{Im}\mathbb{H} \Leftrightarrow (v_1, v_2, v_3) \in \mathbb{R}^3$$

This leads to the following geometric interpretation of multiplication of two imaginary quaternions.

[15] Note that the imaginary part includes the basis vectors unlike in the complex case.

[16] It is meaningful to write this as a fraction, since $|q|^2$ is real and therefore real invertible while commuting with every quaternion.

Lemma 4.4. *Let $v, w \in \mathrm{Im}\mathbb{H}$. Then*

$$vw = -\underbrace{\langle v, w\rangle}_{\in\mathbb{R}} + \underbrace{v \times w}_{\in \mathrm{Im}\mathbb{H}} \in \mathbb{H}.$$

Proof.

$$\begin{aligned}&(v_1\mathbb{i} + v_2\mathbb{j} + v_3\mathbb{k})(w_1\mathbb{i} + w_2\mathbb{j} + w_3\mathbb{k})\\ &= -v_1w_1 - v_2w_2 - v_3w_3 + (v_2w_3 - v_3w_2)\mathbb{i} + (v_3w_1 - v_1w_3)\mathbb{j} + (v_1w_2 - v_2w_1)\mathbb{k}.\end{aligned}$$

□

So we get the cross product and the scalar product of $v, w \in \mathrm{Im}\mathbb{H}$ in terms of commutator and anti-commutator.

$$\begin{aligned}v \times w &= \frac{1}{2}(vw - wv) =: \frac{1}{2}[v, w]\\ \langle v, w\rangle &= -\frac{1}{2}(vw + wv)\end{aligned}$$

In particular, two imaginary non-vanishing quaternions $v, w \neq 0$ are parallel if and only if they commute, and they are perpendicular if and only if they anti-commute:

$$\begin{aligned}vw - wv = 0 &\Leftrightarrow v \times w = 0 \Leftrightarrow v \parallel w\\ vw + wv = 0 &\Leftrightarrow \langle v, w\rangle = 0 \Leftrightarrow v \perp w\end{aligned}$$

Lemma 4.5. *Unitary quaternions $q \in \mathbb{H}_1$ can be parametrized as*

$$q = \cos\alpha + (\sin\alpha)n,$$

where $n \in \mathrm{Im}\mathbb{H}$ with $|n| = 1$ and $\alpha \in [0, \pi]$.

Proof. For $q \in \mathbb{H}_1$ we can write $\mathrm{Re}q = q_0 \in \mathbb{R}$ and $\mathrm{Im}q = cn$ with $c \geqslant 0$, $n \in \mathrm{Im}\mathbb{H}$, $|n| = 1$. Then

$$1 = |q|^2 = (q_0 + cn)(q_0 - cn) = q_0^2 + c^2$$

which can be parametrized as

$$\begin{aligned}q_0 &= \cos\alpha\\ c &= \sin\alpha\end{aligned}$$

with $\alpha \in [0, \pi]$. □

Remark 4.4. This parametrization is a double covering since

$$q(-\alpha, -n) = q(\alpha, n).$$

Proposition 4.6 (quaternionic rotation in $\mathbb{R}^3$)**.** *For $q \in \mathbb{H}_1$, $q = \cos\alpha + (\sin\alpha)n$, $n \in \mathrm{Im}\mathbb{H}$, $|n| = 1$, $\alpha \in [0, \pi]$ the map $\mathcal{R}_q : \mathbb{R}^3 \to \mathbb{R}^3$ given by*

$$\mathcal{R}_q(v) \coloneqq qvq^{-1}$$

is a rotation about the axis n by the angle 2α.[17]

[17] Instead of $q \in \mathbb{H}_1$ one can take $q \in \mathbb{H}_*$, since the absolute value of q cancels in qvq^{-1}.

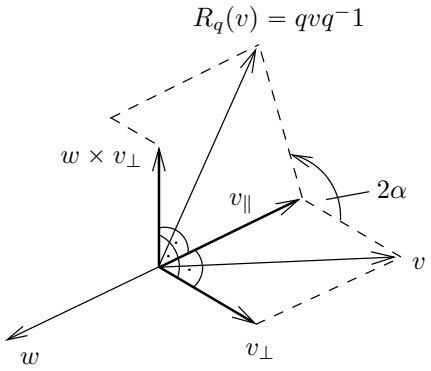

Figure 4.4. Decomposition of a vector v into its part along the rotation axis and along the orthogonal complement.

Proof. Decompose $v \in \mathrm{Im}\mathbb{H}$ into the part parallel and the part perpendicular to n, i.e.

$$v = v_\parallel + v_\perp,$$

where $v_\parallel w = w v_\parallel$ and $v_\perp w = -w v_\perp$. Then

$$\begin{aligned} q v_\parallel q^{-1} &= v_\parallel \\ q v_\perp q^{-1} &= (\cos\alpha + (\sin\alpha)n) v_\perp (\cos\alpha - (\sin\alpha)n) \\ &= (\cos^2\alpha - \sin^2\alpha 2(\cos\alpha\sin\alpha)n) v_\perp \\ &= (\cos 2\alpha) v_\perp + (\sin 2\alpha) w \times v_\perp. \end{aligned}$$

□

Remark 4.5. The map $\mathbb{H}_1 \to \mathrm{SO}(3), \quad q \mapsto \mathcal{R}_q$ is a double covering of $\mathrm{SO}(3)$ since

$$\mathcal{R}_{-q} = \mathcal{R}_q.$$

Multiplication of unitary quaternions corresponds to the composition of rotations

$$\mathcal{R}_{q_2 q_1} = \mathcal{R}_{q_2} \circ \mathcal{R}_{q_1},$$

i.e. multiplication in $\mathrm{SO}(3)$.

An *Euclidean motion* is a composition of rotation and translation:

$$v \mapsto q v q^{-1} + p, \quad v \in \mathrm{Im}\mathbb{H},$$

where $q \in \mathbb{H}_1$, $p \in \mathrm{Im}\mathbb{H}$. Consider an *Euclidean flow*

$$\Phi_t(v) = q(t) v q(t)^{-1} + p(t), \quad t \in \mathbb{R}.$$

The infinitesimal generator of this flow

$$\varphi_t(\Phi_t(v)) \coloneqq \frac{\mathrm{d}}{\mathrm{d}t}\Phi_t(v)$$

gives a time-dependent vector field which is called an *infinitesimal Euclidean motion*.

Corollary 4.7 (Infinitesimal Euclidean motions)**.** *Infinitesimal Euclidean motions are vector fields of the form*

$$v \mapsto \frac{1}{2}[a, v] + b = a \times v + b, \quad v \in \mathrm{Im}\mathbb{H},$$

where $a, b \in \mathrm{Im}\mathbb{H}$ *are called the angular and translational velocity.*

Proof. We have to compute the time derivative of an Euclidean flow

$$\begin{aligned}\frac{\mathrm{d}}{\mathrm{d}t}\Phi_t(v) &= (q(t)vq(t)^{-1})' + p'(t)\\ &= q'vq^{-1} - qv(q^{-1})' + p'\\ &= q'vq^{-1} - qvq^{-1}q'q^{-1} + p'\\ &= [q'q^{-1}, \Phi_t(v)] + p' - [q'q^{-1}, p]\\ &= \frac{1}{2}[a(t), \Phi_t(v)] + b(t),\end{aligned}$$

where we set $a(t) \coloneqq 2q'(t)q^{-1}(t) \in \mathrm{Im}\mathbb{H}$ and $b(t) \coloneqq p'(t) - \frac{1}{2}[a(t), p(t)] \in \mathrm{Im}\mathbb{H}$. □

Conversely, given a one-parameter family of infinitesimal Euclidean motions

$$\varphi_t(v) = a(t) \times v + b(t),$$

there exists an essentially unique corresponding one-parameter family of Euclidean motions $\Phi_t(v)$ which is the flow generated by $\varphi_t(v)$.
It can be obtained by integrating the quaternionic linear differential equations

$$\begin{aligned}q' &= \frac{1}{2}aq\\ p' &= b + \frac{1}{2}[a, p].\end{aligned}$$

This completes the proof of Corollary 4.3.

4.3 Discrete elastic curves

We consider discrete arc length parametrized curves

$$\gamma : I \to \mathbb{R}^3, \quad T_k = \gamma_{k+1} - \gamma_k, \quad |T_k| = 1.$$

What is the proper bending energy for discrete elastica?

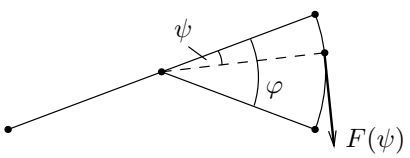

Figure 4.5. Bending energy as the integral of the bending force.

Assume that the bending force at an inner vertex $k \in I$ (depending on the bending angle φ_k) is proportional to the curvature

$$\kappa_k = 2 \tan \frac{\varphi_k}{2}$$

we defined for discrete arc length parametrized curves.
Then we obtain the corresponding local energy at vertex k

$$\begin{aligned}\int_0^{\varphi_k} \kappa(\psi) \mathrm{d}\psi &= 2 \int_0^{\varphi_k} \tan \frac{\psi}{2} \mathrm{d}\psi = -4 \log \cos \frac{\psi}{2} \Big|_0^{\varphi_k} = -4 \log \cos \frac{\varphi_k}{2} \\ &= -2 \log \cos^2 \frac{\varphi_k}{2} = 2 \log \left(1 + \tan^2 \frac{\varphi_k}{2}\right) = 2 \log \left(1 + \frac{\kappa_k^2}{4}\right).\end{aligned}$$

We define the local bending energy

$$\mathcal{E}_k \coloneqq \log \left(1 + \frac{\kappa_k^2}{4}\right).$$

With

$$\frac{1}{2} \left\| T_k + T_{k-1} \right\|^2 = 1 + \langle T_k, T_{k-1} \rangle = 1 + \cos \varphi_k = 2 \cos^2 \frac{\varphi_k}{2}$$

we find alternate expressions

$$\mathcal{E}_k = -\log \left(1 + \langle T_k, T_{k-1} \rangle\right) + \log 2 = -log \left\| T_k + T_{k-1} \right\|^2 + \log 4.$$

Remark 4.6.

- The discrete local bending energy is invariant under Euclidean transformations.
- In the smooth limit we have $\varphi_k \to 0$ and therefore $\kappa_k \to 0$. We find that

  $$\mathcal{E}_k = \log \left(1 + \frac{\kappa_k^2}{4}\right) = \frac{\kappa_k^2}{4} + o(\kappa^2)$$

  is quadratic in the curvature.
- At singular vertices we have $\varphi_k \to \pi$ and therefore $\kappa_k \to \infty$. We obtain

  $$\mathcal{E}_k = \log \left(1 + \frac{\kappa_k^2}{4}\right) \to \infty.$$

  So discrete elastic curves are regular.

For finite curves with $I = [0, n]$ we consider variations of the total energy on $\mathcal{C}_I^{\mathrm{arc}}$

$$\sum_{k=1}^{n-1} \mathcal{E}_k,$$

where the sum goes over all "inner vertices" of I.
Admissible variations should fix end points and end tangent vectors and preserve the arc length.

Definition 4.2 (Discrete elastic curve)**.** A discrete arc length parametrized curve $\gamma : I \to \mathbb{R}^3$, $I = [0, n] \subset \mathbb{Z}$ with tangent vector $T : I \to \mathbb{R}^3$, $T_k = \gamma_{k+1} - \gamma_k$ is called *discrete elastic curve* if it is a critical point of the functional

$$\mathcal{E}[\gamma] \coloneqq \sum_{k=1}^{n-1} \log\left(1 + \frac{\kappa_k^2}{4}\right) \sim \sum_{k=1}^{n-1} \log\left(1 + \langle T_k, T_{k-1}\rangle\right) \sim \sum_{k=1}^{n-1} \log \|T_k + T_{k-1}\|$$

under variations on $\mathcal{C}_I^{\text{arc}}$ with fixed $\gamma_0, \gamma_n, T_0, T_{n-1}$, where $\kappa_k = 2\tan\frac{\varphi_k}{2}$ is the discrete curvature. The $\sim$ denotes equivalent functionals, i.e. functionals which have the same critical points.

Remark 4.7.

- Closed arc length parametrized curves $I = \mathbb{Z}_{n-1}$ can be treated as a special case of $I = [0, n]$ with $\gamma_0 = \gamma_{n-1}, \gamma_1 = \gamma_n$ and therefore $T_{n-1} = T_0$.

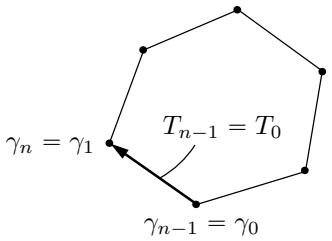

Figure 4.6. Closed elastic curves as a special case.

  We note that factorizing by Euclidean motions we can get rid of any fixed points and directions in this case.

- Factorizing by translations we reformulate the variational problem in terms of $T : I \to \mathbb{R}^3$ only. Admissible variations of T have to
  - fix $T_0, T_{n-1} \in \mathbb{S}^2$,
  - satisfy $\sum_{k=0}^{n-1} T_k = \gamma_n - \gamma_0 \in \mathbb{R}^3$,
  - preserve $\|T_k\| = 1$ for $i = 0, \dots, n-1$.
- Functionals are functions of many variables in the discrete case. Applying that $T_0, T_{n-1} \in \mathbb{S}^2$ are fixed,

$$\mathcal{E}[T] = \mathcal{E}(T_0, \dots, T_{n-1}) = \mathcal{E}(T_1, \dots, T_{n-2})$$

  is a function of $3(n-2)$ variables which has to be varied under the constraints
  - $\sum_{k=1}^{n-2} T_k = const. \in \mathbb{R}^3$,
  - $\|T_k\| = 1$ for $i = 1, \dots, n-2$.

Theorem 4.8 (Euler-Lagrange equations for discrete elastic curve)**.** *A discrete arc length parametrized curve $\gamma : I \to \mathbb{R}^3$, $I = [0, n] \subset \mathbb{Z}$ is a discrete elastic curve if and only if there exists $a, b \in \mathbb{R}^3$ such that*

$$\frac{T_k \times T_{k-1}}{1 + \langle T_k, T_{k+1}\rangle} = a \times \gamma_k + b, \qquad k = 1, \dots, n-1,$$

where $T_k = \gamma_{k+1} - \gamma_k$.

Proof. We want to derive equations for the critical points of

$$\mathcal{E}(T_1, \dots, T_{n-2}) = \sum_{k=1}^{n-1} \log\left(1 + \langle T_k, T_{k-1}\rangle\right)$$

under the constraints

- $\sum_{k=1}^{n-2} T_k = const. \in \mathbb{R}^3$,
- $\|T_k\| = 1$ for $k = 1, \dots, n-2$.

We implement these constraints using Lagrange-multipliers $c_k \in \mathbb{R}, k = 1, \dots, n-2$ and $a = (a_1, a_2, a_3) \in \mathbb{R}^3$, and obtain

$$\mathcal{E}_\lambda \coloneqq \sum_{k=1}^{n-1} \log\left(1 + \langle T_k, T_{k-1}\rangle\right) - \sum_{k=1}^{n-2} \left(c_k \langle T_k, T_k\rangle + \langle a, T_k\rangle\right).$$

The corresponding Euler-Lagrange equations are

$$\nabla_{T_k} \mathcal{E}_\lambda = 0, \qquad k = 1 \dots, n-2.$$

Using $\nabla_{T_k}\langle T_k, a\rangle = b$ and $\nabla_{T_k}\langle T_k, T_k\rangle = 2T_k$, we find for $k = 1, \dots, n-2$

$$\nabla_{T_k} \mathcal{E}_\lambda = \frac{T_{k-1}}{1 + \langle T_k, T_{k-1}\rangle} + \frac{T_{k+1}}{1 + \langle T_{k+1}, T_k\rangle} - 2c_k T_k - a = 0. \tag{4.2}$$

Taking the cross-product with T_k, we obtain

$$\frac{T_{k+1} \times T_k}{1 + \langle T_{k+1}, T_k\rangle} - \frac{T_{k-1} \times T_k}{1 + \langle T_k, T_{k-1}\rangle} = a \times T_k = a \times (\gamma_{k+1} - \gamma_k), \tag{4.3}$$

which is equivalent to

$$\frac{T_k \times T_{k-1}}{1 + \langle T_k, T_{k+1}\rangle} - a \times \gamma_k = b = const. \in \mathbb{R}^3.$$

Noting that (4.2) and (4.3) are equivalent, we obtain the claim. □

Remark 4.8.

- If we identify the left-hand side of the Euler-Lagrange equations as the discrete Heisenberg flow, which we denote by ∂_t, we have shown

$$\begin{aligned} \gamma \text{ discrete elastica } &\Leftrightarrow \partial_t \gamma_k = a \times \gamma_k + b \\ &\Leftrightarrow \partial_t T_k = a \times T_k, \end{aligned}$$

  where the second line are the equivalent equations in terms of the tangent vector which are written down explicitly in (4.3).

- Recalling the smooth limit of the Heisenberg flow (3.12) and (3.13), we obtain for the smooth limit of the Euler-Lagrange equations

$$\begin{aligned} T' \times T = a \times \gamma + b &\Leftrightarrow \gamma'' \times \gamma' = a \times \gamma + b \\ &\Leftrightarrow T'' \times T = a \times T, \end{aligned}$$

  which are the Euler-Lagrange equations for smooth elastic curves as stated in Theorem 4.2.

Corollary 4.9. *A discrete arc length parametrized curve is a discrete elastic curve if and only if the Heisenberg flow preserves its form, i.e. under the action of the Heisenberg flow the curve evolves by an Euclidean motion.*

Proof. Same as in the smooth case. □

Definition 4.3 (discrete spherical pendulum)**.** A *discrete spherical pendulum* is a mechanical system on $\mathbb{S}^2$ with discrete time and Lagrangian

$$\mathcal{L}_k \coloneqq \log\left(1 + \langle T_k, T_{k-1}\rangle\right) - \langle a, T_k\rangle$$

with some $a \in \mathbb{R}^3$. This means that the trajectories $T : I \to \mathbb{S}^2$ are critical points of the action functional $\mathcal{S} = \sum_k \mathcal{L}_k$.

Remark 4.9. The terms $\mathcal{T}_k \coloneqq \log\left(1 + \langle T_k, T_{k-1}\rangle\right)$ and $\mathcal{U}_k \coloneqq \langle a, T_k\rangle$ are interpreted as kinetic and potential energies of the pendulum with gravitation vector a. In the smooth limit

$$\begin{aligned}\mathcal{U}_k &\to \langle a, T\rangle,\\ \mathcal{T}_k &\sim \log\left(1 + \frac{\kappa_k}{4}\right) = \frac{\kappa_k^2}{4} + o(\kappa_k^2),\end{aligned}$$

where $\kappa_k \to \|T'\|$. So in the smooth limit the kinetic energy is quadratic in the velocity.

From this definition we immediately obtain a discrete analog of Theorem 4.1.

Theorem 4.10 (Kirchhoff analogy for discrete elastic curves)**.** *A discrete arc length parametrized curve $\gamma : I \to \mathbb{R}^3$ is a discrete elastic curve if and only if its tangent vector $T_k = \gamma_{k+1} - \gamma_k$ describes the evolution of a discrete spherical pendulum.*

Proof. Analogous to the proof of Theorem 4.1. □

4.4 Moving frames and framed curves

Let $T, N, B : I \to \mathbb{R}^3$ be three smooth maps such that $T(s), N(s), B(s)$ is an orthonormal basis for any $s \in I$, i.e. the matrix $\mathcal{R}(s) \coloneqq (T(s), N(s), B(s)) \in \mathrm{SO}(3)$. We can think of it as a coordinate frame fixed inside a rigid body which rotates around some fixed point. In this interpretation we call (T, N, B) the *body frame*.

Definition 4.4 (moving frame)**.** Let $I \subset \mathbb{R}$ be an interval. A *moving frame* is a differentiable map

$$\mathcal{R} : I \to \mathrm{SO}(3).$$

This is a special case of an Euclidean motion where the rotation $\mathcal{R}$ describes the movement of the frame with respect to the stationary coordinate system (e_1, e_2, e_3):

$$T = \mathcal{R}e_1, \quad N = \mathcal{R}e_2, \quad B = \mathcal{R}e_3.$$

On the other hand $\mathcal{R}$ is the coordinate transformation mapping points

$$X = X_1 e_1 + X_2 e_2 + X_3 e_3$$

in the rotating body frame to points

$$x(s) = X_1 T(s) + X_2 N(s) + X_3 B(s) = x_1(s) e_1 + x_2(s) e_2 + x_3(s) e_3$$

in the stationary coordinate system by

$$x = \mathcal{R} X.$$

We usually suppose the frame to be aligned with the fixed coordinate system for $s = 0$, i.e. $\mathcal{R}(0) = \mathrm{id}_{\mathbb{R}^3}$.

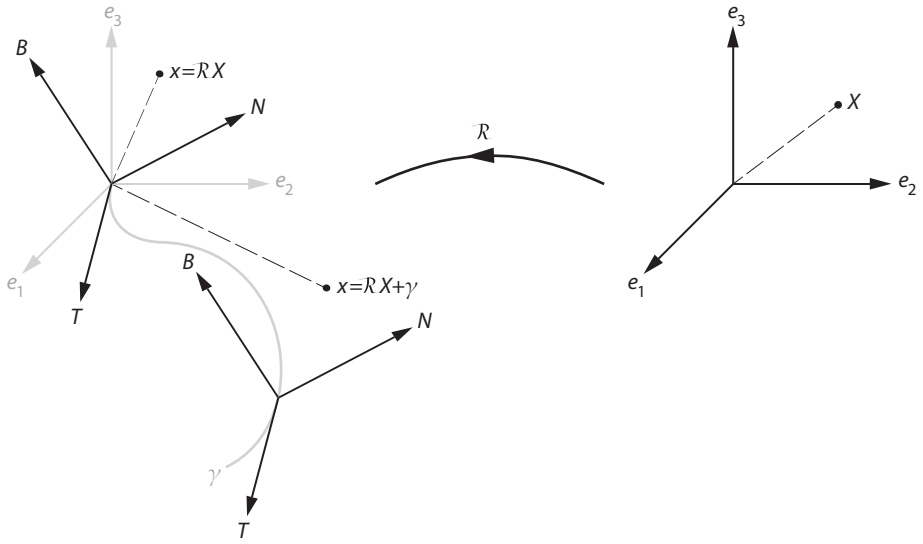

Figure 4.7. $\mathcal{R}$ describes the rotation of a moving frame. It is the coordinate transformations from the rotating coordinate system to a stationary coordinate system. The translational part along the corresponding framed curve can be obtained by integration.

Curvatures κ_1, κ_2 and torsion τ of a frame $\mathcal{R} = (T, N, B)$ are defined as

$$\begin{aligned} \kappa_1 &\coloneqq \langle T', N \rangle \\ \kappa_2 &\coloneqq \langle T', B \rangle \\ \tau &\coloneqq \langle N', B \rangle. \end{aligned}$$

Remark 4.10. A moving frame can be recovered from the differentiable data $\kappa_1, \kappa_2, \tau : [0, L] \to \mathbb{R}$ up to rotation using the *frame equations*

$$\begin{pmatrix} T \\ N \\ B \end{pmatrix}' = \underbrace{\begin{pmatrix} 0 & \kappa_1 & \kappa_2 \\ -\kappa_1 & 0 & \tau \\ -\kappa_2 & -\tau & 0 \end{pmatrix}}_{=:A} \begin{pmatrix} T \\ N \\ B \end{pmatrix}. \tag{4.4}$$

Definition 4.5 (framed curve)**.** A *framed curve* is given by an arc length parametrized curve $\gamma : I \to \mathbb{R}^3$, $T \coloneqq \gamma'$ together with a unit normal field $N : I \to \mathbb{S}^2$, i.e. $\langle N, T\rangle = 0$.

A framed curve is carrying a moving frame $\mathcal{R} : I \to \mathrm{SO}(3)$, $\mathcal{R} \coloneqq (T, N, B)$, where $B \coloneqq T \times N$. Vice versa, given an orthonormal frame we can recover the curve γ (up to translation) by integration of T.
So framed curves and moving frames are in one-to-one correspondence.
The curvature $\kappa \coloneqq \|\gamma''\| = \|T'\|$ of the curve γ satisfies

$$\kappa^2 = \kappa_1^2 + \kappa_2^2.$$

for any frame.

Remark 4.11. The transformation $x = \mathcal{R}X$ captures only the rotation of the frame, not the translation along the curve. The coordinates in the moving frame –as it moves along the curve– are given by

$$x(s) = \mathcal{R}(s)X + \gamma(s),$$

where $\gamma = \int T$.

Using $\mathbb{H}_1$ as a double covering of $\mathrm{SO}(3)$ we apply the quaternionic description for Euclidean motions. We identify $\mathcal{R} : I \to \mathrm{SO}(3)$ with[18]

$$\Phi : I \to \mathbb{H}_1,$$

i.e.

$$\mathcal{R} \in \mathrm{SO}(3) \text{ acts on } X \in \mathbb{R}^3 \text{ by } x = \mathcal{R}X$$

becomes

$$\Phi \in \mathbb{H}_1 \text{ acts on } X \in \mathrm{Im}\mathbb{H} \text{ by } x = \Phi X \Phi^{-1}.$$

Then the movement of some static point $X = X_1\mathbb{i} + X_2\mathbb{j} + X_3\mathbb{k} \in \mathrm{Im}\mathbb{H}$ in the rotating frame as it is seen in the stationary frame is described by the differential equation

$$\begin{aligned} x' &= \Phi' X \Phi^{-1} - \Phi X \Phi^{-1}\Phi'\Phi^{-1} \\ &= [\Phi'\Phi^{-1}, x] = \frac{1}{2}[\omega, x] = \omega \times x, \end{aligned}$$

where $\omega \coloneqq 2\Phi'\Phi^{-1}$, i.e.

$$\Phi' = \frac{1}{2}\omega\Phi. \tag{4.5}$$

Here, ω is called the *angular velocity* in the stationary frame. In the rotating frame the angular velocity is seen as Ω where $\omega = \Phi\Omega\Phi^{-1}$, i.e. $\Omega = 2\Phi^{-1}\Phi'$. The movement of the frame in terms of Ω can be expressed as

$$\Phi' = \frac{1}{2}\Phi\Omega. \tag{4.6}$$

[18]Note that Φ is not the Euclidean flow as before, but the quaternion –denoted by q before– corresponding to the rotation of the flow.

Remark 4.12. In this form it corresponds directly to (4.4). Indeed,

$$\begin{aligned}(4.4) &\Leftrightarrow (T,N,B)'^T = A(T,N,B)^T\\ &\Leftrightarrow \mathcal{R}'^T = A\mathcal{R}^T\\ &\Leftrightarrow \mathcal{R}' = \mathcal{R}A^T.\end{aligned}$$

The components κ_1, κ_2, τ of $A \in \mathrm{so}(3)$ correspond to the components of $\Omega \in \mathrm{Im}\mathbb{H}$ as we will see below.

For the basis vectors of the frame

$$T, N, B : I \to \mathrm{Im}\mathbb{H}$$

we have

$$T = \Phi \mathbb{i} \Phi^{-1}, \quad N = \Phi \mathbb{j} \Phi^{-1}, \quad B = \Phi \mathbb{k} \Phi^{-1},$$

which becomes

$$\begin{aligned}T' &= \frac{1}{2}[\omega, T] = \omega \times T\\ N' &= \frac{1}{2}[\omega, N] = \omega \times N\\ B' &= \frac{1}{2}[\omega, B] = \omega \times B\end{aligned} \tag{4.7}$$

upon differentiation. From here we obtain

$$\begin{aligned}\kappa_1 &= \langle T', N\rangle = \langle \omega \times T, N\rangle = \langle T \times N, \omega\rangle = \langle B, \omega\rangle = \langle e_3, \Omega\rangle\\ \kappa_2 &= \langle T', B\rangle = \langle \omega \times T, B\rangle = \langle T \times B, \omega\rangle = -\langle N, \omega\rangle = -\langle e_2, \Omega\rangle\\ \tau &= \langle N', B\rangle = \langle \omega \times N, B\rangle = \langle N \times B, \omega\rangle = \langle T, \omega\rangle = \langle e_1, \Omega\rangle.\end{aligned}$$

Remark 4.13. (4.4), (4.5), (4.6), (4.7) are equivalent versions of the frame equations using different choices within the identifications

$$\mathrm{SO}(3) \;\leftrightarrow\; \mathbb{H}_1, \quad \mathbb{R}^3 \;\leftrightarrow\; \mathrm{so}(3) \;\leftrightarrow\; \mathrm{Im}\mathbb{H}$$

or different coordinate systems to express the angular velocity. They describe the relation between the rotating motion and its angular velocity as the infinitesimal generator.

4.4.1 The Lagrange top

The *Lagrange top* is a rigid body with a symmetry axis that rotates around a fixed point on its symmetry axis in a homogeneous gravitational field. Let $\Phi \cong (T, N, B) : I \to \mathrm{SO}(3)$ be the rotating frame fixed within the body such that T is aligned with the axis of symmetry. In this body frame the tensor of inertia is diagonal and looks like

$$J = \begin{pmatrix}\alpha & 0 & 0\\ 0 & 1 & 0\\ 0 & 0 & 1\end{pmatrix}$$

with some $\alpha > 0$. The kinetic energy of the Lagrange-top is

$$\begin{aligned}\mathcal{T} = \langle \Omega, J\Omega\rangle &= \alpha\langle e_1, \Omega\rangle^2 + \langle e_2, \Omega\rangle^2 + \langle e_3, \Omega\rangle^2\\ &= \alpha\langle T, \omega\rangle^2 + \langle N, \omega\rangle^2 + \langle B, \omega\rangle^2\\ &= \alpha\tau^2 + \kappa^2.\end{aligned} \tag{4.8}$$

Alternatively, in terms of T and ω only:

$$\begin{aligned}\langle \Omega, J\Omega\rangle &= \langle \Omega, \Omega\rangle - \langle \Omega, (J-\mathrm{id})\Omega\rangle \\ &= \langle \omega, \omega\rangle + (\alpha-1)\langle T, \omega\rangle^2.\end{aligned} \tag{4.9}$$

For symmetry reasons the Lagrange top has its barycenter on the axis of symmetry, which goes through T. So its potential energy is given by

$$\mathcal{U} = -2\langle a, T\rangle$$

with some $a \in \mathbb{R}^3$.

We obtain the action functional for the Lagrange top

$$\mathcal{S}[\Phi] = \int_0^L \left(\langle \omega, \omega\rangle + (\alpha-1)\langle \omega, T\rangle^2 + 2\langle a, T\rangle\right) \mathrm{d}s. \tag{4.10}$$

Remark 4.14. Note that the functional $\mathcal{S}[\Phi]$ originally depends on $\Phi : I \to \mathbb{H}_1$. In particular it depends on its derivative $\varphi(s) = \Phi'(s) \in \mathrm{T}_{\Phi(s)}\mathbb{H}_1$, or equivalently[19] on $\omega(s) = 2\Phi'(s)\Phi^{-1}(s) \in \mathrm{Im}\mathbb{H}$.
If we want to treat (Φ, φ) as independent variables,[20] we have to impose an additional constraint characterizing the relation $\Phi' = \varphi$. In terms of (Φ, ω) this is $\Phi' = \frac{1}{2}\omega\Phi$. This leads to the phase space $\mathbb{H}_1 \times \mathrm{Im}\mathbb{H}$. Since Φ enters $\mathcal{S}$ only in terms of T we can of course reduce this further, replacing $\mathbb{H}_1$ by $\mathbb{S}^2$.
Finally we end up with a functional $\mathcal{S}[T, \omega]$ on the phase space $\mathbb{S}^2 \times \mathbb{R}^3$ and the additional condition $T' = \omega \times T$.

Remark 4.15. From now on we will not distinguish between $\mathcal{R} \in \mathrm{SO}(3)$ and $\Phi \in \mathbb{H}_1$ anymore.

4.5 Smooth elastic rods

Elastic rods are described by framed curves

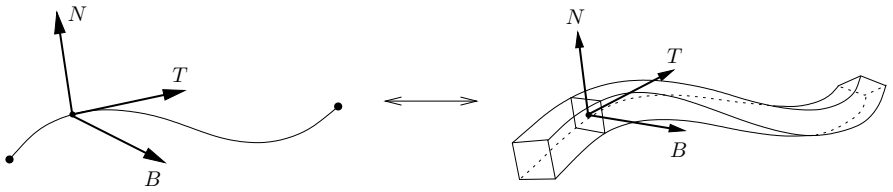

Figure 4.8. Elastic rods as framed curves

We extend variations of the curve $\gamma : [0, L] \to \mathbb{R}^3$ with fixed endpoints and fixed length to the frame $\Phi : [0, L] \to \mathrm{SO}(3)$,

[19] By identifying all tangent spaces of $\mathbb{H}_1$ with $\mathrm{Im}\mathbb{H}$ by right translation.

[20] This means replacing the configuration space SO(3) by the phase space TSO(3) which is the tangent bundle.

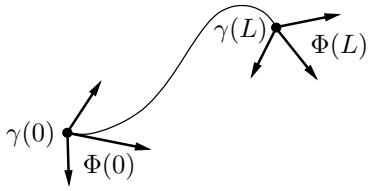

Figure 4.9. Curve with fixed end-frames.

which leads to admissible variations that

- fix $\gamma(0)$, $\gamma(L) \in \mathbb{R}^3$,
- fix $\Phi(0)$, $\Phi(L) \in \mathrm{SO}(3)$,
- preserve orthonormality, i.e. $\Phi(s) \in \mathrm{SO}(3)$ for all $s \in [0, L]$, in particular preserve the arc length parametrization and therefore the length of the curve.

We complement the bending energy of γ by an adjustable torsion energy

$$\mathcal{E}[\Phi] \coloneqq \int_0^L \left(\kappa(s)^2 + \alpha\tau(s)^2\right) \mathrm{d}s$$

with some *torsion coefficient* $\alpha \neq 0$.

Definition 4.6 (Elastic rod)**.** An (isotropic) *elastic rod* is a framed curve (γ, Φ) which is a critical point of the energy functional $\mathcal{E}$ under the described admissible variations.

If we want to formulate the variational problem solely in terms of the moving frame $\Phi : [0, L] \to \mathrm{SO}(3)$, we have to impose the additional constraint

- $\int_0^L T(s)\mathrm{d}s = \gamma(L) - \gamma(L) \in \mathbb{R}^3$

again, to take the fixed endpoints of the curve into account.

We use

$$\kappa^2 + \alpha\tau^2 = \langle\omega, \omega\rangle + (\alpha - 1)\langle\omega, T\rangle^2$$

as follows from (4.8) and (4.9) to express the energy in terms of the angular velocity ω and T only, where $T' = \omega \times T$. Implementing the constraint for the fixed endpoints of the curve $\int_0^L T(s)\mathrm{d}s = const.$ via Lagrange-multiplicators, we finally obtain

$$\mathcal{E}_a[T, \omega] = \int_0^L \left(\langle\omega, \omega\rangle + (\alpha - 1)\langle\omega, T\rangle^2 + 2\langle a, T\rangle\right) \mathrm{d}s.$$

Recognizing the action functional (4.10) of the Lagrange top we formulate the Kirchhoff analogy for elastic rods.

Theorem 4.11 (Kirchhoff analogy for elastic rods)**.** *A arc length parametrized curve $\gamma : [0, L] \to \mathbb{R}^3$ with frame $\Phi : [0, L] \to \mathrm{SO}(3)$ is an elastic rod if and only if its tangent vector $T \coloneqq \gamma' : [0, L] \to \mathbb{S}^2$ describes the evolution of the symmetry axis of the Lagrange top with angular velocity $\omega : [0, L] \to \mathbb{R}^3$ of the frame Φ. The arc length parameter of the framed curve coincides with the time parameter of the top.*

To derive the Euler-Lagrange equations for elastic rods, we investigate how admissible variations of Φ look in terms of ω and T where $T' = \omega \times \Phi$.
Since $\mathbb{H}_1$ is a multiplicative (differentiable) group we can express all variations

$$\tilde{\Phi} : [0, L] \times (-\varepsilon, \varepsilon) \to \mathbb{H}_1$$

as

$$\tilde{\Phi}(s, t) = H(s, t)\Phi(s),$$

where

$$H : [0, L] \times (-\varepsilon, \varepsilon) \to \mathbb{H}_1$$

with $H(s, 0) = 1$, $H(0, t) = H(L, t) = 0$.

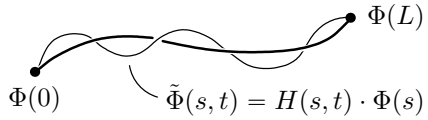

Figure 4.10. Variations of the frame Φ in terms of multiplication by a quaternion.

The variational vector fields along the curve are described by

$$\eta(s) \coloneqq \dot{\eta}(s, 0) = \frac{\partial H}{\partial t}(s, 0) \in \mathrm{Im}\mathbb{H} \qquad \big(\Rightarrow \eta(0) = \eta(L) = 0 \big),$$

which build a vector space.[21]

So admissible variations of $\omega(s) = 2\Phi'(s)\Phi^{-1}(s)$ become

$$\begin{aligned} \tilde{\omega}(s, t) &\coloneqq 2\tilde{\Phi}'(s, t)\tilde{\Phi}^{-1}(s, t) = 2(H\Phi)'(H\Phi)^{-1} \\ &= 2(H'\Phi + H\Phi')\Phi^{-1}H^{-1} = 2(H'\Phi + \frac{1}{2}H\omega\Phi)\Phi^{-1}H^{-1} \\ &= 2H'H^{-1} + H\omega H^{-1}, \end{aligned}$$

and the corresponding variational vector fields

$$\begin{aligned} \dot{\tilde{\omega}}(s, 0) &= \big(2\eta' H^{-1} - 2H'H^{-1}\eta H^{-1} + \eta\omega H^{-1} - H\omega H^{-1}\eta H^{-1}\big)\big|_{t=0} \\ &= 2\eta' + \eta\omega - \omega\eta = 2\eta' + [\eta, \omega] = 2(\eta' + \eta \times \omega). \end{aligned}$$

With $T(0) = \mathbb{i}$ the integral version of $T' = \omega \times T = \frac{1}{2}[\omega, T]$ is $T = \Phi\mathbb{i}\Phi^{-1}$. So admissible variations of T are

$$\tilde{T}(s, t) \coloneqq \tilde{\Phi}\mathbb{i}\tilde{\Phi}^{-1} = H\Phi\mathbb{i}\Phi^{-1}H^{-1} = HTH^{-1},$$

and the corresponding variational vector fields

$$\begin{aligned} \dot{\tilde{T}}(s, 0) &= \big(\eta T H^{-1} - HTH^{-1}\eta H^{-1}\big)\big|_{t=0} \\ &= \eta T - T\eta = [\eta, T] = 2\eta \times T. \end{aligned}$$

This describes admissible variations of $(T, \omega) : [0, L] \to \mathbb{S}^2 \times \mathbb{R}^3$.

[21] We denote partial derivatives w.r.t. s by $'$ and w.r.t. t by $\dot{}$

For the variation of the energy we obtain

$$\begin{aligned}
\frac{\mathrm{d}}{\mathrm{d}t}\Big|_{t=0} \mathcal{E}_a[\tilde{T},\tilde{\omega}] &= \int_0^L \frac{\partial}{\partial t}\Big|_{t=0} \Big(\langle\tilde{\omega},\tilde{\omega}\rangle + (\alpha-1)\langle\tilde{\omega},\tilde{T}\rangle^2 + 2\langle a,\tilde{T}\rangle\Big)\,\mathrm{d}s \\
&= 4\int_0^L \big(\langle\eta'+\eta\times\omega,\omega\rangle + (\alpha-1)\langle\omega,T\rangle(\langle\eta'+\eta\times\omega,T\rangle + \langle\omega,\eta\times T\rangle) \\
&\qquad + \langle a,\eta\times T\rangle\big)\mathrm{d}s \\
&= 4\int_0^L \big(\langle\eta',\omega\rangle + (\alpha-1)\langle\omega,T\rangle\langle\eta',T\rangle + \langle a,\eta\times T\rangle\big)\,\mathrm{d}s \\
&= 4\int_0^L \big(\langle\eta',-\omega+(1-\alpha)\tau T\rangle + \langle\eta,T\times a\rangle\big)\mathrm{d}s \\
&= 4\int_0^L \langle\eta,-\omega'+(1-\alpha)(\tau' T+\tau T') + T\times a\rangle\mathrm{d}s,
\end{aligned}$$

where we used partial integration with vanishing boundary terms due to $\eta(0) = \eta(L) = 0$. So the Euler-Lagrange equations are given by

$$\begin{cases} T' &= \omega\times T \\ \omega' &= (1-\alpha)(\tau' T+\tau T') + T\times a. \end{cases}$$

Further simplification is still possible by the following Lemma.

Lemma 4.12. *The torsion τ of an elastic rod is constant.*

Proof. We have $\tau = \langle\omega, T\rangle$. So

$$\tau' = \langle\omega', T\rangle + \langle\omega, T'\rangle = (1-\alpha)\tau',$$

where we plugged in the Euler-Lagrange equations for T' and ω'. So we get $\tau' = 0$ since $\alpha \neq 0$ for elastic rods. □

Eventually we arrive at the final version of the Euler-Lagrange equations for elastic rods.

Theorem 4.13 (Euler-Lagrange equations for elastic rods)**.** *An arc length parametrized curve $\gamma : [0, L] \to \mathbb{R}^3$ with frame $\Phi : [0, L] \to \mathbb{R}^3$ is an elastic rod with torsion coefficient α if and only if its torsion τ is constant ($\tau' = 0$) and one of the following conditions is satisfied:*

(i) There is $a \in \mathbb{R}^3$ such that

$$\begin{cases} T' &= \omega\times T \\ \omega' &= (1-\alpha)\tau T' + T\times a, \end{cases}$$

where $T = \gamma'$ is the tangent vector and $\omega = 2\Phi'\Phi^{-1}$ the angular velocity of the frame.

(ii) There is $a, b \in \mathbb{R}^3$ such that

$$\gamma''\times\gamma' + c\gamma' = a\times\gamma + b.$$

(iii) There is $a \in \mathbb{R}^3$ such that

$$T'' \times T + cT = a \times T,$$

where $c \coloneqq -\alpha\tau$.

Proof. We are left to show the equivalence of these three equations.

(ii)⇔(iii) By integration/differentiation.

(i)⇒(ii) Integrating $\omega' = (1-\alpha)\tau T' + T \times a$, we obtain

$$\omega + b = (1-\alpha)\tau T + \gamma \times a.$$

From this and $T' = \omega \times T$ we get

$$\begin{aligned} T' \times T = (\omega \times T) \times T &= \langle \omega, T \rangle T - \omega \\ &= \tau T - \omega = \alpha\tau T + a \times \gamma + b. \end{aligned}$$

(iii)⇒(i) Define ω by $T' = \omega \times T$ and $\langle \omega, T \rangle = \tau$.[22]
Then $T'' = \omega' \times T + \omega \times T'$. So

$$T'' \times T = \langle \omega', T \rangle T - \omega' + \langle \omega, T \rangle T' = \tau T' - \omega'.$$

On the other hand we have

$$T'' \times T = \tau\alpha T' + a \times T.$$

Together this implies

$$\omega' = (1-\alpha)\tau T' + T \times a.$$

□

We identify the left hand sides of (ii) and (iii) as a linear combination of the Heisenberg flow ∂_t and the tangent flow ∂_x, i.e.

$$(\partial_t + c\partial_x)\gamma = a \times \gamma + b$$

and

$$(\partial_t + c\partial_x)T = a \times T.$$

Corollary 4.14. *A framed curve is an elastic rod if and only if a linear combination of the Heisenberg flow and the tangent flow with non-zero coefficients preserves its form, i.e. under the action of this combined flow the curve evolves by an Euclidean motion.*

[22] In quaternions this is $\omega \coloneqq (T' - \tau)T^{-1}$.

Remark 4.16 (anisotropic elastic rods). The theory can be generalized to anisotropic elastic rods by using an anisotropic bending energy

$$\mathcal{E} = \int \left(\alpha_1 \kappa_1^2 + \alpha_2 \kappa_2^2 + \alpha_3 \tau^2\right) \mathrm{d}s.$$

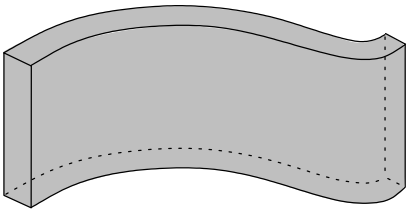

Figure 4.11. Anisotropic rod. The bending energy depends on the cross section.

4.6 Discrete elastic rods

We use the characterization in terms of Heisenberg flow and tangent flow to obtain a definition for discrete elastic rods.

Definition 4.7 (Discrete elastic rods)**.** A discrete arc length parametrized curve $\gamma : I \to \mathbb{R}^3$ is called *discrete elastic rod* if it evolves under a linear combination $(\partial_t + c\partial_x)$, $c \neq 0$ of the discrete Heisenberg flow ∂_t and the discrete tangent flow ∂_x by an Euclidean motion, i.e.

- there is $a, b \in \mathbb{R}^3$ and $c \neq 0$ such that

$$\frac{T_k \times T_{k-1}}{1 + \langle T_k, T_{k-1} \rangle} + c \frac{T_k + T_{k-1}}{1 + \langle T_k, T_{k-1} \rangle} = a \times \gamma_k + b,$$

or equivalently

- there is $a \in \mathbb{R}^3$ and $c \neq 0$ such that

$$\left(\frac{T_{k+1}}{1 + \langle T_{k+1}, T_k \rangle} - \frac{T_{k-1}}{1 + \langle T_k, T_{k-1} \rangle} \right) \times T_k + c \left(\frac{T_{k+1} + T_k}{1 + \langle T_{k+1}, T_k \rangle} + \frac{T_k + T_{k-1}}{1 + \langle T_k, T_{k-1} \rangle} \right) = a \times T_k.$$

Remark 4.17. These equations go to the Euler-Lagrange equations for smooth elastic rods since the discrete Heisenberg flow and discrete tangent flow go to their corresponding smooth counterparts, which we have seen already.

5 Darboux transforms

5.1 Smooth tractrix and Darboux transform

Assume that a point moves along a curve γ and pulls an interval $(\gamma, \hat{\gamma})$ so that the distance $\|\hat{\gamma} - \gamma\|$ ist constant, and the velocity vector $\hat{\gamma}'$ is parallel to $\gamma - \hat{\gamma}$. The curve $\hat{\gamma}$ can be thought of as a trajectory of the second wheel of a bicycle whose first wheel moves along the curve γ.

Definition 5.1 (Smooth tractrix)**.** Let $\gamma : \mathbb{R} \supseteq I \to \mathbb{R}^2$ be a smooth planar curve. A curve $\hat{\gamma} : I \to \mathbb{R}^2$ is called a *tractrix* of γ, if the difference $v := \hat{\gamma} - \gamma$ satisfies

$$\|v\| = const. \qquad \text{and} \qquad \hat{\gamma}' \parallel v.$$

Lemma 5.1. *Let γ be arclength parameterized, let $\hat{\gamma}$ be a tractrix of γ, and let $v = \hat{\gamma} - \gamma$. Then the curve $\tilde{\gamma} := \gamma + 2v$ is also arclength parametrized and $\hat{\gamma}$ is a tractrix of $\tilde{\gamma}$ as well.*

Proof. We will show that $\|\tilde{\gamma}'\|^2 - \|\gamma'\|^2 = 0$. Note that

$$\|\tilde{\gamma}'\|^2 - \|\gamma'\|^2 = \langle \tilde{\gamma}' + \gamma', \tilde{\gamma}' - \gamma' \rangle = 2\langle \tilde{\gamma}' + \gamma', v' \rangle.$$

But $\frac{1}{2}(\tilde{\gamma} + \gamma) = \gamma + v$ is the tractrix of γ. The derivative $\tilde{\gamma}' + \gamma'$ is therefore parallel to v. Now the claim follows from $0 = (\|v\|^2)' = 2\langle v, v' \rangle$. □

Definition 5.2 (Smooth Darboux transform)**.** Two arclength parameterized curves $\gamma, \tilde{\gamma}$ are called *Darboux transforms* of each other if

$$\|\tilde{\gamma}(s) - \gamma(s)\| = const.,$$

and $\tilde{\gamma}$ is not just a translate of γ.

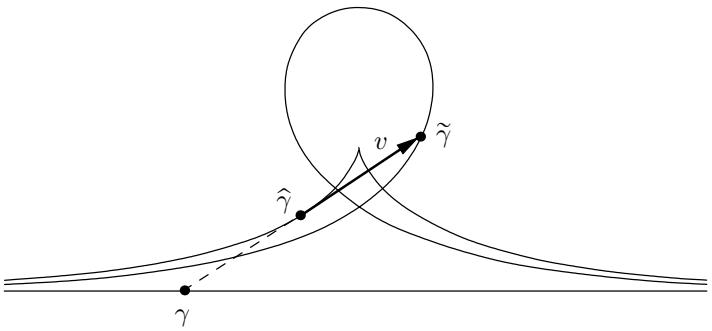

Figure 5.1. A Traktrix and the corresponding Darboux transform of γ.

Theorem 5.2. *Let $\gamma : I \to \mathbb{R}^2$ be an arclength parametrized curve. Then the following claims are equivalent:*

(i) $\tilde{\gamma}$ is a Darboux transform of γ

(ii) $\hat{\gamma} := \frac{1}{2}(\gamma + \tilde{\gamma})$ is a tractrix of γ (and of $\tilde{\gamma}$).

Proof. (ii) ⇒ (i): This is the statement of Lemma 5.1.

(i) ⇒ (ii): It is clear that $v := \frac{1}{2}(\tilde{\gamma} - \gamma)$ is of constant length. It remains to show that $\hat{\gamma}' \parallel v$ which is the same as $\hat{\gamma}' \perp v'$ in this case. This is true since

$$\langle \hat{\gamma}', v' \rangle = \langle \frac{1}{2}(\gamma' + \tilde{\gamma}'), \frac{1}{2}(\tilde{\gamma}' - \gamma') \rangle = \frac{1}{4}(1 - 1) = 0.$$

□

5.2 Discrete Darboux transform

For discrete curves the definition is the same:

Definition 5.3 (Discrete Darboux transform)**.** Two discrete arclength parametrized curves $\gamma, \tilde{\gamma} : I \to \mathbb{R}^2$ are called Darboux transforms of each other if their corresponding points are at constant distance, $\|\tilde{\gamma}_k - \gamma_k\| = const$, and $\tilde{\gamma}$ is not a parallel translation of γ.

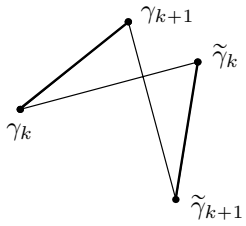

Figure 5.2. An elementary quadrilateral of the Darboux transformation ("Darboux butterfly").

There are two important generalizations of the Darboux transformation:

1. Möbius geometric (cross-ratio condition)
2. Space curves (non-commutative).

Next we will discuss the Möbius geometric generalization in detail.

5.3 Cross-ratio generalization and consistency

Definition 5.4 (Cross-ratio)**.** The *cross-ratio* of four points $z_1, z_2, z_3, z_4 \in \hat{\mathbb{C}} \cong \mathbb{CP}^1$ is defined as

$$\mathrm{cr}(z_1, z_2, z_3, z_4) = \frac{(z_1 - z_2)(z_3 - z_4)}{(z_2 - z_3)(z_4 - z1)}.$$

Important poperties:

1. The cross-ratio is preserved by *fractional linear transformations*

$$z \mapsto \frac{az + b}{cz + d}, \quad ad - bc \neq 0.$$

These are isomorphic to the group $\mathrm{PSL}(2, \mathbb{C})$:

$$\frac{az + b}{cz + d} \leftrightarrow \begin{pmatrix} a & b \\ c & d \end{pmatrix} \in \mathrm{PSL}(2, \mathbb{C}),$$

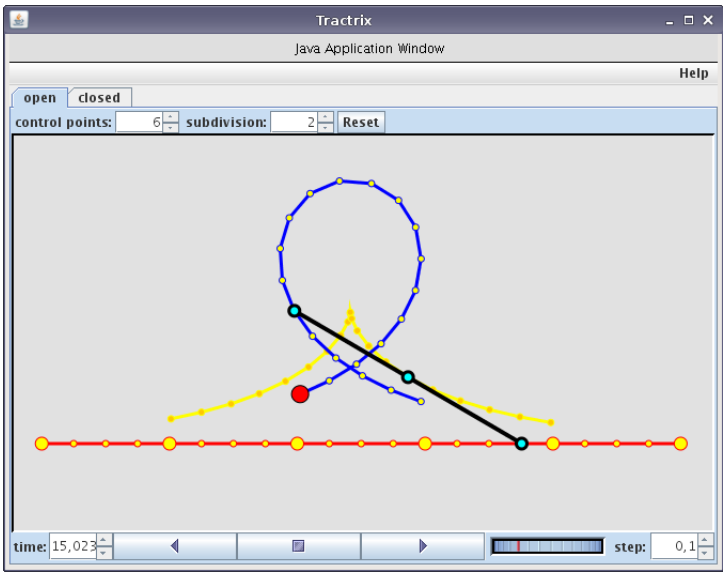

Figure 5.3. A pair of discrete curves in Darboux relation together with the curve traced out by the midpoint of the assembly. For this and other applications look at: http://www.math.tu-berlin.de/geometrie/lab/

where

$$\mathrm{PSL}(2,\mathbb{C}) == \{A \in GL(2,\mathbb{C}) \mid \det(A) = 1\}/_{\{\pm \mathrm{id}\}}.$$

Extended by the complex conjugation $z \mapsto \bar{z}$ these group expands to the group of *Möbius transformations* of the plane. The real part and the absolute value of the cross-ratio are preserved by Möbius transformations since the complex conjugation $z \mapsto \bar{z}$ induces $\mathrm{cr} \mapsto \overline{\mathrm{cr}}$.

2. $\mathrm{cr}(z_1, z_2, z_3, z_4) \in \mathbb{R} \Leftrightarrow$ the points z_1, z_2, z_3, z_4 are concircular. Moreover cross-ratios of embedded circular quads are negative, and of non-embedded ones are positive.

$$\mathrm{cr}\left(\quad\right) < 0, \quad \mathrm{cr}\left(\quad\right) > 0.$$

3. Möbius transformations map circles and straight lines to circles and straight lines

Lemma 5.3. *Assume $\gamma_k, \gamma_{k+1}, \tilde{\gamma}_k$ satisfying $|\gamma_{k+1} - \gamma_k| = \Delta$ and $|\tilde{\gamma}_k - \gamma_k| = l$ are given. Let $\tilde{\gamma}_{k+1}$ be the point determined from the condition*

$$\mathrm{cr}(\gamma_k, \gamma_{k+1}, \tilde{\gamma}_{k+1}, \tilde{\gamma}_k) = \frac{\Delta^2}{l^2}.$$

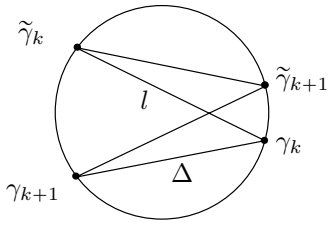

Then $[\tilde{\gamma}_{k+1}, \tilde{\gamma}_k]$ *is the Darboux transform of* $[\gamma_{k+1}, \gamma_k]$.

Proof. The Darboux transform $\tilde{\gamma}_{k+1}$ is geometrically uniquely determined by γ_k, γ_{k+1} and $\tilde{\gamma}_k$. From the definition of the cross-ratio follows

$$\mathrm{cr}(\gamma_k, \gamma_{k+1}, \tilde{\gamma}_{k+1}, \tilde{\gamma}_k) = \frac{\Delta^2}{l^2}$$

(the value of the cross-ratio is greater 0 since the quadrilateral is not embedded). Since the cross-ratio for three fixed points and one variable argument is a bijective function, the former equation also determines $\tilde{\gamma}_{k+1}$ uniquely. □

This leads to the following Möbius generalization of the Darboux transformation.

Definition 5.5 (Möbius Darboux transform)**.** Let $\gamma : I \to \mathbb{C}$ be a discrete curve, and let $\alpha_i \in \mathbb{R}$ (or $\mathbb{C}$) associated to the edges $[\gamma_i, \gamma_{i+1}]$. A curve $\tilde{\gamma} : I \to \mathbb{C}$ is called a *Möbius Darboux transform* of γ with parameter $\lambda \in \mathbb{R}$ (or $\mathbb{C}$), if

$$\mathrm{cr}(\gamma_i, \gamma_{i+1}, \tilde{\gamma}_{i+1}, \tilde{\gamma}_i) = \frac{\alpha_i}{\lambda}.$$

Lemma 5.3 shows that the standard Euclidean definition 5.3 of the Darboux transformation corresponds to $\lambda = \frac{1}{l^2}$ and $\alpha_i = 1\ \forall i$ in the Möbius generalization, where $l = |\tilde{\gamma} - \gamma|$ is the constant distance.

Note that the cross-ratio condition can also be applied to non-arclength parametrized curves.

Now consider a three dimensional combinatorial cube and assume that all edges of the cube parallel to the axis j carry a label α_j. Suppose that the values $z, z_1, z_2, z_3 \in \mathbb{C}$ are given at a vertex and its three neighbours. Then the *cross-ratio equation*

$$\mathrm{cr}(z, z_i, z_{ij}, z_j) = \frac{\alpha_i}{\alpha_j}$$

applied to the three faces intersecting at z uniquely determines the values z_{12}, z_{13}, z_{23}.

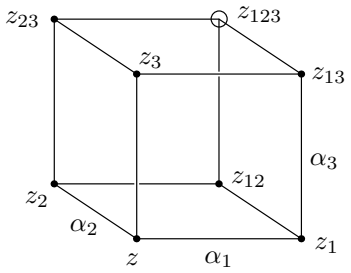

After that the cross-ratio equation delivers three a priori different values for z_{123}, coming from the three different faces containing z_{123} on which the equation can be imposed.

In general, if for such a system these values, which can be computed in several ways, coincide for any choice of the initial data z, z_1, z_2, z_3, then the system is called *3D-consistent*.

It is not difficult to show that any 3D-consistent system is ND-consistent for any $N \geqslant 3$, thus can be consistently defined on a $\mathbb{Z}^N$-lattice.

Theorem 5.4. *The cross-ratio equation is 3D-consistent.*

Proof. $\mathrm{cr}(z, z_1, z_{13}, z_3) = \frac{\alpha_1}{\alpha_3}$ can be rewritten as

$$\begin{aligned} & \frac{\alpha_1}{\alpha_3}\frac{z_{13}-z_1}{z_1-z} = \frac{z_{13}-z_3}{z_3-z} \\ \Leftrightarrow \quad & \frac{\alpha_1}{\alpha_3}(z_{13}-z_1)\frac{z_3-z_1}{z_1-z} = (z_{13}-z_1)+(z_1-z_3) \\ \Leftrightarrow \quad & (z_{13}-z_1)\left(1+\frac{\alpha_1}{\alpha_3}\frac{z_3-z}{z-z_1}\right) = z_3-z_1 = z_3-z+z-z_1. \end{aligned}$$

Thus $(z_{13}-z_1)$ is a Möbius transformation of (z_3-z):

$$z_{13}-z_1 = L(z_1, z, \alpha_1, \alpha_3)[z_3-z],$$

where

$$L(z_1, z, \alpha_1, \alpha_3) = \begin{pmatrix} 1 & z-z_1 \\ \frac{\alpha_1}{\alpha_3(z-z_1)} & 1 \end{pmatrix}.$$

is its matrix representation and

$$\tilde{z} = \begin{pmatrix} a & b \\ c & d \end{pmatrix} z :\Leftrightarrow \tilde{z} = \frac{az+b}{cz+d}.$$

Going arround the cube once, we have

$$\begin{aligned} z_{123}-z_{12} &= L(z_{12}, z_1, \alpha_2, \alpha_3)[z_{13}-z_1] \\ z_{123}-z_{12} &= L(z_{12}, z_2, \alpha_1, \alpha_3)[z_{23}-z_2]. \end{aligned}$$

This equality of these two values of z_{123} follows from the stronger claim

$$L(z_{12}, z_1, \alpha_2, \alpha_3)L(z_1, z, \alpha_1, \alpha_3) = L(z_{12}, z_2, \alpha_1, \alpha_3)L(z_2, z, \alpha_2, \alpha_3).$$

which shall be checked as an exercise.

The last equation (on the top face) then follows from symmetry. □

Now we will show that the Darboux butterflies can be put to all the faces of a combinatorial cube consistently.

Corollary 5.5 (Consistency of the 2D Darboux transformation)**.** *Given a point z and its three neighbours $z_1, z_2, z_3 \in \mathbb{C}$, let z_{ij} be the Darboux transforms associated to the faces of a cube. Then there exists a unique $z_{123} \in \mathbb{C}$ such that the faces $(z_1, z_{13}, z_{123}, z_{12})$, $(z_2, z_{23}, z_{123}, z_{12})$, and $(z_3, z_{13}, z_{123}, z_{23})$ are Darboux butterflies.*

Proof. This follows from the previous Theorem 5.4 if one sets $\alpha_i = l_i^2$, where $l_i = |z - z_i|$. □

The idea of consistency (or compatibility) is in the core of the theory of integrable systems. One is faced with it already in the very beginning when defining *complete integrability* of a Hamiltonian flow in the Liouville-Arnold sence, which means exactly that the flow may be included into a complete family of commuting (compatible) Hamiltonian flows. The 3D-consistency is an example of this phenomenon in the discrete setup. Moreover, the consistency phenomenon has developed into one of the fundamental principles of discrete differential geometry, the *consistency principle* already mentioned in Section **??**.

Next we give a simple example to show how this principle implies some facts from the corresponding smooth theory.

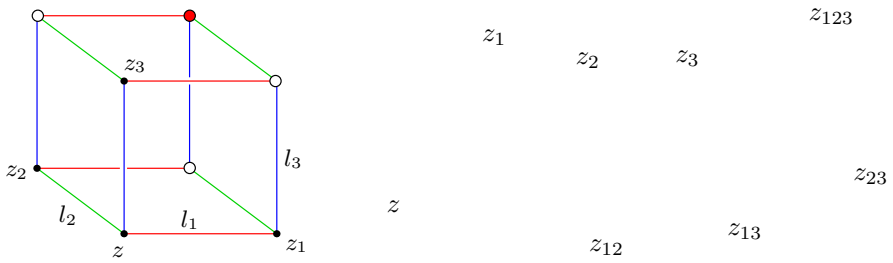

Figure 5.4. The combinatorial Darboux cube for the given data and the two dimensional embeding of the corresponding Darboux butterflies together with the unique consistent completion.

5.4 Darboux transformation and tangent flow

The tangent flow can be seen as an infinitesimal Darboux transformation. This observation is based upon a simple

Lemma 5.6 (Tangent flow as infinitesimal Darboux transformation)**.** *Let $\gamma_{k-1}, \gamma_k, \gamma_{k+1}$ be three consecutive vertices of an arclength parametrized curve. A Darboux transform of this curve is determined by choosing a vertex η_k corresponding to the vertex γ_k infinitesimally close to γ_{k-1}:*

$$\eta_k = \gamma_{k-1} + \varepsilon w + o(\varepsilon), \quad \varepsilon \to 0$$

with some $w \in \mathbb{C}$. Then the next vertex of the Darboux transform is given by

$$\eta_{k+1} = \gamma_k + \varepsilon v_k \langle w, T_{k-1} \rangle + o(\varepsilon), \tag{5.1}$$

where v_k is the tangent flow at γ_k:

$$v_k = \frac{T_k + T_{k-1}}{1 + \langle T_k, T_{k-1} \rangle}.$$

In particular, if $w = v_{k-1}$ then also $\eta_{k+1} = \gamma_k + \varepsilon v_k + o(\varepsilon)$.

Proof. The distance between γ and its Darboux transform η is given by

$$l^2 = \|\gamma - \eta\|^2 = \|T_{k-1} - \varepsilon w + o(\varepsilon)\|^2 = 1 - 2\varepsilon \langle w, T_{k-1} \rangle + o(\varepsilon).$$

For the cross-ratio this implies

$$q := \mathrm{cr}(\gamma_{k-1}, \gamma_k, \eta_k, \eta_{k-1}) = \frac{1}{l^2} = 1 + 2\varepsilon \langle w, T_{k-1} \rangle + o(\varepsilon).$$

Resolving the cross-ratio formula $q = \mathrm{cr}(\gamma_k, \gamma_{k+1}, \eta_{k+1}, \eta_k)$ for η_{k+1} we obtain

$$\eta_{k+1} - \gamma_k = \frac{(1-q)(\gamma_k - \gamma_{k+1})(\eta_k - \gamma_k)}{\gamma_k - \gamma_{k+1} + q(\eta_k - \gamma_k)}.$$

In the limit $\varepsilon \to 0$ this yields

$$\eta_{k+1} - \gamma_k = \varepsilon \langle w, T_{k-1} \rangle \frac{T_k \cdot T_{k-1}}{T_k + T_{k-1}} + o(\varepsilon),$$

which is equivalent to (5.1). □

If we apply such a Darboux transformation to the left end vertex of γ_0 of a discrete curve $\gamma : \{0, .., N\} \to \mathbb{R}^2$ we obtain an infinitesimal tangent flow of all vertices (except maybe γ_0).

Theorem 5.7. *The Darboux tranformation of discrete arclength parametrized curves is compatible with its tangent flow. This means:*
Given two discrete arclength parametrized curves $\gamma, \tilde{\gamma} : I \to \mathbb{R}^2$ evolving under the tangential flow $t \mapsto \gamma(t, \cdot)$, $t \mapsto \tilde{\gamma}(t, \cdot)$. If the curves are in Darboux correspondence at some $t = t_0$, then they are Darboux transforms of each other for all t.

Proof. This fact can be derived from the permutability of the Darboux transformations. The three directions of the compatibility cube for Darboux transformations get three different interpretations:

Let γ and $\tilde{\gamma}$ be a Darboux pair. Let η be an infinitesimal Darboux transform of γ as in Lemma 5.6, i.e. with $\eta_k \to \gamma_{k-1}$. The Darboux condition determines vertices $\tilde{\eta}_k$ and $\tilde{\eta}_{k+1}$, as in the picture, uniquely (from Corollary 5.5 we know that everything is consistent).

From the cross-ratio $\mathrm{cr}(\gamma_k, \eta_k, \tilde{\eta}_k, \tilde{\gamma}_k)$ it is easy to see that the vertex $\tilde{\eta}_k$ of the Darboux cube also satisfies $\tilde{\eta}_k \to \tilde{\gamma}_{k-1}$ and therefore, due to Lemma 5.6, the curve $\tilde{\eta}$ is given by the tangent flow of $\tilde{\gamma}$.

Passing to the limit $\varepsilon \to 0$ we obtain the claim of the theorem.

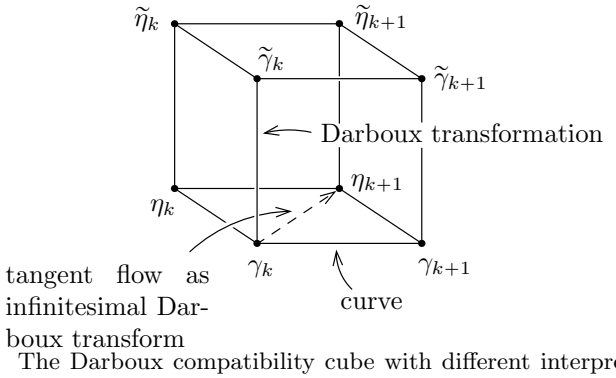

Figure 5.5. The Darboux compatibility cube with different interpretations of the three dimensions.

□

Remark 5.1. (Möbius geometry tangent flow).
For the Möbius Darboux transformation the corresponding construction leads to the flow

$$\gamma_t = \frac{\Delta\gamma_k \cdot \Delta\gamma_{k-1}}{\Delta\gamma_k + \Delta\gamma_{k-1}}$$

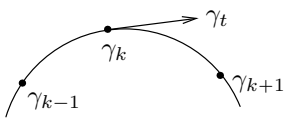

which is tangent to the circle through γ_{k-1}, γ_k and γ_{k+1}.

Remark 5.2. (Generalization to space curves).
There exists also a generalization of the Darboux transformation to a consistent

system in an associative algebra $\mathcal{A}$. The case of quaternions, $\mathcal{A} = \mathbb{H}$, leads to a Darboux transformation for space curves (with twist).

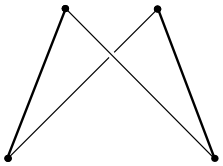

Figure 5.6. A Darboux butterfly for space curves is not planar.

Part II
Discrete Surfaces

There is no canonical way of defining a discrete surface. We usually think of discrete surfaces as surfaces build from vertices, edges and faces. As an example consider

simplicial surfaces Surfaces glued from triangles.
We see that not every possibility of gluing together triangles constitutes in something we want to call a discrete surface.

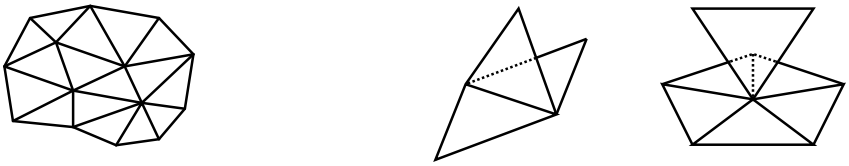

discrete surface not discrete surfaces

Generalizing the faces to be polygons we obtain the notion of

polyhedral surfaces Surfaces glued from planar polygons.

In particular

simple surfaces Polyhedral surfaces with all vertices of valence three.
They can be seen as an analogue of the characterization of a surface via enveloping tangent planes. Start with a simplicial surface and add a plane at every vertex. By intersecting neighboring planes we obtain another polyhedral surface. Since three planes generically intersect in one point we obtain a vertex for every face of the original surface and a face for each vertex. This means that the obtained surface is combinatorically dual to the simplicial surface. The faces are now planar polygons and all vertices of valence three.

Another special case of polyhedral surfaces are

quad-surfaces Surfaces glued from quadrilaterals
They are analogues of parametrized surfaces. For each quad there is two unique transversal directions given by pairs of opposite edges leading to parameter lines consisting of strips of quadrilaterals.
A reasonable generalization here is to consider non-planar quads.

Dropping the combinatorial structure completely one might consider

point samples Surfaces generated by sets of points. But it is not clear when a set of points without further structure should be considered a discrete surface or how to obtain this additional structure. E.g. In the domain of computer graphics the non-trivial problem of obtaining a water tight polyhedral surface from a “point cloud” is considered.

Reasonable data from an experiment, e.g. scanning a 3D-object could be not only positions but also normal directions. Providing each point with a normal vector or equivalently with a tangent plane leads to

contact elements Points with planes. This can be seen as a notion of a surface together with its Gauss map.

We will mainly deal with polyhedral surfaces and begin by specifying how vertices, edges and faces constitute a discrete surface.

6 Abstract discrete surfaces

We consider discrete surfaces consisting of vertices, edges and faces from the point of view of topology (abstract discrete surfaces), metric geometry (piecewise flat surfaces) and Euclidean geometry (polyhedral surfaces).

6.1 Cell decompositions of surfaces

From the topological point of view a discrete surface is a decomposition of a two-dimensional manifold into vertices, edges and faces. This is what we call the *combinatorics* of a discrete surface.

First some preliminary definitions

Definition 6.1 (surface)**.** A *surface* is a real two-dimensional connected manifold, possibly with boundary.

Remark 6.1. We mainly focus on compact surfaces and compact closed surfaces.

Definition 6.2 (n-cell)**.** We denote the open disk in $\mathbb{R}^n$ by

$$D^n \coloneqq \{x \in \mathbb{R}^n \mid \|x\| < 1\}$$

and its boundary by

$$\partial D^n \coloneqq \overline{D^n} \backslash D^n,$$

where the bar denotes the topological closure.
An *n-dimensional cell* or *n-cell* is a topological space homeomorphic to D^n.

Remark 6.2. Note that $D^0 = \{0\}$ is a point and its boundary $\partial D^0 = \varnothing$.

Definition 6.3 (cell decomposition)**.** Let M be a surface and $T = \{U_i\}_{i=1}^N$ a covering of M by pairwise disjoint 0-, 1- and 2-cells.
T is called a finite *cell decomposition* of M if for any n-cell $U_i \in T$ there is a continuous map

$$\varphi_i : \overline{D^n} \to M$$

which maps D^n homeomorphic to U_i and ∂D^n to a union of cells of dimension at most $n-1$, i.e. 1-cells are bounded by 0-cells and 2-cells by 1- and 0-cells.
0-cells are called *vertices*, 1-cells *edges* and 2-cells *faces*.

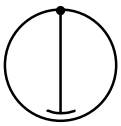

Figure 6.1. This is not a cell decomposition.

Remark 6.3.

- More requirements are needed to define infinite cell decompositions.
- The existence of a finite cell decomposition makes a surface necessarily compact.
- Cell decompositions of surfaces are a special case of *cell complexes*. E.g. a 1-dimensional cell complex is a *graph*.

Example 6.1. A convex polyhedron induces a cell decomposition of $\mathbb{S}^2$.

We introduce some additional properties coming from polyhedra theory but mostly deal with general cell decompositions.

Definition 6.4 (regular and strongly regular)**.** A cell decomposition $T = \{U_i\}_{i=1}^N$ of a surface M is called *regular* if the maps $\varphi_i : \overline{D^n} \to M$ are homeomorphisms.
A regular cell decomposition is called *strongly regular* if for any two cells U_i and U_j the intersection of their closures $\overline{U_i} \cap \overline{U_j}$ is either empty or the closure of *one* cell.

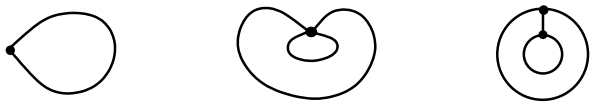

Figure 6.2. Examples of non-regular cell decompositions. Cells with boundary identifications –i.e. self-touching cells– are not allowed. E.g. no loops.

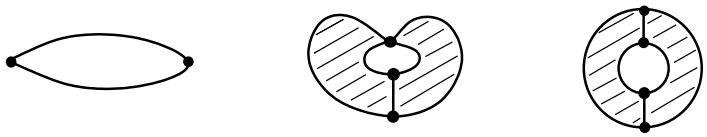

Figure 6.3. Examples of non-strongly regular cell decompositions. Cells with multiple common boundary components are not allowed. E.g. no double edges.

Example 6.2.

(1) The cell decompositions of $\mathbb{S}^2$ induced by convex polyhedra are strongly regular.

(2) Cube with a hole:

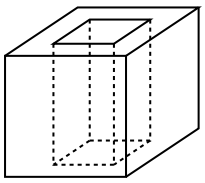

This is not a cell-decomposition of the cube with a hole.

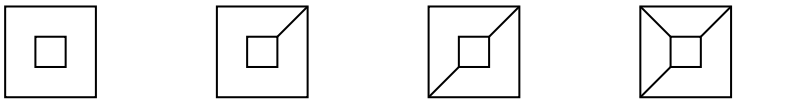

Figure 6.4. Cube with a hole. From "not a cell decomposition" to a strongly regular cell decomposition by adding edges.

Definition 6.5 (abstract discrete surface)**.** Let T be a cell decomposition of a surface M. Then we call the combinatorial data $\mathcal{S} \coloneqq (M, T)$ an *abstract discrete surface* and a homeomorphism $f : M \to \mathbb{R}^n$ its *geometric realization*. We write this as $f : \mathcal{S} \to \mathbb{R}^n$.

Remark 6.4.

- Abstract discrete surfaces are compact.
- We use the terms vertices, edges and faces for the combinatorial cells $U_i \in T$ as well as for the images under the geometric realization $f(U_i) \subset f(M) \subset \mathbb{R}^n$.

Example 6.3 (quad-graph)**.** A *quad-graph* is an abstract discrete surface with all faces being quadrilaterals. A geometric realization with planar faces is called a *Q-net*.

6.2 Topological classification of compact surfaces

We outline the topological classification of compact surfaces. This means that we are interested in topological invariants which uniquely identify a compact surface up to homeomorphisms. A cell decomposition of a surface induces the following topological invariant.

Definition 6.6 (Euler characteristic)**.** Let V, E, F be the sets of vertices, edges and faces of an abstract discrete surface $\mathcal{S} \coloneqq (M, T)$ and $|V|$, $|E|$, $|F|$ their cardinalities. Then

$$\chi(M) \coloneqq |V| - |E| + |F|$$

is called the *Euler characteristic* of M.

Remark 6.5. Since the Euler characteristic is independent of the cell decomposition T of M and every compact surface has a cell decomposition[23], this indeed defines a topological invariant of the surface M.

Example 6.4.

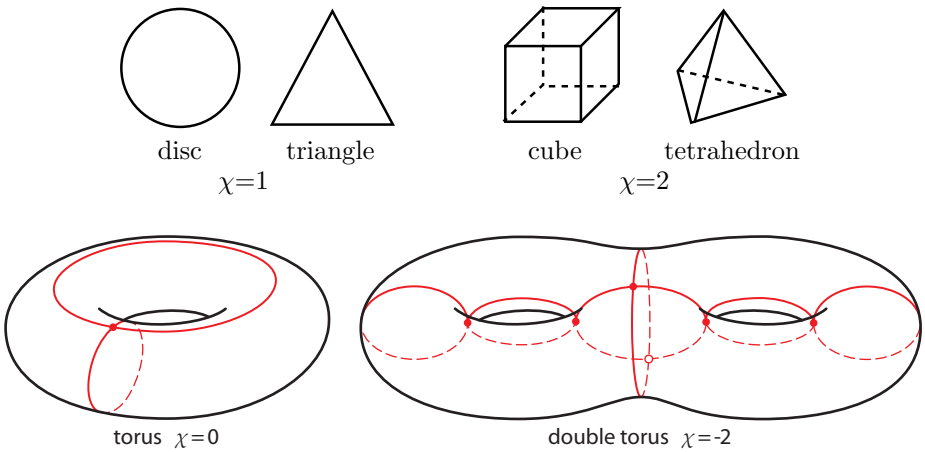

Figure 6.5. Cell decompositions of a disk, sphere, torus and double torus. With Euler characteristic $\chi = |V| - |E| + |F|$.

We describe the construction of closed surfaces by combining some elementary compact closed surfaces of high Euler characteristic using the connected sum. The classification theorem then states that this already yields all possible compact closed surfaces up to homeomorphisms.

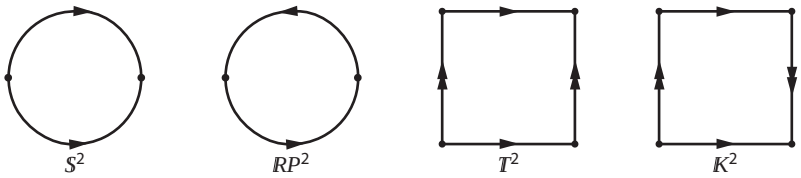

Figure 6.6. Elementary closed surfaces from identifying edges of bigons and quadrilaterals.

There are two essentially different ways of orienting the two edges of a bigon. Identifying the two edges along these orientations yields the *sphere* $\mathbb{S}^2$ and the *real projective plane* $\mathbb{R}\mathrm{P}^2$ respectively. The first of which is orientable while the second is not. Counting vertices, edges and faces of the cell decompositions induced by the original bigon we obtain the Euler characteristics

$$\chi(\mathbb{S}^2) = 2 - 1 + 1 = 2, \quad \chi(\mathbb{R}\mathrm{P}^2) = 1 - 1 + 1 = 1.$$

Pairwise identifying the four edges of a quadrilateral gives us two additional

[23] Even stronger: Every compact surface has a triangulation.
Note that abstract discrete surfaces –which is our case of interest– are compact and always come with a cell decomposition.

surfaces which are the *torus* $\mathbb{T}^2$ and the *Klein bottle* $\mathbb{K}^2$ with

$$\chi(\mathbb{T}^2) = 1 - 2 + 1 = 0, \quad \chi(\mathbb{K}^2) = 1 - 2 + 1 = 0.$$

We notice that the torus and the Klein bottle can not be distinguished by their Euler characteristic alone. But the torus is orientable while the Klein bottle is not.

For two surfaces M and N their connected sum $M\#N$ is obtained by removing an open disk from each and gluing the resulting surfaces together along the circular boundary components of the missing disks.
This operation is associative, commutative and the sphere is the identity element, i.e.

$$M\#\mathbb{S}^2 = \mathbb{S}^2\#M = M$$

Let us determine the Euler characteristic of the connected sum $M\#N$. Consider a cell decomposition of M and N respectively. A cell decomposition of M° which is the surface M with an open disk removed can be obtained by adding one edge as a loop at one vertex of the cell decomposition of M, so

$$\chi(M^\circ) = \chi(M) - 1.$$

Same for N°. Gluing along the circular boundaries is then equivalent to the identification of these new edges and the adjacent vertex. So we have one edge less and one vertex less in the connected sum which cancel out in the Euler characteristic

$$\chi(M\#N) = \chi(M^\circ) + \chi(N^\circ) - 1 + 1 = \chi(M) + \chi(N) - 2.$$

Starting with a sphere as the identity element we construct surfaces of lower Euler characteristic by connecting tori, projective planes and Klein bottles to it. Connecting g tori to the sphere[24] yields an orientable surface with g holes, i.e.

$$\chi((\mathbb{T}^2)^{\#g}) = \chi(\mathbb{T}^2\#\ldots\#\mathbb{T}^2) = 2 - 2g, \qquad g \geqslant 0,$$

where we define $M^{\#0} \coloneqq \mathbb{S}^2$ by the identity element. g is called the *genus* of the resulting surface.

Building the connected sum of h projective planes we obtain surfaces of odd and even Euler characteristic all of them non-orientable.[25]

$$\chi((\mathbb{RP}^2)^{\#h}) = \chi(\mathbb{RP}^2\#\ldots\#\mathbb{RP}^2) = 2 - h, \qquad h \geqslant 1.$$

Any other combination of connected sums of our elementary surfaces $\mathbb{S}^2$, $\mathbb{T}^2$, $\mathbb{RP}^2$ and $\mathbb{K}^2$ does not yield new surfaces. Indeed building the connected sum of two projective planes already gives us a Klein bottle

$$\mathbb{RP}^2\#\mathbb{RP}^2 = \mathbb{K}.$$

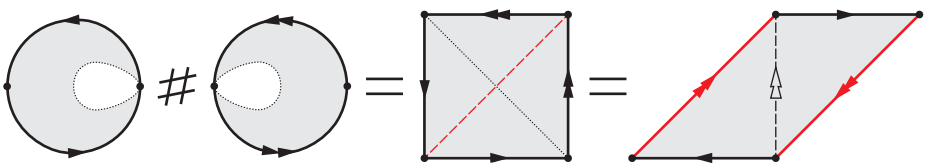

Figure 6.7. The connected sum of two projective planes is a Klein bottle.

[24] Or equivalently to each other.
[25] Any connected sum containing at least one projective plane is non-orientable.

Attaching another projective plane to the Klein bottle is the same as attaching it to a torus[26]

$$\mathbb{K}\#\mathbb{R}\mathrm{P}^2 = \mathbb{T}^2\#\mathbb{R}\mathrm{P}^2.$$

So any mixed combinations of tori and projective planes are already included.[27]

$\mathbb{T}^2$ and $\mathbb{R}\mathrm{P}^2$ together with the connected sum # generate a monoid of which the classification theorem states that it already includes all compact closed surfaces.

Theorem 6.1 (classification by connected sums)**.** *Any compact closed surface M is either homeomorphic to the connected sum of $g \geqslant 0$ tori*

$$M = (\mathbb{T}^2)^{\#g}$$

or to the connected sum of $h \geqslant 1$ real projective planes

$$M = (\mathbb{R}\mathrm{P}^2)^{\#h}.$$

In the first case M is orientable and in the second non-orientable.

And as an immediate consequence of our considerations about the Euler characteristics

Corollary 6.2 (classification by orientability and Euler characteristic)**.** *Any compact closed surface is uniquely determined by its orientability and Euler characteristic up to homeomorphisms.*

Remark 6.6.

- A compact closed orientable surface can be classified by its Euler characteristic only, or equivalently by its genus g since

$$\chi(M) = 2 - 2g.$$

- The classification theorem can be generalized to compact surfaces with boundary by adding another topological invariant which is the number of connected boundary components k. In this case the Euler characteristic for orientable surfaces becomes

$$\chi(M) = 2 - 2g - k.$$

- The easiest and most recent proof of the classification theorem is Conway's ZIP proof which can be found in [**zip-proof**].
- The procedure of identifying edges of bigons and quadrilaterals to obtain compact closed surfaces can be generalized to the pairwise identification of edges of even-sided polygons. This leads to other possible ways of classification.

[26] We see that the connected sum has no inverse operation.

[27] This can be restated more general in the following way. On any non-orientable surface there is no way to distinguish a handle from an attached Klein-bottle.

7 Polyhedral surfaces and piecewise flat surfaces

We start with a short presentation of curvature in the classical smooth theory.

7.1 Curvature of smooth surfaces

Extrinsic curvatures of a smooth surface immersed in $\mathbb{R}^3$ are defined as follows. Consider the one parameter family of tangent spheres $S(\kappa)$ with signed curvature κ touching the surface at a point p. κ is positive if the sphere lies at the same side of the tangent plane as the normal vector and negative otherwise. Let M be the set of tangent spheres intersecting any neighborhood U of p in more than one point. The values

$$\kappa_1 \coloneqq \inf_{S\in M} \kappa(S), \quad \kappa_2 \coloneqq \sup_{S\in M} \kappa(S)$$

are called the *principal curvatures* of the surface at p.

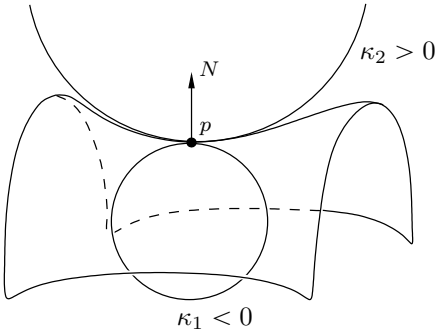

Figure 7.1. The curvature spheres touching the surface in p.

The spheres $S(\kappa_1)$ and $S(\kappa_2)$ are called *principal curvature spheres* and are in second order contact with the surface. The contact directions are called *principal directions* and are orthogonal.

The *Gaussian curvature* and *mean curvature* are defined as

$$K \coloneqq \kappa_1\kappa_2, \quad H \coloneqq \frac{1}{2}(\kappa_1 + \kappa_2).$$

The Gaussian curvature of a surface at a point p is also the quotient of oriented areas $A(\cdot)$:

$$K(p) = \lim_{\varepsilon\to 0} \frac{A(N(U_\varepsilon(p)))}{A(U_\varepsilon(p))},$$

where $U_\varepsilon(p)$ is an ε-neighborhood of p on the surface, and $N(U_\varepsilon(p)) \subset S^2$ is its image under the Gauss map.
The following classical theorems hold.

Theorem 7.1 (Gauss' Theorema Egregium)**.** *The Gaussian curvature of a surface is preserved by isometries.*

Theorem 7.2 (Gauss-Bonnet)**.** *The total Gaussian curvature of a compact closed surface S is given by*

$$\int_S K \mathrm{d}A = 2\pi\chi(S).$$

7.1.1 Steiner's formula

The *normal shift* of a smooth surface S with normal map N is defined as

$$S_\rho := S + \rho N.$$

For sufficiently small ρ the surface S_ρ is also smooth. Interpreting S as an enveloping surface of the principal sphere congruences one can show that the centers of the principal curvature spheres of S and S_ρ coincide. The signed radii are reduced by ρ so the principal curvatures change as

$$\frac{1}{\kappa_{1\rho}} = \frac{1}{\kappa_1} - \rho, \quad \frac{1}{\kappa_{2\rho}} = \frac{1}{\kappa_2} - \rho.$$

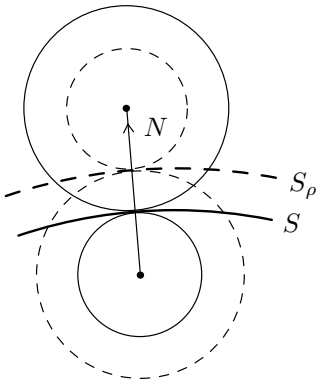

Theorem 7.3 (Steiner's formula)**.** *Let S be a smooth surface and S_ρ its smooth normal shift for sufficiently small ρ. Then the area of S_ρ is a quadratic polynomial in ρ,*

$$A(S_\rho) = A(S) - 2H(S)\rho + K(S)\rho^2,$$

where $K(S) = \int_S K \mathrm{d}A$ and $H(S) = \int_S H \mathrm{d}A$ are the total Gaussian and total mean curvature of S.

Proof. Let $\mathrm{d}A$ and $\mathrm{d}A_\rho$ be the area forms of S and S_ρ. The normal shift preserves the Gauss map, therefore one has

$$K\mathrm{d}A = K_\rho \mathrm{d}A_\rho,$$

where K and K_ρ are the corresponding Gaussian curvatures. For the area this implies

$$\begin{aligned} A(S_\rho) &= \int_{S_\rho} \mathrm{d}A_\rho = \int_S \frac{K}{K_\rho}\mathrm{d}A \\ &= \int_S \kappa_1\kappa_2(\frac{1}{\kappa_1} - \rho)(\frac{1}{\kappa_2} - \rho)\mathrm{d}A \\ &= \int_S \left(1 - (\kappa_1 + \kappa_2)\rho + \kappa_1\kappa_2\rho^2\right)\mathrm{d}A \\ &= A(S) - 2H(S)\rho + K(S)\rho^2. \end{aligned} \tag{7.1}$$

□

Remark 7.1. Equation (7.1) also holds true without integration. We can state Steiner's formula in the differential version

$$\mathrm{d}A_\rho = (1 - 2H(p)\rho + K(p)\rho^2)\mathrm{d}A,$$

where $K(p)$ and $H(p)$ are the (local) Gaussian and mean curvature at p.

7.2 Curvature of polyhedral surfaces

Definition 7.1 (polyhedral surface)**.** A *polyhedral surface* in $\mathbb{R}^n$ is a geometric realization $f : \mathcal{S} \to \mathbb{R}^n$ of an abstract discrete surface $\mathcal{S} = (M, T)$ such that the edges are intervals of straight lines and the faces are planar.
A *simplicial surface* is a polyhedral surface with all faces being triangles.

7.2.1 Discrete Gaussian curvature

For a polyhedral surface the Gaussian curvature is concentrated at vertices in the following sense: The area of $N(U_\varepsilon(p))$ vanishes for all internal points on faces and edges. For a vertex it is equal to the oriented area of the corresponding spherical polygon.

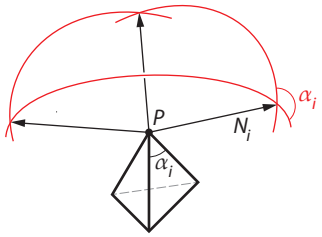

Figure 7.2. The angle α_i at vertex p is the external angle of the spherical polygon at vertex N_i.

Let N_i be the normal vectors of the faces adjacent to the vertex p. Each two neighboring normals define a geodesic line on $\mathbb{S}^2$, which all together constitute a spherical polygon. The angle α_i at vertex p of the face on the polyhedral surface with normal vector N_i is equal to the external angle of the spherical polygon at the vertex N_i. So the angle defect $2\pi - \sum \alpha_i$ at the vertex p is the area of the spherical polygon where $\sum \alpha_i$ is the total angle on the polyhedral surface around the vertex p.[28]

Definition 7.2 (discrete Gaussian curvature)**.** For a closed polyhedral surface S the angle defect

$$K(p) := 2\pi - \sum_i \alpha_i \tag{7.2}$$

at a vertex p is called the *Gaussian curvature* of S at p.
The *total Gaussian curvature* is defined as the sum

$$K(S) := \sum_{p \in V} K(p).$$

The points with $K(p) > 0$, $K(p) = 0$ and $K(p) < 0$ are called *elliptic*, *flat* and *hyperbolic* respectively.

[28] This is an oriented area since the "external angle" depends on the orientation of the polygon.

Remark 7.2. The angle defect at a vertex p is bounded from above by 2π but unbounded from below.

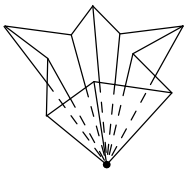

Figure 7.3. The discrete Gaussian curvature at a vertex p can be made arbitrarily low by "folding" a vertex star.

Lemma 7.4. *Let p be an inner point of a polyhedral surface. Then*

$$\begin{aligned} p \text{ convex} &\Rightarrow p \text{ elliptic} \\ p \text{ planar} &\Rightarrow p \text{ flat} \\ p \text{ saddle} &\Rightarrow p \text{ hyperbolic}, \end{aligned}$$

where

$$\begin{aligned} p \text{ convex} &:\Leftrightarrow \text{the spherical polygon of the normal vectors around } p \text{ is convex} \\ p \text{ planar} &:\Leftrightarrow p \text{ and its neighbors lie in a plane} \\ p \text{ saddle} &:\Leftrightarrow p \text{ lies in the convex hull of its neighbors (and } p \text{ not planar).} \end{aligned}$$

Remark 7.3. In general, none of the implications in Lemma 7.4 is reversible.

Since the discrete Gaussian curvature is defined intrinsically[29] we immediately obtain a discrete version of Gauss' Theorema Egregium.

Theorem 7.5 (polyhedral Gauss' Theorema Egregium)**.** *The Gaussian curvature of a polyhedral surface is preserved by isometries, i.e. depends on the polyhedral metric only.*

There also holds a discrete version of the Gauss-Bonnet theorem.

Theorem 7.6 (polyhedral Gauss-Bonnet)**.** *The total Gaussian curvature of a closed polyhedral surface S is given by*

$$K(S) = 2\pi\chi(S).$$

Proof. We have

$$K(S) = \sum_{p \in V} K(p) = 2\pi\,|V| - \sum_{\text{all angles of } S} \alpha_i.$$

The angles $\pi - \alpha_i$ are the (oriented) external angles of a polygon. Their sum is

$$\sum_{\substack{\text{all angles of} \\ \text{one polygon}}} (\pi - \alpha_i) = 2\pi.$$

[29] The cone angle $\sum \alpha_i$ is invariant under isometries. We discuss this and polyhedral metrics in more detail in Section 7.3.

The sum over all faces gives

$$2\pi\,|F| = \sum_{\text{all angles of } S} (\pi - \alpha_i) = 2\pi|E| - \sum_{\text{all angles of } S} \alpha_i,$$

where we used that the number of angles is equal to $2|E|$ (each edge is associated with 4 attached angles but each angle comes with two edges).
Finally

$$K(S) = 2\pi(|V| - |E| + |F|) = 2\pi\chi(S).$$

□

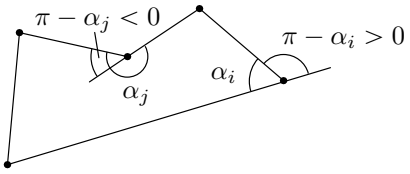

Figure 7.4. Oriented external angles of a polygon.

Example 7.1 (Gaussian curvature of a cube)**.** Consider a standard cube with all vertex angles equal to $\frac{\pi}{2}$. Then the Gaussian curvature at every vertex p is

$$K(p) = 2\pi - 3\frac{\pi}{2} = \frac{\pi}{2}.$$

So the sum over all eight vertices yields $K(S) = 4\pi$.
On the other hand $\chi(S) = \chi(\mathbb{S}^2) = 2$.

Remark 7.4. The polyhedral Gauss-Bonnet theorem can be extended to polyhedral surfaces with boundary. Since the boundary components of a polyhedral surface are piecewise geodesic we only have to add the turning angle of the boundary curve

$$\varphi(p) \coloneqq \pi - \sum_i \alpha_i$$

at each boundary vertex p to the total discrete Gaussian curvature.[30]

7.2.2 Discrete mean curvature

Definition 7.3 (discrete mean curvature)**.** The *discrete mean curvature* of a closed polyhedral surface S at the edge $e \in E$ is defined by

$$H(e) := \frac{1}{2}\theta(e)l(e),$$

where $l(e)$ is the length of e, and $\theta(e)$ is the oriented angle between the normals of the adjacent faces sharing the edge e (the angle is considered to be positive in the convex case and negative otherwise).
The *total mean curvature* is defined as the sum over all edges

$$H(S) := \sum_{e\in E} H(e) = \frac{1}{2}\sum_{e\in E} \theta(e)l(e).$$

[30] Or alternatively define the discrete Gaussian curvature at boundary vertices by the turning angle.

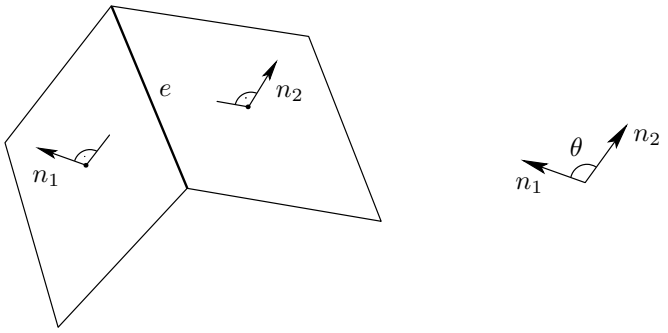

Figure 7.5. Discrete mean curvature for polyhedral surfaces.

With this definition the following discrete version of Steiner's formula holds true.

Theorem 7.7 (Steiner's formula for convex polyhedra)**.** *Let $\mathcal{P}$ be a convex polyhedron with boundary surface $S = \partial\mathcal{P}$. Let $\mathcal{P}_\rho$ be the parallel body at the distance ρ*

$$\mathcal{P}_\rho := \left\{p \in \mathbb{R}^3 \mid d(p, \mathcal{P}) \leqslant \rho\right\}.$$

Then the area of the boundary surface $S_\rho := \partial\mathcal{P}_\rho$ is given by

$$A(S_\rho) = A(S) + 2H(S)\rho + 4\pi\rho^2. \tag{7.3}$$

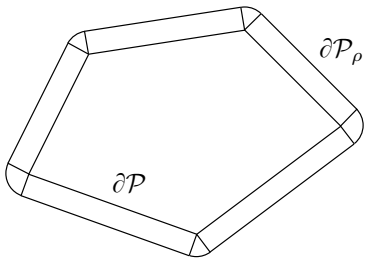

Figure 7.6. Boundary surface S of a convex polyhedron and S_ρ of its parallel body at distance ρ.

Proof. The parallel surface S_ρ consists of three parts:

- Plane pieces congruent to the faces of S.
  Their areas sum up to $A(S)$.
- Cylindrical pieces of radius ρ, angle $\theta(e)$ and length $l(e)$ along the edges e of S with area $\theta(e)l(e)\rho = 2H(e)\rho$.
- Spherical pieces at the vertices p of S with area $K(p)\rho^2$. Since a convex polyhedron is a topological sphere the Gaussian curvature sums up to $K(S) = 4\pi$, i.e. merged together by parallel translation the spherical pieces comprise a round sphere of radius ρ.

□

Remark 7.5 (Steiner's formula for polyhedral surfaces). At non-convex edges and vertices we can define the parallel surface as depicted in Figure 7.7

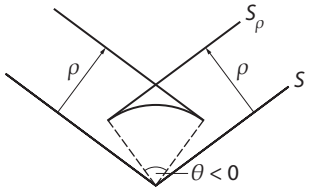

Figure 7.7. On the definition of the parallel surface S_ρ in the non-convex case.

and take the area of the corresponding cylindrical and spherical pieces as negative. Then Steiner's formula for an arbitrary closed polyhedral surface S reads as follows:

$$A(S_\rho) = A(S) + 2H(S)\rho + K(S)\rho^2,$$

where $K(S) = 2\pi\chi(S)$ is the total Gaussian curvature.

7.3 Polyhedral Metrics

We want to investigate the intrinsic geometry induced by polyhedral surfaces.

Definition 7.4. A *metric* on a set M is a map

$$d : M \times M \to \mathbb{R}$$

such that for any $x, y, z \in M$

(i) $d(x, y) \geqslant 0$

(ii) $d(x, y) = 0 \Leftrightarrow x = y$

(iii) $d(x, y) = d(y, x)$

(iv) $d(x, y) + d(y, z) \geqslant d(x, z)$

The pair (M, d) is called a *metric space*.
Let (M, d) and $(\tilde{M}, \tilde{d})$ be two metric spaces. Then a map $f : M \to \tilde{M}$ such that for any $x, y \in M$

$$\tilde{d}(f(x), f(y)) = d(x, y)$$

is called an *isometry*.
(M, d) and $(\tilde{M}, \tilde{d})$ are called *isometric* if there exists a bijective isometry $f : M \to \tilde{M}$ called a *global isometry*.
(M, d) is called *locally isometric* to $(\tilde{M}, \tilde{d})$ at a point $x \in M$ if there exists a neighborhood U of x and a neighborhood $\tilde{U} \subset \tilde{M}$ such that (U, d) is isometric to $(\tilde{U}, \tilde{d})$.

Remark 7.6.

- Every isometry is continuous and every global isometry a homeomorphism.
- An abstract discrete surface $\mathcal{S} = (M, T)$ equipped with a metric becomes a *metric space* (M, d).
- For a geometric realization $f : \mathcal{S} \to \mathbb{R}^n$ the Euclidean metric on $\mathbb{R}^n$ induces a metric on $f(M) \subset \mathbb{R}^n$. To study this metric intrinsically on the corresponding abstract discrete surface $\mathcal{S}$ we pull it back, i.e. we define the metric on $\mathcal{S}$ such that f is an isometry.

Let $f : \mathcal{S} \to \mathbb{R}^n$ be a polyhedral surface. We examine the metric induced by the Euclidean metric of $\mathbb{R}^n$. For two points $x, y \in f(M)$ we are interested in the length $L(\gamma)$ of the shortest curve γ lying on $f(M)$ connecting x and y:

$$d(x, y) = \inf_{\gamma} \{L(\gamma) \mid \gamma : [0, 1] \to f(M), \gamma(0) = x, \gamma(1) = y\}.$$

Example 7.2 (shortest paths on a polyhedral surface)**.** Isometrically unfolding a cube to a plane we see that connecting two points by a straight line might not always constitute a shortest path.

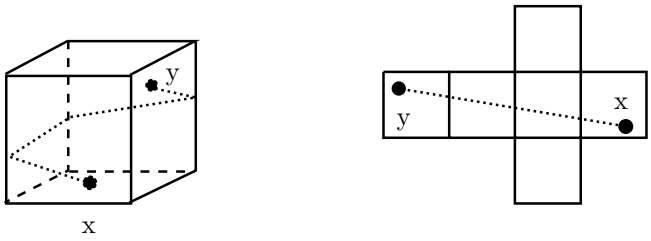

Figure 7.8. Straight line on a cube which is not the shortest path connecting x and y.

Shortest paths are a global property of the metric.

We start by investigating locally shortest paths which are called geodesics. We look for local isometries to some planar domain where we already know the geodesics.

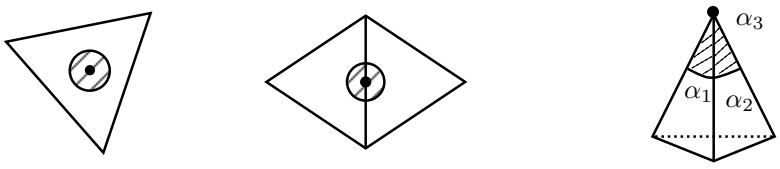

Figure 7.9. Neighborhoods of a point on a face, edge and vertex of a polyhedral surface.

Consider a point $p \in M$ on a face $A \in F$. Then a small enough neighborhood of $f(p)$ on $f(M)$ is entirely contained in the planar face $f(A)$. So the neighborhood can be mapped isometrically to a disk D^2.

For points on edges a small neighborhood intersects the interior of two planar faces. Isometrically unfolding those two faces to a plane we find that the neighborhood is also isometric to a disk.
For points on a vertex we could also unfold the adjacent faces to a plane. But this leaves a cut in the neighborhood. What we can do isometrically is map the small neighborhood to the tip of a cone characterized by the angle θ which is the sum of angles α_i between the edges adjacent to the vertex. The *angle defect*

$$K(p) \coloneqq 2\pi - \theta$$

is a measure for the non-flatness of the metric at p.
In general θ can be greater than 2π in which case the cone becomes a saddle. We make the following classification

$K > 0$ elliptic point, locally isometric to a cone.

$K = 0$ flat point, locally isometric to a disk,
i.e. the vertex and its adjacent edges could be completely removed from the combinatorics without changing the polyhedral surface.

$K < 0$ hyperbolic point, locally isometric to a saddle.

We find that the metric induced on the polyhedral surface $f(M)$ by the Euclidean metric in $\mathbb{R}^n$ is locally equivalent to the Euclidean metric of $\mathbb{R}^2$ everywhere except for the vertices.

Pulling back the metric with the map f to the abstract discrete surface $\mathcal{S}$ we obtain a metric with the same properties, i.e. a small neighborhood of a point $p \in M$ on a

- face is isometric to a disk D^2.
- edge is isometric to a disk D^2.
- vertex is isometric to the tip of a cone.

We can now forget about the combinatorics and obtain an abstract surface M with a polyhedral metric which we call piecewise flat surface.

Definition 7.5 (piecewise flat surface)**.** A metric d on a surface M is called a *polyhedral metric* if (M, d) is locally isometric to a cone at finitely many points $V = \{P_1, \dots, P_N\} \subset M$ (*conical singularities* of the metric) and locally isometric to a plane elsewhere.
The pair (M, d) of a surface and a polyhedral metric is called a *piecewise flat surface.*

Remark 7.7. A polyhedral metric d on a surface M carries no obvious information about edges and faces, only about the vertices.

How to prescribe a polyhedral metric?

We investigate how the information about the metric gets transferred from a polyhedral surface to its corresponding piecewise flat surface (w.l.o.g. we consider simplicial surfaces).
A simplicial surface induces a piecewise flat surface (M, d) together with a triangulation T such that the vertex set includes the conical singularities and all edges are geodesics on (M, d).

Definition 7.6 (geodesic triangulation)**.** Let (M, d) be a piecewise flat surface with conical singularities V_0.
Then a *geodesic triangulation* of (M, d) is a triangulation of M such that its vertex set includes the conical singularities $V_0 \subset V$ and all edges are geodesics on (M, d).

Remark 7.8. In general a geodesic triangulation on a piecewise flat surface does not have to come from a polyhedral surface.

The geodesic triangulation fixes the polyhedral metric of the piecewise flat surface. Its triangles are isometric to Euclidean triangles with straight edges and the polyhedral metric is determined by the lengths of the edges.
The Euclidean triangles on the other hand are uniquely determined by the lengths of its edges if and only if these satisfy the triangle-inequality.
We obtain the following general construction on how to prescribe a polyhedral metric.[31]

- Start with an abstract discrete surface $\mathcal{S} = (M, T)$ where T is a triangulation.
- Define a length function $l : E \to \mathbb{R}_+$ on the edges E of T such that on every face the triangle-inequality is satisfied.

From this data we can construct unique Euclidean triangles which fit together along corresponding edges of T. We can always glue the obtained Euclidean triangles together along the edges around one common vertex –thus obtaining a polyhedral metric on the abstract surface $\mathcal{S}$– but we cannot be sure that they will fit together to constitute a whole polyhedral surface. Summing up the angles at corresponding vertices we obtain the angle defect of the conical singularities of the polyhedral metric.

We get closer to the answer of the questions:

> Is a piecewise flat surface always realizable as a polyhedral surface?
> And is the corresponding polyhedral surface uniquely determined?

Isometric deformations of a simplicial surface preserve its polyhedral metric and therefore the corresponding piecewise flat surface.

Example 7.3 (pushing a vertex in)**.** If all neighbors of a vertex p are coplanar we can reflect the whole vertex star in this plane without changing any angles.

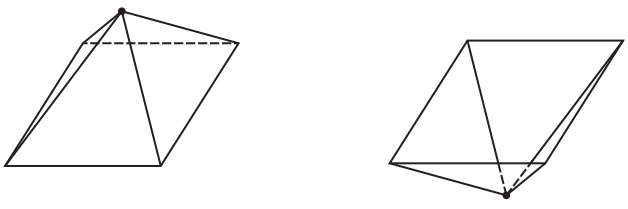

Figure 7.10. Pushing a vertex in does not change the metric.

We obtain the same piecewise flat surface with the same geodesic triangulation. So the polyhedral surface generating a piecewise flat surface is in general not unique.

[31] Note that choosing a triangulation of M –i.e. gluing M together from triangles– to prescribe the polyhedral metric is still eminent in this construction.

Example 7.4 (isometric bending of a polyhedral quadrilateral and edge flipping)**.** Consider two planar triangles with a common edge. Isometrically unfolding the two triangles along the common edge we obtain a planar quadrilateral. If the quadrilateral is convex we can replace the edge by the other diagonal and fold the quadrilateral along this new edge.

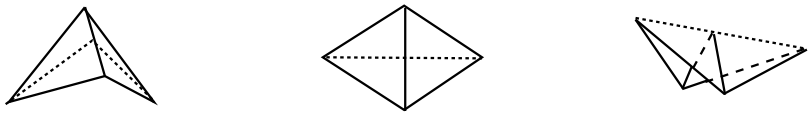

Figure 7.11. Edge flip. Isometrically unfold a quadrilateral to a plane and fold it along the other diagonal.

The edge flip can be done directly on the polyhedral surface without any folding by introducing a non-straight edge.
We obtain a different geodesic triangulation on the same piecewise flat surface which does not necessarily come from a polyhedral surface anymore.

Lemma 7.8 (Possibility of an edge-flip)**.** *Let (M, d) be a piecewise flat surface with a geodesic triangulation T.*
Then an edge e of T can be flipped if its two neighboring triangles are distinct and unfolding them into a plane yields a convex quadrilateral.

Remark 7.9. Since we admit non-regular triangulations we need the condition of the two triangles to be distinct to make the edge flip combinatorially possible.

Example 7.5 (tetrahedron)**.** Four congruent equilateral triangles can be glued together to obtain a tetrahedron.

Figure 7.12. Two geodesic triangulations of the piecewise flat surface given by a tetrahedron.

An edge-flip of one of their edges constitute four triangles which do not fit together as a whole polyhedral surface with the given combinatorics.

We have seen that not every geodesic triangulation of a piecewise flat surface is realizable as a polyhedral surface. Nor is the polyhedral surface we seek uniquely determined even if we know the combinatorics.

We finish this section by stating two classical theorems.

Theorem 7.9 (Burago-Zalgaller, 1960)**.** *Every piecewise flat surface can be realized as a polyhedral surface embedded in* $\mathbb{R}^3$*.*

Remark 7.10*.*

- Note that the ambient space can always be taken to be $\mathbb{R}^3$.
- This is a pure existence statement and the proof gives no indication on how to construct the polyhedral surface.

For convex polyhedral metrics the corresponding polyhedral surface which is convex is unique and can be obtained via a construction algorithm.

Theorem 7.10 (Alexandrov)**.** *Let* (M, d) *be a piecewise flat sphere with a convex polyhedral metric* d*. Then there exists a convex polytope* $\mathcal{P} \subset \mathbb{R}^3$ *such that the boundary of* $\mathcal{P}$ *is isometric to* (M, d)*. Besides,* $\mathcal{P}$ *is unique up to a rigid motion.*

Remark 7.11*.*

- A polyhedral metric d with conical singularities $P_1, \ldots, P_N$ is called convex if all its conical singularities are elliptic, i.e. $K(P_i) \geqslant 0$.
- The edges of $\mathcal{P}$ are a complicated functions of d, since the metric does not distinguish points on edges from points on faces.
- For a proof of this theorem with a construction algorithm see [**alexandrov-theorem**].
- An implementation of the algorithm can be found at [**sechel**].

8 Discrete cotan Laplace operator

We introduce a discrete Laplace operator naturally induced by a simplicial surface (or more general by a geodesic triangulation of a piecewise flat surface).

8.1 Smooth Laplace operator in $\mathbb{R}^N$

Let $\Omega \subset \mathbb{R}^N$ be an open set with boundary $\partial\Omega$. We denote the coordinates in $\mathbb{R}^N$ by $x = (x_1, ..., x_N)$. The Laplace operator of a function $f : \Omega \to \mathbb{R}$ is defined by

$$\Delta f = \sum_{i=1}^{N} \frac{\partial^2 f}{\partial x_i^2}$$

A function with $\Delta f = 0$ is called *harmonic*.
The problem of finding a harmonic function with prescribed boundary data $g : \partial\Omega \to \mathbb{R}$

$$\Delta f|_\Omega = 0, \quad f|_{\partial\Omega} = g \tag{DBVP}$$

is known as the *Dirichlet boundary value problem*.
The *Dirichlet energy* is given by

$$E(f) = \frac{1}{2} \int_\Omega |\nabla f|^2 \, \mathrm{d}A,$$

where ∇f is the gradient of f.
Let $\varphi \in \mathcal{C}_0^1(\Omega)$ be a continuously differentiable function with compact support on Ω. Then due to Green's formula

$$\frac{d}{dt} E(f + t\varphi)|_{t=0} = \int_\Omega \langle \nabla f, \nabla \varphi \rangle \mathrm{d}A = \int_\Omega \varphi(\Delta f) \mathrm{d}A.$$

This integral vanishes for arbitrary φ if and only if f is harmonic. So harmonic functions are the critical points of the Dirichlet energy.
For sufficient smooth boundary[32] one can prove the existence and uniqueness of solutions of the Dirichlet boundary value problem (DBVP) for arbitrary continuous $g \in \mathcal{C}(\partial\Omega)$. This solution minimizes the Dirichlet energy.

Remark 8.1. Sometimes the Laplace operator is defined with minus sign to obtain a positive definite operator.

[32] For example of Hölder class $\partial\Omega \in \mathcal{C}^{1+a}$, with some $a > 0$.

8.2 Laplace operator on graphs

Definition 8.1 (Laplace operator and Dirichlet energy on graphs)**.** Let $G = (V, E)$ be a finite graph with vertices V and edges E. Let $\nu : E \to \mathbb{R}$ be a *weight function* defined on the edges of G.
Then the *discrete Laplace operator* on G with weights ν is defined by

$$(\Delta f)(i) = \sum_{j:(ij)=e\in E} \nu(e)(f(i) - f(j))$$

for all $i \in V$ and all functions $f : V \to \mathbb{R}$ on vertices.
The *Dirichlet energy* of f is defined by

$$E(f) = \frac{1}{2} \sum_{(ij)=e\in E} \nu(e)(f(i) - f(j))^2.$$

A function $f : V \to \mathbb{R}$ satisfying $\Delta f = 0$ is called *discrete harmonic*.

Example 8.1. By setting $\nu(e) = 1$ for all $e \in E$ one obtains the *combinatorial Laplace operator*

$$(\Delta f)(i) = \sum_{j:(ij)\in E} (f(i) - f(j))$$

on any graph G.
In the case $G = \mathbb{Z}$ we obtain

$$(\Delta f)(n) = 2f(n) - f(n + 1) - f(n - 1),$$

and for $G = \mathbb{Z}^2$

$$(\Delta f)(n, m) = 4f(m, n) - f(m - 1, n) - f(m + 1, n) - f(m, n - 1) - f(m, n + 1).$$

Let $V_0 \subset V$ (treated as the "boundary" of G).

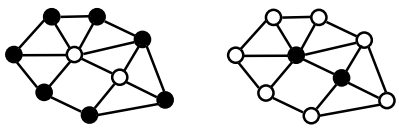

Figure 8.1. The set V_0 of "boundary" vertices on a graph (black vertices in the figure) is arbitrary.

Given some $c : V_0 \to \mathbb{R}$ consider the space of functions with prescribed values on the boundary

$$\mathcal{F}_{V_0,c} = \left\{ f : V \to \mathbb{R} \mid \ f|_{V_0} = c|_{V_0} \right\}.$$

This is an affine space over the vector space $\mathcal{F}_{V_0,0}$.

Theorem 8.1. *A function $f : V \to \mathbb{R}$ is a critical point of the Dirichlet energy $E(f)$ on $\mathcal{F}_{V_0,c}$ if and only if it is harmonic on $V\backslash V_0$, i.e.*

$$\Delta f(i) = 0 \quad \forall i \in V\backslash V_0.$$

Proof. Consider a variation $f + t\varphi \in \mathcal{F}_{V_0,c}$ of $f \in \mathcal{F}_{V_0,c}$, i.e. $\varphi \in \mathcal{F}_{V_0,0}$. We have

$$\begin{aligned} E(f + t\varphi) &= E(f) + t^2 E(\varphi) + t \sum_{(ij)\in E} \nu(ij)(f(i) - f(j))(\varphi(i) - \varphi(j)) \\ &= E(f) + t^2 E(\varphi) + t \sum_{i\in V} \varphi(i) \sum_{j:(ij)\in E} \nu(ij)(f(i) - f(j)) \\ &= E(f) + t^2 E(\varphi) + t \sum_{i\in V} \varphi(i)(\Delta f)(i). \end{aligned}$$

So

$$\left.\frac{\mathrm{d}}{\mathrm{d}t}\right|_{t=0} E(f + t\varphi) = \sum_{i\in V} \varphi(i)(\Delta f)(i)$$

vanishes for all $\varphi \in \mathcal{F}_{V_0,0}$ if and only if $\Delta f(i) = 0$ for all $i \in V\backslash V_0$. □

If all the weights are positive $\nu : E \to \mathbb{R}_+$ then the discrete harmonic functions have properties familiar from the smooth case.

Theorem 8.2 (maximum principle)**.** *Let $G = (V, E)$ be a connected graph and $V_0 \subset V$. Let Δ be a discrete Laplace operator on G with positive weights. Then a function $f : V \to \mathbb{R}$ which is harmonic on $V\backslash V_0$ can not attain its maximum (and minimum) on $V\backslash V_0$.*

Proof. At a local maximum $i \in V \subset V_0$ of f one has $\Delta f(i) = \sum_{j:(ij)\in E} \nu(ij)(f(i) - f(j)) > 0$, therefore f cannot be harmonic. □

For $V_0 = \varnothing$ this implies:

Corollary 8.3 (discrete Liouville theorem)**.** *A harmonic function on a connected graph is constant.*

and for $V_0 \neq \varnothing$:

Corollary 8.4 (dDBVP, uniqueness)**.** *The solution of the discrete Dirichlet boundary value problem*

$$\Delta f|_{V\backslash V_0} = 0, \quad f|_{V_0} = c \tag{dDBVP}$$

is unique.

Proof. Let $f, \tilde{f}$ be two solutions of (dDBVP). Then $\varphi \coloneqq \tilde{f} - f \in \mathcal{F}_{V_0,0}$ for which the maximum principle implies $\varphi|_V = 0$. □

Theorem 8.5. *Let $G = (E, V)$ be a finite connected graph with positive weights $\nu : E \to \mathbb{R}_+$ and $\varnothing \neq V_0 \subset V$. Given some $c : V_0 \to \mathbb{R}$ there exists a unique minimum $f : V \to \mathbb{R}$ of the Dirichlet energy on $\mathcal{F}_{V_0,c}$.*
This minimum is the unique solution of the discrete Dirichlet boundary value problem (dDBVP).

Proof. The Dirichlet energy is a function on $\mathcal{F}_{V_0,c} \cong \mathbb{R}^{|V\setminus V_0|}$. We investigate its behavior for $\left\| f|_{V\setminus V_0} \right\| \to \infty$. Define

$$\nu_0 := \min_E\{\nu(e)\}, \quad c_0 := \max_{i\in V_0}\{c(i)\}.$$

For $R > c_0$ let $f(k) > R$ at some vertex $k \in V\setminus V_0$. Let $\gamma_k \subset E$ be a path connecting k to some vertex in V_0. It has at most $|E|$ edges. For the Dirichlet energy this gives the following rough estimate:[33]

$$\begin{aligned} E(f) &\geqslant \frac{1}{2}\nu_0 \sum_{(ij)\in\gamma_k} (f(i) - f(j))^2 \\ &\geqslant \frac{1}{2}\nu_0 \frac{(R - c_0)}{|E|} \to \infty \quad (R \to \infty). \end{aligned}$$

Thus the minimum of the Dirichlet energy is attained on a compact set $\{f \in \mathcal{F}_{V_0,c} \mid |f(i)| < R \ \forall i\}$ with some $R \in \mathbb{R}$.
The uniqueness has already been shown in Corollary 8.4. □

Summarizing we have the following equivalent statements:

- $f \in \mathcal{F}_{V_0,c}$ harmonic, i.e. $\Delta f|_{V\setminus V_0} = 0$, $f|_{V_0} = c$.
- f is a critical point of the Dirichlet energy on $\mathcal{F}_{V_0,c}$, i.e. $\nabla_f E = 0$.
- f is the unique minimum of the Dirichlet energy E on $\mathcal{F}_{V_0,c}$.

[33] Where we use $\sum_{i=1}^n a_i^2 \geqslant \frac{1}{n}\left(\sum_{i=1}^n a_i\right)^2$.

8.3 Dirichlet energy of piecewise affine functions

We compute the Dirichlet energy of an affine function on a triangle.
Denote by 1, 2, 3 the vertices of a triangle F and by $\varphi_1, \varphi_2, \varphi_3$ the basis of affine functions on F given by

$$\varphi_j(i) = \delta_{ij}, \quad i, j = 1, 2, 3.$$

Then $\varphi_1 + \varphi_2 + \varphi_3 = 1$ and an affine function $f : F \to \mathbb{R}$ on the triangle F is determined by its values $f_i = f(i)$ at the vertices:

$$f = \sum_{i=1}^{3} f_i \varphi_i.$$

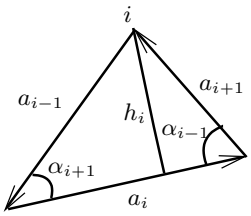

Figure 8.2. Triangle F with vertices i, sides a_i, angles α_i and heights h_i.

For gradient of f we get

$$|\nabla f|^2 = \left| \sum_{i=1}^{3} f_i^2 \nabla \varphi_i \right|^2 = \sum_{i=1}^{3} f_i \left|\nabla \varphi_i\right|^2 + 2 \sum_{i=1}^{3} f_i f_{i+1} \langle \nabla \varphi_i, \nabla \varphi_{i+1} \rangle, \tag{8.1}$$

where the indices are considered modulo 3.
For the gradient $\nabla \varphi_i$ we calculate further

$$\begin{aligned} \left|\nabla \varphi_i\right|^2 &= \frac{1}{h_i^2} = \frac{1}{2A(F)} \frac{|a_i|}{h_i} = \frac{1}{2A(F)} (\cot \alpha_{i-1} + \cot \alpha_{i+1}), \\ \langle \nabla \varphi_i, \nabla \varphi_{i+1} \rangle &= \frac{\langle a_i, a_{i+1} \rangle}{4A(F)^2} = \frac{|a_i|\,|a_{i+1}| \cos \alpha_{i-1}}{4A(F)^2} = -\frac{\cot \alpha_{i-1}}{2A(F)}, \end{aligned}$$

where $a_i \in \mathbb{R}^2$ is the side opposite i and h_i the height at the vertex i. The area of the triangle is $A(F) = \frac{1}{2} h_i \,|a_i|$.
For the gradient (8.1) of f this implies

$$|\nabla f|^2 = \frac{1}{2A(F)} \sum_{i=1}^{3} (f_{i+1} - f_{i-1})^2 \cot \alpha_i.$$

Multiplying by $\frac{1}{2} A(F)$ we obtain the Dirichlet energy of f on F:

$$E(f) = \frac{1}{2} \int_F |\nabla f|^2 \, \mathrm{d}A = \frac{1}{4} \sum_{i=1}^{3} (f_{i+1} - f_{i-1})^2 \cot \alpha_i.$$

Theorem 8.6. *Let S be a simplicial surface and $f : S \to \mathbb{R}$ a continuous and piecewise affine function (affine on each face of S).*
Then its Dirichlet energy is

$$E(f) = \frac{1}{2} \sum_{(ij)\in E} \nu(ij)(f(i) - f(j))^2,$$

with weights

$$\nu(ij) = \begin{cases} \frac{1}{2} \ (\cot \alpha_{ij} + \cot \alpha_{ji}) & \textit{for internal edges} \\ \frac{1}{2} \ \cot \alpha_{ij} & \textit{for external edges} \end{cases} \tag{8.2}$$

called cotan-weights.

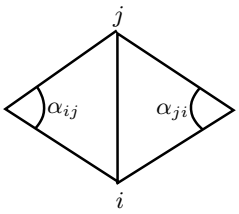

Figure 8.3. α_{ij} and α_{ji} are the angles opposite the edge (ij).

A discrete function $f : V \to \mathbb{R}$ defined at the vertices of a simplicial surface S uniquely extends to a piecewise affine function $f : S \to \mathbb{R}$.
Even more for a discrete function $f : V \to \mathbb{R}$ defined at the vertices of a geodesic triangulation of a piecewise flat surface (M, d) we can unfold each triangle to the Euclidean plane and define its Dirichlet energy by the affine extension to this triangle in the same way. We define the corresponding discrete Laplace operator on triangulated piecewise flat surfaces.

Definition 8.2 (discrete cotan Laplace operator)**.** Let (M, d) be a piecewise flat surface, $V \subset M$ a finite set of points that contains all conical singularities. Let $T \in \mathcal{T}_{M,V}$ be a geodesic triangulation of M.
Then we define the *discrete cotan Laplace operator* of T by

$$(\Delta f)(i) \coloneqq \sum_{j:(ij)\in E} \nu(ij)(f(i) - f(j))$$

for all $i \in V$ and all discrete functions $f : V \to \mathbb{R}$, with cotan-weights as defined in (8.2).

8.4 Simplicial minimal surfaces (I)

The area of simplicial surfaces can be represented as a Dirichlet energy.
The area of the triangle ABC with angles α, β, γ and edge lengths a, b, c is equal to

$$\frac{1}{4}(a^2 \cot\alpha + b^2 \cot\beta + c^2 \cot\gamma).$$

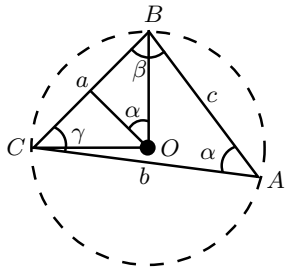

Figure 8.4. Subdivide the triangle ABC into three triangles by connecting the center O of the circumcircle to its vertices. The area of the triangle OBC is $\frac{1}{4}a^2 \cot\alpha$

Let $f : \mathcal{S} \to \mathbb{R}^N$ be a simplicial surface $S \coloneqq f(\mathcal{S})$. Then its total area is given by

$$A(S) = \frac{1}{2} \sum_{(i,j)\in E} \nu(ij)\|f(i) - f(j)\|^2$$

with cotan-weights ν as defined in (8.2). The square of the edge lengths is

$$\|f(i) - f(j)\|^2 = \sum_{k=1}^{N} |f_k(i) - f_k(j)|^2.$$

Theorem 8.7. *Let $f : \mathcal{S} \to \mathbb{R}^N$, $S \coloneqq f(\mathcal{S})$ be a simplicial surface. It is completely determined by its vertices $f : V \to \mathbb{R}^N$. Its area is given by*

$$A(S) = \sum_{k=1}^{N} E(f_k),$$

where $E(f_k)$ is the Dirichlet energy of the k-th coordinate function.
The area gradient at the vertex $f(i)$ is equal to the discrete cotan Laplace operator of f at i

$$\nabla_{f(i)} A(S) = (\Delta f)(i) = \sum_{j:(i,j)\in E} \nu(ij)(f(i) - f(j)).$$

Proof. Consider a variation $f + t\varphi$ of the vertex $i \in V$ only, i.e.

$$\varphi(j) = y\delta_{ij}$$

for all $j \in V$ with some $y \in \mathbb{R}^N$. Then

$$\begin{aligned}\left.\frac{\mathrm{d}}{\mathrm{d}t}\right|_{t=0} A(f + t\varphi) &= \sum_{k=1}^{N} \left.\frac{\mathrm{d}}{\mathrm{d}t}\right|_{t=0} E(f_k + t\varphi_k) \\ &= \sum_{k=1}^{N} y_k \Delta f_k(i) = \langle y, \Delta f(i)\rangle,\end{aligned}$$

which is

$$\nabla_{f(i)} A(S) = (\Delta f)(i).$$

□

Remark 8.2.

- Note that f is involved in the definition of Δ since the weights are determined by the geometry of the simplicial surface.
- For $u : V \to \mathbb{R}^N$ the equation $\Delta u = 0$ is to be understood component-wise, i.e.
$$\Delta u = 0 \;\Leftrightarrow\; \Delta u_k = 0 \;\forall k = 1, \ldots, N.$$

We have

f harmonic (w.r.t. cotan Laplace) $\;\Leftrightarrow\;$ S critical for the area functional.

So we might define *simplicial minimal surfaces* as suggested in [**cotan-minimal**] by

$$S \text{ discrete minimal surface } :\Leftrightarrow\; \Delta f = 0,$$

which immediately comes with a computation algorithm.

Data: Simplicial surface $f : \mathcal{S} \to S \subset \mathbb{R}^N$
Result: Simplicial minimal surface (w.r.t. cotan Laplace operator).
while *S is not critical for the area functional* **do**
  Compute $\tilde{f}$ such that
  $$\Delta \tilde{f} = 0$$
  which defines a new simplicial surface $\tilde{S}$;
  Replace S by the new surface $\tilde{S}$;
end

Figure 8.5. Simplicial minimal surface algorithm (with cotan Laplace operator).

Remark 8.3. In each step a new simplicial surface is generated which carries a new cotan Laplace operator.

The weights ν of the discrete cotan Laplace operator can be negative. So it lacks the following property which is a reformulation of the maximum principle for $\mathbb{R}^N$-valued functions.

Proposition 8.8 (local maximum principle)**.** *Let Δ be a discrete Laplace operator on a graph G with positive weights. Let $u : V \to \mathbb{R}^N$ be a map which is harmonic at a vertex $i \in V$.*
Then the value $u(i)$ at the vertex i lies in the convex hull of the values of its neighbors.

Proof. With

$$C \coloneqq \sum_{j:(ij)\in E} \nu(ij)$$

we have

$$\begin{aligned}(\Delta f)(i) &= \sum_{j:(ij)\in E} \nu(ij)\,(f(i) - f(j)) = 0\\ \Leftrightarrow\ f(i) &= \sum_{j:(ij)\in E} \frac{\nu(ij)}{C} f(j).\end{aligned}$$

□

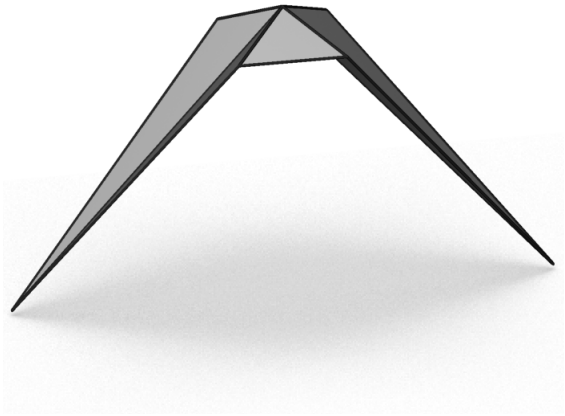

Figure 8.6. Simplicial minimal surface violating the maximum principle. One vertex does not lie in the convex hull of its neighbors.

The maximum principle is a desirable feature analogous to the smooth property of all points of a minimal surface being hyperbolic. So we ask the question

When does the cotan Laplace operator have positive weights?

For an edge $(ij) \in E$ we have

$$\begin{aligned}\nu(ij) &= \frac{1}{2}(\cot\alpha_{ij} + \cot\alpha_{ji})\\ &= \frac{1}{2}\left(\frac{\cos\alpha_{ij}\sin\alpha_{ji} + \cos\alpha_{ji}\sin\alpha_{ij}}{\sin\alpha_{ij}\sin\alpha_{ji}}\right)\\ &= \frac{\sin(\alpha_{ij}+\alpha_{ji})}{\sin\alpha_{ij}\sin\alpha_{ji}} \geqslant 0 \ \Leftrightarrow\ \alpha_{ij}+\alpha_{ji} \leqslant \pi,\end{aligned} \tag{8.3}$$

which is not satisfied for the long edges in Figure 8.6. We will come back to this when introducing the discrete Laplace-Beltrami operator.

9 Delaunay tessellations

We have noted that the polyhedral metric of a piecewise flat surface (M, d) carries no obvious information about edges and faces. In the following we show how to use the metric to obtain a distinguished geodesic tessellation of (M, d). After recalling the notion of Delaunay tessellations of the plane we demonstrate how to generalize it to piecewise flat surfaces.

9.1 Delaunay tessellations of the plane

9.1.1 Delaunay tessellations from Voronoi tessellations

Consider n distinct points in the plane $V = \{P_1, \dots, P_n\} \subset \mathbb{R}^2$. For each $P_i \in V$ one defines the *Voronoi region*

$$W_{P_i} \coloneqq \left\{P \in \mathbb{R}^2 \mid |PP_i| < |PP_j| \ \forall j \neq i\right\}.$$

With $H_{ij} \coloneqq \left\{P \in \mathbb{R}^2 \mid |PP_i| < |PP_j|\right\}$ we have $W_{P_i} = \bigcap_{j \neq i} H_{ij}$. Thus Voronoi regions are convex polygons.

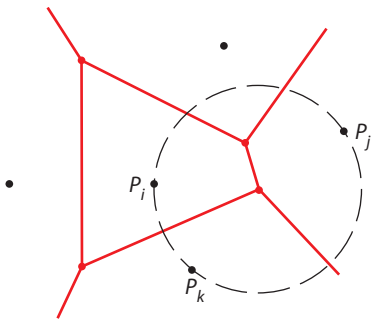

Figure 9.1. Voronoi tessellation for some given points $V = \{P_1, \dots, P_n\}$ in the plane. A vertex Q of the Voronoi tessellation has equal shortest distance to at least three points of V.

Voronoi regions are the 2-cells of the *Voronoi tessellation*.[34]
For $P \in \mathbb{R}^2$ consider

$$\Gamma_{P,V} \coloneqq \left\{P_j \in V \mid |PP_j| = \min_{P_k \in V} |PP_k|\right\}.$$

We can identify points of 2-cells, 1-cells and 0-cells of the Voronoi tessellation by counting points in V that have equal shortest distance to P.
The 2-cells of the Voronoi tessellation are the connected components of

$$\left\{P \in \mathbb{R}^2 \mid \#\Gamma_{P,V} = 1\right\},$$

the 1-cells are the connected components of

$$\left\{P \in \mathbb{R}^2 \mid \#\Gamma_{P,V} = 2\right\},$$

[34] A tessellation is a cell-decomposition with polygonal 2-cells.

and the 0-cells are the points in

$$\left\{P \in \mathbb{R}^2 \mid \#\Gamma_{P,V} \geqslant 3\right\}.$$

For $P' \in \mathbb{R}^2$ with $\#\Gamma_{P',V} = 2$, $P_i, P_j \in \Gamma_{P',V}$, $P_i \neq P_j$ the corresponding 1-cell is given by

$$\left\{P \in \mathbb{R}^2 \mid |PP_i| = |PP_j| < |PP_k| \ \forall k \neq i,j\right\},$$

and for $P \in \mathbb{R}^2$ with $\#\Gamma_P \geqslant 3$, $P_i, P_j, P_k \in \Gamma_{P,V}$ different, the corresponding 0-cell is given by

$$\left\{P \in \mathbb{R}^2 \mid |PP_i| = |PP_j| = |PP_k| \leqslant |PP_m| \ \forall m\right\}.$$

Let Q be a vertex of the Voronoi tessellation, i.e.

$$\exists i,j,k \ \forall m: \ r_Q \coloneqq |PP_i| = |PP_j| = |PP_k| \leqslant |PP_m|.$$

Define the disk

$$D_Q \coloneqq \left\{P \in \mathbb{R}^2 \mid |PQ| < r_Q\right\}.$$

It contains no points of V. But its closure $\bar{D}_Q$ contains at least three. Thus

$$H_Q \coloneqq \operatorname{conv}\left\{P_i \in V \mid |QP_i| = r_Q\right\}$$

is a convex circular polygon.

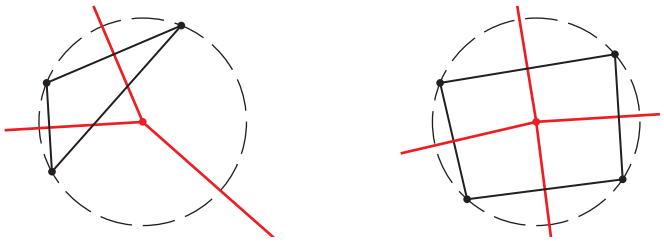

Figure 9.2. Delaunay cells are convex circular polygons. They are triangles in the generic case.

The H_Q are the 2-cells of the *Delaunay tessellation*.
The vertices of this tessellation are V and the edges (P_iP_j) where i,j are indices of neighboring Voronoi cells, i.e. there exists a corresponding Voronoi edge.

Remark 9.1.

- Voronoi and Delaunay tessellations are dual cell-decompositions.
- Corresponding edges of the Voronoi and Delaunay tessellation are orthogonal but do not necessarily intersect (see Figure 9.2). The Voronoi edge bisects the corresponding Delaunay edge.
- Voronoi and Delaunay tessellations of the plane are strongly regular.

- One can also introduce a Delaunay-Voronoi quad-tessellation as a composition of both:

Figure 9.3. Voronoi-Delaunay quad tessellation. Faces (dotted lines) are convex or non-convex kites.

Vertices are the union of Voronoi and Delaunay vertices.
Edges are the intervals connecting the centers of Voronoi cells with their vertices or alternatively the centers of Delaunay cells with their vertices.
Faces are embedded quads with orthogonal diagonals and the diagonal which is a Delaunay-edge is bisected into two equal intervals by the line through the orthogonal Voronoi-edge.

Theorem 9.1. *Given a set of distinct points* $V = \{P_1, \ldots, P_n\} \in \mathbb{R}^2$ *there exists a unique Voronoi and Delaunay tessellation.*
These tessellations are dual to each other: The Delaunay vertices V *are the generating points of the Voronoi tessellation. The Delaunay faces are convex circular polygons centered at Voronoi vertices. The corresponding edges of the Voronoi and Delaunay tessellations are orthogonal.*

9.1.2 Delaunay tessellations in terms of the empty disk property

How to define Delaunay tessellations without referring to Voronoi?
We noticed that:

> All faces of a Delaunay tessellation are convex circular polygons.
> The corresponding Delaunay open disks D_Q contain no vertices.

and call this the *empty disk property*.

Definition 9.1. A tessellation of a planar domain is called *Delaunay* if it possesses the empty disk property.
An edge of a tessellation is called *Delaunay edge* if two faces sharing this edge do not have any of their vertices in the interior of their disks.

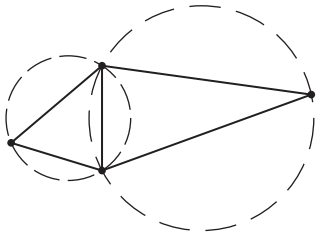

Figure 9.4. Empty disk property of Delaunay tessellations.

Theorem 9.2. *The property of being a Delaunay tessellation is invariant under Möbius transformations.*

Proof. Follows directly from the empty disk property being Möbius invariant. □

Remark 9.2. Delaunay tessellations on $\mathbb{S}^2$ can be obtained by stereographic projection.

Lemma 9.3 (angle criterion for circular quadrilaterals)**.** *Let $P_1, P_2, P_3, P_4 \in \mathbb{R}^2$ be four points in the plane cyclically ordered. Let C be the circle through P_1, P_2, P_3,*

$$\alpha \coloneqq \measuredangle P_1P_2P_3, \quad \beta \coloneqq \measuredangle P_3P_4P_1.$$

Then

$$\begin{aligned} P_4 \text{ lies outside } C &\Leftrightarrow \alpha + \beta < \pi \\ P_4 \text{ lies on } C &\Leftrightarrow \alpha + \beta = \pi \\ P_4 \text{ lies inside } C &\Leftrightarrow \alpha + \beta > \pi. \end{aligned}$$

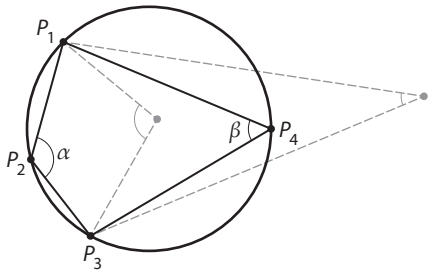

Figure 9.5. Angle criterion for circular quadrilaterals.

Proposition 9.4 (angle criterion for Delaunay triangulations)**.** *A triangulation of the plane is Delaunay if and only if for each edge the sum of the two angles opposite to this edge is less than or equal to π.*

9.2 Delaunay tessellations of piecewise flat surfaces

9.2.1 Delaunay tessellations from Voronoi tessellations

Let (M, d) be a piecewise flat surface. Let $V = \{P_1, \ldots, P_n\}$ be points on M such that $V \supset \{\text{conical singularities of } (M, d)\}$.
On M –in contrast to the planar case– it can happen that the distance between two points is realized by more than one geodesic. The suitable generalization of counting points of equal shortest distance to V is counting geodesics that realize this distance. For $P \in M$ we define

$$\Gamma_{P,V} \coloneqq \{\gamma : [0,1] \to M \text{ geodesic} \mid \gamma(0) = P,\ \gamma(1) \in V,\ \mathrm{L}(\gamma) = d(P,V)\}.$$

The 2-cells of the *Voronoi tessellation* of M with vertex set V are the connected components of

$$\{P \in M \mid \#\Gamma_{P,V} = 1\},$$

the 1-cells are the connected components of

$$\{P \in M \mid \#\Gamma_{P,V} = 2\},$$

and the 0-cells are the points in

$$\{P \in M \mid \#\Gamma_{P,V} \geqslant 3\}.$$

We can try to describe the cells in a similar manner as in the planar case. E.g. for $P' \in M$ with $\#\Gamma_{P',V} = 2$, $\gamma_1, \gamma_2 \in \Gamma_{P'}$, $\gamma_1 \neq \gamma_2$, $P_i = \gamma_1(1), P_j = \gamma_2(1) \in V$ (possibly $i = j$) the corresponding 1-cell is given by

$$\left\{P \in M \mid d(P, P_i) = d(P, P_j) < d(P, P_k)\ \forall k \neq i, j \text{ (and } \#\Gamma_{P,\{P_i,P_j\}} = 2)\right\}.$$

Example 9.1 (Voronoi tessellation of a cube)**.** Let V be the set of vertices of a cube.

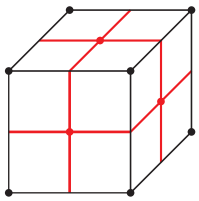

Figure 9.6. Voronoi tessellation of a cube.

Let P be an internal point of a Voronoi edge. Then there is $P_i, P_j \in V$ (possibly $i = j$) such that

$$d(P, P_i) = d(P, P_j) < d(P, P_k)\ \forall k \neq i, j.$$

This describes an *empty immersed disk* centered at P with exactly two elements of V on the boundary.[35]
The endpoints of Voronoi edges are Voronoi vertices. Let Q be such a point. Then there is $P_i, P_j, P_k \in V$ such that

$$d(Q, P_i) = d(Q, P_j) = d(Q, P_k) \leqslant d(Q, P_l)\ \forall l.$$

This describes an empty immersed disk centered at Q with at least three elements of V on the boundary.[36]
As in the plane the Delaunay tessellation is defined as dual to the Voronoi tessellation.

[35] Or one element but two different geodesics minimizing the distance to P.
[36] Or less but with at least three different geodesics minimizing the distance to P.

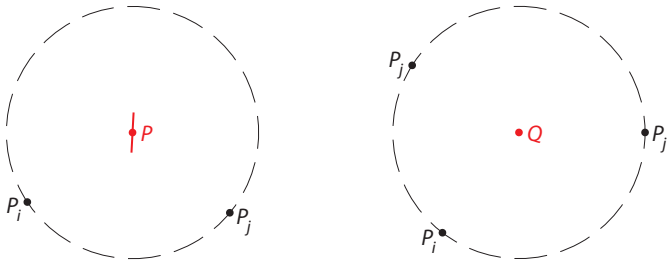

Figure 9.7. (left) An internal point P of a Voronoi edge. (right) A Voronoi vertex Q. Both are the center of an empty immersed disk on M with vertices on the boundary. The Delaunay edges are geodesic arcs connecting the points of V on the boundary, i.e. the Delaunay faces are flat circular polygons.

Remark 9.3. A *geodesic tessellation* of a piecewise flat surface (M, d) is a tessellation with flat polygonal 2-cells (compare Definition 7.6).
Delaunay tessellations are geodesic tessellations on M. The edges of Voronoi tessellations are geodesic arcs but it is not a geodesic tessellation since the faces are not flat.

Theorem 9.5. *Let (M, d) be a piecewise flat surface without boundary, $V \subset M$ a finite set of points that contains all conical singularities.*
Then there exists a unique Delaunay tessellation of M with vertex set V.

Remark 9.4.

- The proof via construction of the Voronoi tessellation can be found in [**masur˙hausdorff**].
- If one triangulates all Delaunay faces by triangulating the corresponding circular polygons in the corresponding empty immersed disks one can obtain *Delaunay triangulations*.[37]
  On the contrary, the unique Delaunay tessellation can be recovered from any Delaunay triangulation by deleting edges.
- We will show later how to construct a Delaunay triangulation starting from an arbitrary triangulation by applying an algorithm of consecutive edge flips.

9.2.2 Delaunay tessellations in terms of the empty disk property

We define Delaunay tessellations on a piecewise flat surface in a selfcontained way without referring to Voronoi.

Definition 9.2 (empty immersed disk)**.** Let (M, d) be a piecewise flat surface without boundary, $V \subset M$ a finite set of points that contains all conical singularities.
Then an *immersed empty disk* is a continuous map $\varphi : \bar{D} \to M$ such that $\varphi|_D$ is an isometric immersion[38] and $\varphi(D) \cap V = \varnothing$.

[37] In contrast to the Delaunay tessellation the Delaunay triangulation is not unique as soon as one has circular polygons which are not triangles.
[38] An isometric immersion is a local isometry, i.e. each $P \in D$ has a neighborhood which is mapped to M isometrically.

Definition 9.3 (Delaunay tessellation)**.** Let (M, d) be a piecewise flat surface without boundary, $V \subset M$ a finite set of points that contains all conical singularities.
The *Delaunay tessellation* of M with vertex set V is a cell-decomposition with the following cells:
$C \subset M$ is a closed cell of the Delaunay tessellation if there exists an immersed empty disk $\varphi : \bar{D} \to M$ such that $\varphi^{-1}(D) \neq \varnothing$ and $C = \varphi(\text{conv}\varphi^{-1}(V))$.
The cell is a 0-, 1-, 2-cell if $\varphi^{-1}(V)$ contains 1, 2, or more points respectively.

Claim 9.6. *This is indeed a tessellation.*

Remark 9.5. For the proof see [**laplace-beltrami**].

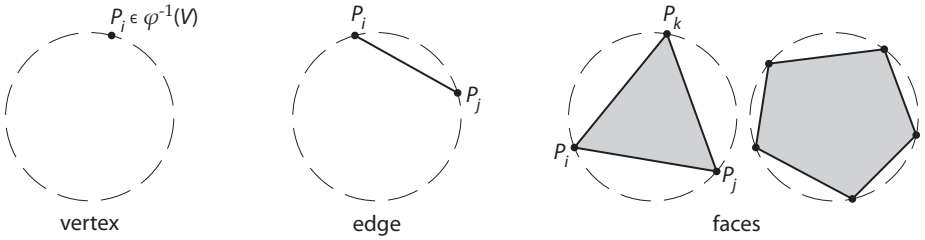

Figure 9.8. Delaunay cells and their corresponding empty immersed disks.

We characterize Delaunay triangulations in terms of a local edge property.

Definition 9.4 (Delaunay edge)**.** Let T be a geodesic triangulation of a piecewise flat surface (M, d). Let e be an interior edge of T. We can isometrically unfold the two triangles of T that are adjacent to e. e is called a *Delaunay edge* if the vertices of these unfolded triangles are not contained inside the circumcircles of the triangles.

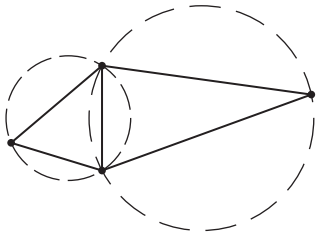

Figure 9.9. Unfolded triangles adjacent to a Delaunay edge. The inside of the circumcircles contain no vertices.

Theorem 9.7 (Characterization of Delaunay triangulations in terms of Delaunay edges)**.** *Let (M, d) be a piecewise flat surface without boundary, $V \subset M$ a finite set of points that contains all conical singularities.*
A geodesic triangulation $T \in \mathcal{T}_{M,V}$ of (M, d) is Delaunay if and only if all of its edges are Delaunay edges.

Remark 9.6. We first explain the general scheme used in the proof to obtain a locally isometric model in the Euclidean plane for parts of our surface M. We do some notably identifications on the way.

- For any face $\Delta \in F(T)$ there is a triangle in the Euclidean plane which can be isometrically immersed into the piecewise flat surface M (continuous on the boundary) such that its image corresponds to the face.
  Notationally we identify the combinatorial/metrical face on M and the unfolded Euclidean triangle.
- We extend the isometric immersion such that it stays an isometric immersion in the interior and continuous on the boundary.
  E.g. by some circular piece or a neighboring triangle.
- Note that we might not be able to extend it to the circumcircle of the unfolded triangle in the plane.
  That is why it is not obvious whether Delaunay edges imply the existence of empty immersed disks for their adjacent faces.
- Only inside the domain of this extended immersion can we be sure to draw straight lines and obtain geodesics on M and measure lengths and angles as they are on M, i.e. measure quantities in our planar isometric model that are well-defined by the piecewise flat surface.

Proof. If T is Delaunay obviously all edges are Delaunay edges.
Assume that all edges are Delaunay but the triangulation is not.

Any face $\Delta \in F(T)$ can be isometrically unfolded into the plane. We denote its circumcircle in the plane by D_Δ.
For an edge a of Δ consider the one-parameter family of circles in the plane through its endpoints. a divides the corresponding open disks into two parts of which we take the one that does not intersect Δ. We call them disk segments which fit to Δ along a.

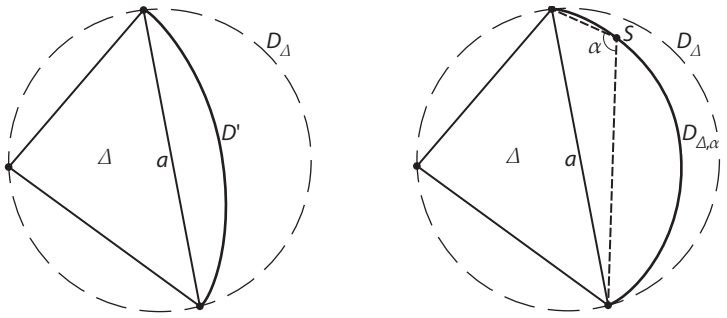

Figure 9.10. (left) Unfolded face Δ with circumcircle D_Δ and disk segment D' fitting to Δ along a. (right) We extend the isometric immersion of Δ behind the edge a to the largest possible disk segment $D_{\Delta,a}$. To every $(\Delta, a, S) \in \mathcal{A}$ we associate an angle α.

$$\mathcal{D}_{\Delta,a} \coloneqq \{D' \mid \text{disk segment fitting to } \Delta \text{ along } a,\\ \text{the isometric immersion of } \Delta \text{ can be extended to } D'\\ \text{(continuously to } \bar{D}'),\\ D' \cap V = \varnothing\}$$

For any edge a of a face Δ we denote the largest such disk segment by

$$D_{\Delta,a} \coloneqq \bigcup_{D' \in \mathcal{D}_{\Delta,a}} D'.$$

If $\mathcal{D}_{\Delta,a}$ is bounded, then $D_{\Delta,a} \in \mathcal{D}_{\Delta,a}$ and there has to be a vertex on the circular arc bounding $D_{\Delta,a}$, i.e.

$$(\partial D_{\Delta,a} \backslash \bar{a}) \cap V \neq \varnothing.$$

Otherwise we could enlarge $D_{\Delta,a}$.

A face Δ which has no empty immersed disk must have an edge a such that $(\bar{D}_{\Delta,a} \backslash \bar{a}) \subset D_\Delta$. Thus the set

$$\mathcal{A} \coloneqq \{(\Delta, a, S) \in F \times E \times V \mid \Delta \text{ has no empty immersed disk},\\ a \text{ is edge of } \Delta \text{ with } (\bar{D}_{\Delta,a} \backslash \bar{a}) \subset D_\Delta,\\ S \in (\partial D_{\Delta,a} \backslash \bar{a}) \cap V\}$$

is not empty.

We introduce the angle $\alpha : \mathcal{A} \to (0, \pi)$,

$$\alpha\,(\Delta, (BC), S) \coloneqq \measuredangle BSC.$$

Let $(\Delta, a, S) \in \mathcal{D}$ such that

$$\alpha(\Delta, a, S) = \max_{(\tilde{\Delta}, \tilde{a}, \tilde{S}) \in \mathcal{A}} \alpha(\tilde{\Delta}, \tilde{a}, \tilde{S}). \tag{9.1}$$

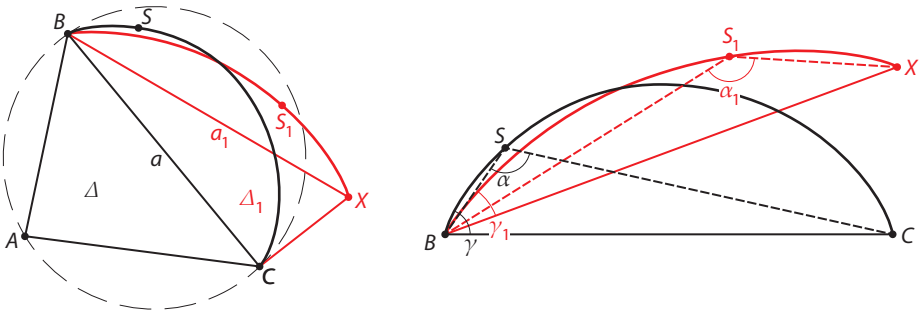

Figure 9.11. (left) For $(\Delta, a, S) \in \mathcal{A}$ we obtain a neighboring element $(\Delta_1, a_1, S_1 \in \mathcal{A}$. (right) We find $\alpha(\Delta_1, a_1, S_1) > \alpha(\Delta, a, S)$ since $\gamma_1 < \gamma$ in contradiction to the assumption.

Let Δ_1 be the face sharing the edge a with Δ. We can isometrically unfold it to the same plane as Δ. Let B, C be the endpoints of a and X the opposite vertex of Δ_1.

$$a \text{ Delaunay edge } \Rightarrow X \notin D_\Delta.$$

Since no triangle may contain any vertices we also have $S \notin \Delta_1$.
Let a_1 be the edge of Δ_1 closest to S, say $a_1 = (BX)$. Then there is $S_1 \in V$ (possibly $S_1 = S$) such that

$$(\Delta_1, a_1, S_1) \in \mathcal{A}.$$

Let us denote the corresponding angles by $\alpha \coloneqq \alpha(\Delta, a, S)$ and $\alpha_1 \coloneqq \alpha(\Delta_1, a_1, S_1)$. Due to Lemma 9.8 the angle $\gamma \coloneqq \pi - \alpha$ is the intersection angle of the circular arc of $\partial D_{\Delta,a}$ with a at B. Similarly γ_1.
Clearly, $\gamma > \gamma_1$ which implies

$$\alpha < \alpha_1$$

in contradiction to (9.1). □

Lemma 9.8. *Let B, S, C be three points on a circle, $\alpha \coloneqq \sphericalangle BSC$. Then the intersection angle between the tangent to the circle at B and the secant (BC) as depicted in Figure 9.12 is equal to α.*

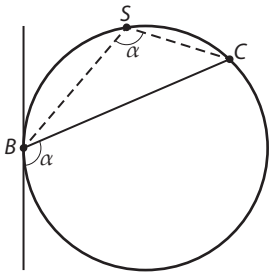

Figure 9.12. Angle in a circular arc.

Proof. While moving S along the circular arc the angle $\alpha = \sphericalangle BSC$ stays constant. In the limit $S \to B$ the edge (BS) becomes the tangent at B and $(SC) \to (BC)$. □

The characterization of Delaunay triangulations in terms of Delaunay edges allows us to formulate an angle criterion as in the planar case.

Proposition 9.9 (Angle criterion for Delaunay triangulations)**.** *A geodesic triangulation of a piecewise flat surface is Delaunay if and only if for every edge the sum of the two angles opposite to this edge is less than or equal to π.*

This is a practical geometric characterization since angles can be measured directly on the piecewise flat surface without any need to find empty immersed disks. Recalling (8.3) we notice at this point

Proposition 9.10. *The discrete cotan Laplace operator of a geodesic triangulation T of a piecewise flat surface (M, d) has non-negative weights if and only if T is Delaunay.*

9.3 The edge-flip algorithm

Let T be a geodesic triangulation of a piecewise flat surface (M, d).
If we unfold two adjacent triangles of T into the plane, we obtain a quadrilateral Q, where one of its diagonals e corresponds to the shared edge of the triangles and the other one e^* corresponds to the edge resulting in an edge flip of e if possible.

Lemma 9.11. *Every non-Delaunay edge of T can be flipped and the flipped edge is then Delaunay.*

Proof. Let e be a non-Delaunay edge.
We use Lemma 7.8 to characterize whether e can be flipped. The sum of the angles opposite to e in the adjacent triangles is greater than π. Therefore the two triangles have to be different since the sum of all angles in a triangle is equal to π. The two triangles form a convex quadrilateral as can be seen e.g. from Figure 9.5. So e can be flipped and the sum of the angles opposite to the flipped edge e^* is less than or equal to π. □

The following question emerges.

> Can any given triangulation be made Delaunay by consecutive edge-flips?

Definition 9.5. We denote the set of all geodesic triangulations of a given piecewise flat surface (M, d) with vertex set V by $\mathcal{T}_{M,V}$.

The edge-flip algorithm acts on $\mathcal{T}_{M,V}$ in the following way.

Data: Some $T \in \mathcal{T}_{M,V}$.
Result: A Delaunay triangulation $T \in \mathcal{T}_{M,V}$.
while T *is not Delaunay* **do**
  Take any non-Delaunay edge e of T;
  Flip e in T;
end

Figure 9.13. Edge-flip algorithm.

Example 9.2. We make the triangulation of the tetrahedron shown in Figure 9.14 Delaunay by applying the edge-flip algorithm.

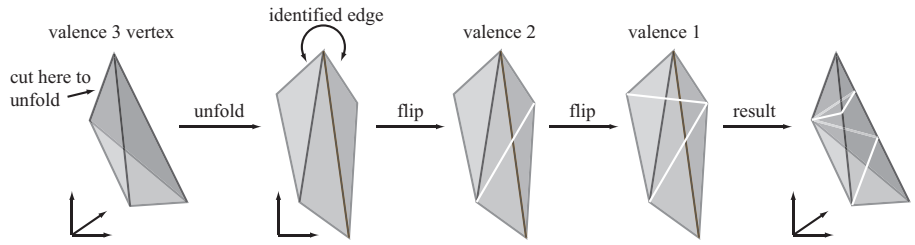

Figure 9.14. Making a given triangulation Delaunay.

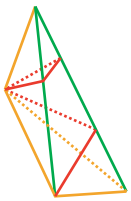

Figure 9.15. Result with colored edges. Green and yellow edges are original edges. Red and yellow edges are Delaunay edges.

Note that the resulting triangulation is not regular and has a vertex of valence one.

Theorem 9.12. *The edge-flip algorithm terminates for any start triangulation $T \in \mathcal{T}_{M,V}$ after a finite number of steps.*

Remark 9.7. Removing all edges which would stay Delaunay upon an edge-flip we obtain the unique Delaunay tessellation. Claiming the existence of some geodesic triangulation on any piecewise flat surface this implies Theorem 9.5. In practice having some start triangulation is not an issue since the standard ways of prescribing a piecewise flat surface already includes a triangulation.

The state of the algorithm is determined by the current triangulation in $\mathcal{T}_{M,V}$. We address the question of possible loops in the algorithm later by means of a function $f : \mathcal{T}_{M,V} \to \mathbb{R}$ that decreases on each step.

For a piecewise flat surface –in contrast to triangulations of a finite set of points in the plane– the set of all triangulations $\mathcal{T}_{M,V}$ is an infinite set in general.

Example 9.3 (infinitely many triangulations of the cube with arbitrary long edges)**.** Consider a standard cube with vertex set V. Unwrapping the cube as in Figure 7.8 suggests how to create an arbitrary long edge between two vertices of V. Completing to a triangulation we conclude that there are infinitely many triangulations of the cube.

So even with the exclusion of loops the algorithm might not terminate.

Definition 9.6 (proper function)**.** We call a function $f : \mathcal{T}_{M,V} \to \mathbb{R}$ proper if for each $c \in \mathbb{R}$ the sublevel set $\{T \in \mathcal{T}_{M,V} \mid f(T) \leqslant c\}$ is finite.

Having a proper decreasing function we can ensure termination after a finite number of steps.

Example 9.4 (edge length function)**.** For an edge e of a triangulation T we denote its length by $l(e)$. Consider the function $l : \mathcal{T}_{M,V} \to \mathbb{R}$ which assigns to each triangulation its maximal edge length

$$l(T) \coloneqq \max_{e \in E(T)} l(e).$$

As we have seen in Example 9.3 the function l might be unbound on $\mathcal{T}_{M,V}$. Nonetheless bounding l only leaves a finite number of triangulations.

Claim 9.13. *The edge length function l is proper.*

9.3.1 Dirichlet energy and edge-flips

Let T be a geodesic triangulation of a piecewise flat surface (M, d). We investigate the local change in the Dirichlet energy of a discrete function $u : V(T) \to \mathbb{R}$ upon an edge-flip.

The geometry of a convex non-degenerate quadrilateral Q with vertices $1, 2, 3, 4$ denoted in counter-clockwise direction is completely determined by the values of $r_1, r_2, r_3, r_4 > 0$ and $\theta \in (0, \pi)$ as depicted in Figure 9.16. We denote such a quadrilateral by $Q(r_1, r_2, r_3, r_4, \theta)$.

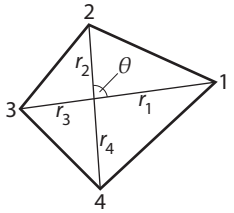

Figure 9.16. A convex non-degenerate quadrilateral $Q(r_1, r_2, r_3, r_4, \theta)$.

Lemma 9.14 (Rippa's Lemma)**.** *Let u_1, u_2, u_3, u_4 be the values of a function on the vertices of the convex non-degenerate quadrilateral $Q(r_1, r_2, r_3, r_4, \theta)$. Let $u_{13} : Q \to \mathbb{R}$ and be the linear interpolation which is affine on the triangles* (123) *and* (134) *whereas $u_{24} : Q \to \mathbb{R}$ is the linear interpolation affine on* (234) *and* (241)*. Let u_0 and u_0^* be the values at the intersection point of the diagonals of u_{13} and u_{24} respectively.*
Then the difference of the corresponding Dirichlet energies is

$$E(u_{13}) - E(u_{24}) = \frac{1}{4} \frac{(u_0 - u_0^*)^2}{\sin\theta} \frac{(r_1 + r_3)(r_2 + r_4)}{r_1 r_2 r_3 r_4} (r_1 r_3 - r_2 r_4). \tag{9.2}$$

Proof. The diagonals of Q separate the quadrilateral into four triangles Δ_1, Δ_2, Δ_3, Δ_4. Both linear interpolations are affine on each of these triangles while the Dirichlet energy of any affine function $u : \Delta_i \to \mathbb{R}$ on the triangle Δ_i is given by

$$E_{\Delta_i}(u) = \frac{1}{2} \int_{\Delta_i} |\nabla u|^2 \, \mathrm{d}A = \frac{1}{2}(u_x^2 + u_y^2) A(\Delta_i).$$

Consider the triangle Δ_1. The interpolation $u \coloneqq u_{13}$ is determined by the values u_0, u_1, u_2 and the geometric data r_1, r_2, θ of the triangle. Choosing a coordinate system such that the x-axis is aligned with the edge r_1 of Δ_1

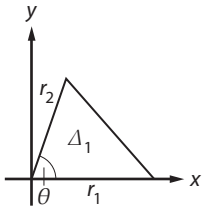

Figure 9.17. Triangle Δ_1 in suitable coordinate system.

we find

$$\begin{aligned} u_1 - u_0 &= u_x r_1 \\ u_2 - u_0 &= u_x r_2 \cos\theta + u_y r_2 \sin\theta, \end{aligned}$$

from which we obtain the partial derivatives u_x and u_y of u on Δ_1

$$\begin{aligned} u_x &= \frac{u_1 - u_0}{r_1} \\ u_y &= \frac{1}{\sin\theta}\left(\frac{u_2 - u_0}{r_2} - \frac{u_1 - u_0}{r_1}\cos\theta\right). \end{aligned}$$

For the gradient we get

$$|\nabla u|^2 = u_x^2 + u_y^2 = \frac{1}{\sin^2\theta}\left(\left(\frac{u_1 - u_0}{r_1}\right)^2 + \left(\frac{u_2 - u_0}{r_2}\right)^2 - 2\frac{(u_1 - u_0)(u_2 - u_0)\cos\theta}{r_1 r_2}\right).$$

The gradient of the interpolation $u^* \coloneqq u_{24}$ on Δ_1 is obtained by replacing u_0 by u_0^*. With $A(\Delta_1) = \frac{1}{2} r_1 r_2 \sin\theta$ the difference of the Dirichlet energies on Δ_1 is

$$\begin{aligned} E_{\Delta_1}(u) - E_{\Delta_1}(u^*) &= \frac{1}{2}\Big(|\nabla u|^2 - |\nabla u^*|^2\Big) A(\Delta_1) \\ &= \frac{r_1 r_2}{4\sin\theta}\Bigg((u_0^2 - u_0^{*2})\left(\frac{1}{r_1^2} + \frac{1}{r_2^2} - \frac{2\cos\theta}{r_1 r_2}\right) \\ &\quad + 2(u_0 - u_0^*)\left(-\frac{u_1}{r_1^2} - \frac{u_2}{r_2^2} + \frac{(u_1 + u_2)\cos\theta}{r_1 r_2}\right)\Bigg) \\ &= \frac{u_0 - u_0^*}{4\sin\theta}\Bigg((u_0 + u_0^*)\left(\frac{r_2}{r_1} + \frac{r_1}{r_2} - 2\cos\theta\right) \\ &\quad + 2\left(-u_1\frac{r_2}{r_1} - u_2\frac{r_1}{r_2} + (u_1 + u_2)\cos\theta\right)\Bigg). \end{aligned}$$

For the difference on Δ_2 we replace $r_1 \to r_2$, $r_2 \to r_3$, $\theta \to \pi - \theta$ and obtain

$$\begin{aligned} E_{\Delta_2}(u) - E_{\Delta_2}(u^*) = \frac{u_0 - u_0^*}{4\sin\theta}\Bigg((u_0 + u_0^*)\left(\frac{r_3}{r_2} + \frac{r_2}{r_3} + 2\cos\theta\right) \\ + 2\left(-u_2\frac{r_3}{r_2} - u_3\frac{r_2}{r_3} - (u_2 + u_3)\cos\theta\right)\Bigg). \end{aligned}$$

Similarly for Δ_3 and Δ_4.

We sum up over all four triangles obtaining the difference of the Dirichlet energies on the whole quadrilateral

$$\begin{aligned}
E(u) - E(u^*) &= \sum_{i=1}^{4} \Big(E_{\Delta_i}(u) - E_{\Delta_i}(u^*) \Big) \\
&= \frac{u_0 - u_0^*}{4 \sin\theta} \Bigg((u_0 + u_0^*) \Big(\frac{r_1}{r_2} + \frac{r_2}{r_3} + \frac{r_3}{r_4} + \frac{r_4}{r_1} + \frac{r_2}{r_1} + \frac{r_3}{r_2} + \frac{r_4}{r_3} + \frac{r_1}{r_4} \Big) \\
&\quad - 2 \Big(u_1 \Big(\frac{r_2}{r_1} + \frac{r_4}{r_1} \Big) + u_2 \Big(\frac{r_3}{r_2} + \frac{r_1}{r_2} \Big) + u_3 \Big(\frac{r_4}{r_3} + \frac{r_2}{r_3} \Big) + u_4 \Big(\frac{r_1}{r_4} + \frac{r_3}{r_4} \Big) \Big) \Bigg) \\
&= \frac{u_0 - u_0^*}{4 \sin\theta} \Bigg((u_0 + u_0^*) \Big((r_2 + r_4) \Big(\frac{1}{r_1} + \frac{1}{r_3} \Big) + (r_1 + r_3) \Big(\frac{1}{r_2} + \frac{1}{r_4} \Big) \Big) \\
&\quad - 2 \Big((r_2 + r_4) \Big(\frac{u_1}{r_1} + \frac{u_3}{r_3} \Big) \Big) + (r_1 + r_3) \Big(\frac{u_2}{r_2} + \frac{u_4}{r_4} \Big) \Big) \Bigg).
\end{aligned}$$

The values u_0 and u_0^* come from the different linear interpolations along the diagonals (13) and (24) respectively.

$$\begin{aligned}
u_0 &= \frac{r_3 u_1 + r_1 u_3}{r_1 + r_3} \\
u_0^* &= \frac{r_4 u_2 + r_2 u_4}{r_2 + r_4}
\end{aligned}$$

Using

$$\begin{aligned}
\frac{u_1}{r_1} + \frac{u_3}{r_3} &= u_0 \frac{r_1 + r_3}{r_1 r_3} \\
\frac{u_2}{r_2} + \frac{u_4}{r_4} &= u_0 \frac{r_2 + r_4}{r_2 r_4}
\end{aligned}$$

we can eliminate all dependence of the vertex values from the difference of the Dirichlet energies

$$\begin{aligned}
E(u) - E(u^*) &= \frac{u_0 - u_0^*}{4 \sin\theta} (r_1 + r_3)(r_2 + r_4) \left((u_0 + u_0^*) \left(\frac{1}{r_1 r_3} + \frac{1}{r_2 r_4} \right) - 2 \left(\frac{u_0}{r_1 r_3} + \frac{u_0^*}{r_2 r_4} \right) \right) \\
&= \frac{u_0 - u_0^*}{4 \sin\theta} (r_1 + r_3)(r_2 + r_4) \left(u_0 \left(\frac{1}{r_2 r_4} - \frac{1}{r_1 r_3} \right) + u_0^* \left(\frac{1}{r_1 r_3} - \frac{1}{r_2 r_4} \right) \right) \\
&= \frac{(u_0 - u_0^*)^2}{4 \sin\theta} (r_1 + r_3)(r_2 + r_4) \frac{r_1 r_3 - r_2 r_4}{r_1 r_2 r_3 r_4}.
\end{aligned}$$

□

We notice that all factors in (9.2) but the last are positive.[39] The sign of the last factor determines which edge is Delaunay.

[39] Note that for $u_0 - u_0^* \neq 0$ we require that not all of u_1, u_2, u_3, u_4 are equal.

Lemma 9.15 (circular quadrilaterals)**.** *The quadrilateral $Q(r_1, r_2, r_3, r_4, \theta)$ is circular if and only if $r_1 r_3 = r_2 r_4$.*
Furthermore

$$r_1 r_3 > r_2 r_4 \Leftrightarrow (24) \text{ Delaunay}$$
$$r_1 r_3 < r_2 r_4 \Leftrightarrow (13) \text{ Delaunay.}$$

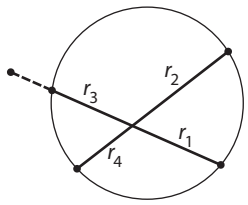

Figure 9.18. Circularity criterion for a convex quadrilateral in terms of lengths of diagonal segments.

Corollary 9.16. *Suppose that not all of the vertex values u_1, u_2, u_3, u_4 are equal. Then*

$$E(u_{13}) = E(u_{24}) \Leftrightarrow Q \text{ circular, i.e. both edges are Delaunay}$$
$$E(u_{13}) > E(u_{24}) \Leftrightarrow (24) \text{ Delaunay}$$
$$E(u_{13}) < E(u_{24}) \Leftrightarrow (13) \text{ Delaunay.}$$

So an edge-flip from a non-Delaunay edge to a Delaunay edge decreases the Dirichlet energy.

Remark 9.8. Note that the Dirichlet energy depends on the triangulation T as well as on the function $u : V(T) \to \mathbb{R}$. To ensure that the Dirichlet energy decreases upon an edge-flip u is required to be non-constant close to the edge.

9.3.2 Harmonic index

We introduce a related function that decreases on each step of the edge-flip algorithm and only depends on the triangulation.

Definition 9.7 (harmonic index)**.** For a triangle Δ with side-lengths a, b, c we define its *harmonic index* to be

$$h(\Delta) \coloneqq \frac{a^2 + b^2 + c^2}{A(\Delta)},$$

and for a geodesic triangulation $T \in \mathcal{T}_{M,V}$ of a piecewise flat surface

$$h(T) \coloneqq \sum_{\Delta \in F(T)} h(\Delta).$$

Lemma 9.17. *Let Δ be a triangle with angles α, β, γ. Then*

$$h(\Delta) = 4(\cot\alpha + \cot\beta + \cot\gamma).$$

Proof. Denote by a, b, c the lengths of the sides of Δ opposite α, β, γ respectively. Consider the height h_a on a.

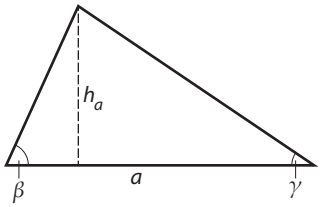

Figure 9.19. Triangle with side lengths a, b, c, corresponding heights h_a, h_b, h_c and angles α, β, γ.

Then

$$a = h_a(\cot\beta + \cot\gamma),$$

and therefore

$$a^2 = 2A(\Delta)(\cot\beta + \cot\gamma).$$

Adding this up with the corresponding formulas for the remaining edge lengths we obtain

$$a^2 + b^2 + c^2 = 4A(\Delta)(\cot\alpha + \cot\beta + \cot\gamma).$$

□

What has the harmonic index of a triangulation T to do with the Dirichlet energy?

Lemma 9.18. *Let T be a geodesic triangulation of a piecewise flat surface, $\varphi_i : V(T) \to \mathbb{R}$, $\varphi_i(j) \coloneqq \delta_{ij}$ the basis functions on T. Then*

$$h(T) = 8 \sum_{i \in V(T)} E(\varphi_i).$$

Proof. The Dirichlet energy of φ_i is given by

$$E(\varphi_i) = \frac{1}{4} \sum_{j \in V : (ij) \in E} (\cot\alpha_{ij} + \cot\alpha_{ji}).$$

Summing along all vertices $i \in V$ amounts in counting every angle twice

$$\sum_{i \in V} E(\varphi_i) = \frac{1}{2} \sum_{(ij) \in E} (\cot\alpha_{ij} + \cot\alpha_{ji}).$$

□

Corollary 9.19. *The harmonic index decreases on each step of the edge-flip algorithm.*

Lemma 9.20. *The harmonic index $h : \mathcal{T}_{M,V} \to \mathbb{R}$ is a proper function.*

Proof. Denote by A the total area of the surface M. We do a very coarse estimation using the maximal edge length $l : \mathcal{T}_{M,V} \to \mathbb{R}$ introduced in Example 9.4:

$$h(T) = \sum_{\Delta \in F(T)} h(\Delta) \geqslant \frac{l(T)}{A}.$$

So for $c \in \mathbb{R}$

$$h(T) \leqslant c \;\Rightarrow\; l(T) \leqslant \sqrt{h(T)A} = \sqrt{cA},$$

and we know that l is proper. □

We conclude that the edge-flip algorithm terminates after a finite number of steps. We have therefore proven Theorem 9.12. But even more

Theorem 9.21. *Let (M, d) be a piecewise flat surface without boundary, $V \subset M$ a finite set of points that contains all conical singularities.*
Let $f : V \to \mathbb{R}$. For each triangulation $T \in \mathcal{T}_{M,V}$ let $f_T : M \to \mathbb{R}$ be the piecewise linear interpolation of f which is affine on the faces of T.
Then the minimum of the Dirichlet energy $E(f_T) = \int_M |\nabla f_T|^2 \, \mathrm{d}A$ among all possible triangulations is attained on a Delaunay triangulation $T_D^\Delta \in \mathcal{T}_{M,V}$ of (M, d):

$$\min_{T \in \mathcal{T}_{M,V}} E(f_T) = E(f_{T_D^\Delta}).$$

9.4 Discrete Laplace-Beltrami operator

Let (M, d) be a piecewise flat surface without boundary, $V \subset M$ a finite set of points that contains all conical singularities.
Let T_D be the Delaunay tessellation of M and $T_D^\Delta \in \mathcal{T}_{M,V}$ some Delaunay triangulation of T_D. Recalling (8.3) we see that for an edge $(ij) \in E$ we have

$$\nu(ij) = 0 \;\Leftrightarrow\; \alpha_{ij} + \alpha_{ji} = \pi,$$

which is the case for circular quadrilaterals. So the edges in T_D^Δ coming from triangulating circular polygons of the Delaunay tessellation T_D have zero weights. The weights of edges on the boundary of circular polygons of T_D are independent of the chosen triangulation as can be seen in Figure 9.20.

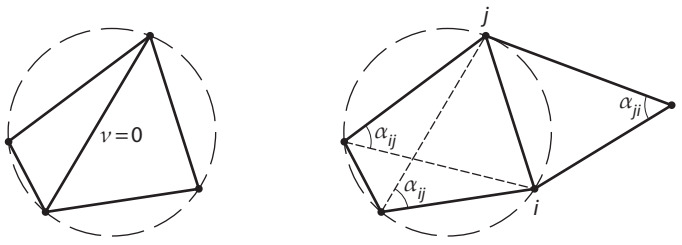

Figure 9.20. Cotan-weights of the Delaunay tessellation. (left) An edge coming from triangulating circular polygons has zero cotan-weight. (right) The cotan-weight of an edge on the boundary of a circular polygon does not depend on the triangulation.

So the cotan-weights are well-defined on the edges of the Delaunay tessellation.

Definition 9.8 (discrete Laplace-Beltrami operator)**.** Let (M, d) be a piecewise flat surface without boundary, $V \subset M$ a finite set of points that contains all conical singularities.
Let T_D be the Delaunay tessellation of M.
Then the *discrete Laplace-Beltrami operator* of (M, d) is defined by

$$\Delta f(i) = \sum_{e=(ij)\in E(T_D)} \nu(e)\,(f(i) - f(j))$$

for any function $f : V \to \mathbb{R}$.
The corresponding Dirichlet energy on (M, d) is defined by

$$E(f) \coloneqq \frac{1}{2} \sum_{e=(ij)\in E(T_D)} \nu(e)\,(f(i) - f(j))^2\,,$$

where ν are the cotan-weights as defined in (8.2) coming from any Delaunay triangulation $T_D^\Delta \in \mathcal{T}_{M,V}$ of T_D.

Remark 9.9.

- The sum can be taken over all edges of any Delaunay triangulation as we have seen above.
  The notion of neighboring vertices might differ from the one given by the "extrinsic triangulation" of a polyhedral surface in $\mathbb{R}^N$. Also triangles of a Delaunay triangulation are not necessarily planar in $\mathbb{R}^N$ anymore.

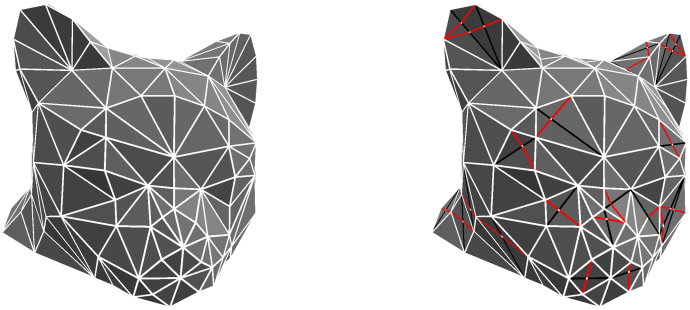

Figure 9.21. Simplicial cat. (left) Triangulation coming from the simplicial surface. (right) Delaunay triangulation (white and red edges).

- The Laplace-Beltrami operator is a well-defined property of the Delaunay tessellation T_D which is uniquely determined by (M, d) and the vertex set V. So we have defined a unique discrete Laplace-Beltrami operator of the piecewise flat surface (M, d), which is determined by the polyhedral metric only, i.e. invariant w.r.t. isometries.
- In Proposition 9.10 we have seen that all weights of the Delaunay triangulation are non-negative. With above considerations we can now conclude that all weights of the Delaunay tessellation are positive. So for the discrete Laplace-Beltrami operator we can apply the results of the theory of discrete Laplace operators with positive weights. We are assured to have the maximum principle and unique minima of the Dirichlet energy.

9.5 Simplicial minimal surfaces (II)

Having the discrete Laplace-Beltrami operator we can improve the definition of simplicial minimal surfaces of Section 8.4.

Definition 9.9 (simplicial minimal surface)**.** Let $f : \mathcal{S} \to S \subset \mathbb{R}^N$ be a simplicial surface and T its triangulation. Then

$$\begin{aligned} S \text{ minimal (in the wide sense)} &:\Leftrightarrow \Delta f = 0 \\ S \text{ minimal (in the narrow sense)} &:\Leftrightarrow \Delta f = 0 \text{ and } T \text{ is Delaunay,} \end{aligned}$$

where in both cases Δ is the discrete Laplace-Beltrami operator of S.

Remark 9.10.

- The Laplace-Beltrami operator coincides with the cotan-Laplace operator only in the narrow definition. So only in this case the surface is actually a critical point of the area functional.
- The Laplace-Beltrami operator has all positive weights. If f is harmonic the maximum principle (Proposition 8.8) implies that any vertex point $f(i)$ lies in the convex hull of its neighbors:

  $$f(i) \in \operatorname{conv}\{f(j) \in \mathbb{R}^n \mid (ij) \in E(T_D)\},$$

  where neighbors are determined by the Delaunay tessellation T_D of S.

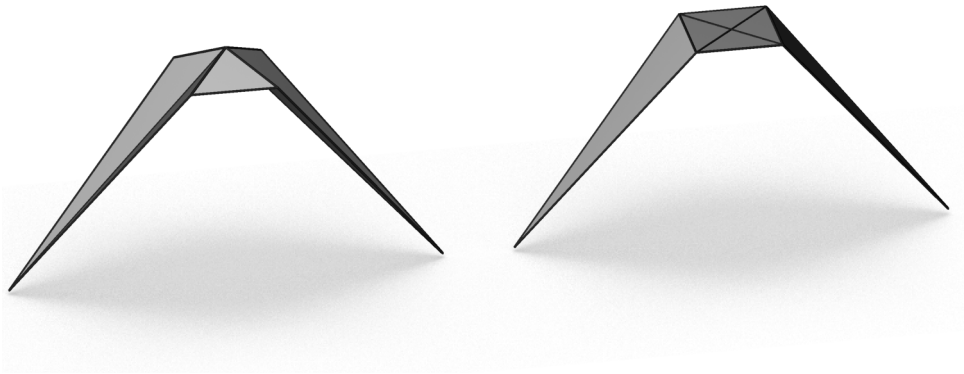

Figure 9.22. (left) Simplicial surface which is minimal with respect to the definition of Section 8.4. It violates the maximum principle. (right) Corresponding minimal surface (in the narrow sense) with respect to Definition 9.9. It satisfies the maximum principle. By "corresponding" we mean that it is obtained by applying Algorithm 9.23 to the left surface.

In the wide definition the neighbors satisfying the maximum principle might be different from the ones given by the triangulation of S, where in the narrow definition they coincide.

This new definition leads to the following algorithm producing minimal surfaces in the narrow sense, if it converges.

Data: Simplicial surface $f : \mathcal{S} \to S \subset \mathbb{R}^N$ with triangulation T.
Result: Simplicial minimal surface in the narrow sense.
while S *is not minimal in the narrow sense* **do**
  Compute Delaunay triangulation $\tilde{T}$ of S (use Algorithm 9.13);
  Compute $\tilde{f}$ such that
$$\Delta_{(S,\tilde{T})}\tilde{f} = 0,$$
  which defines a new simplicial surface $\tilde{S}$;
  Replace S by the new surface $\tilde{S}$;
  Replace T by $\tilde{T}$;
end

Figure 9.23. Simplicial minimal surface algorithm (with intrinsic discrete Laplace-Beltrami-operator and change of combinatorics).

Remark 9.11. The state of the algorithm is determined by the simplicial surface S and its triangulation T.
In each step of the while-loop we replace

$$(S, T) \leftarrow (\tilde{S}, \tilde{T}),$$

where $\tilde{T}$ is the Delaunay triangulation of S which might not be Delaunay anymore for $\tilde{S}$.
Besides using the intrinsic Laplace-Beltrami operator the fundamental difference to Algorithm 8.5 is the change of combinatorics in each step.

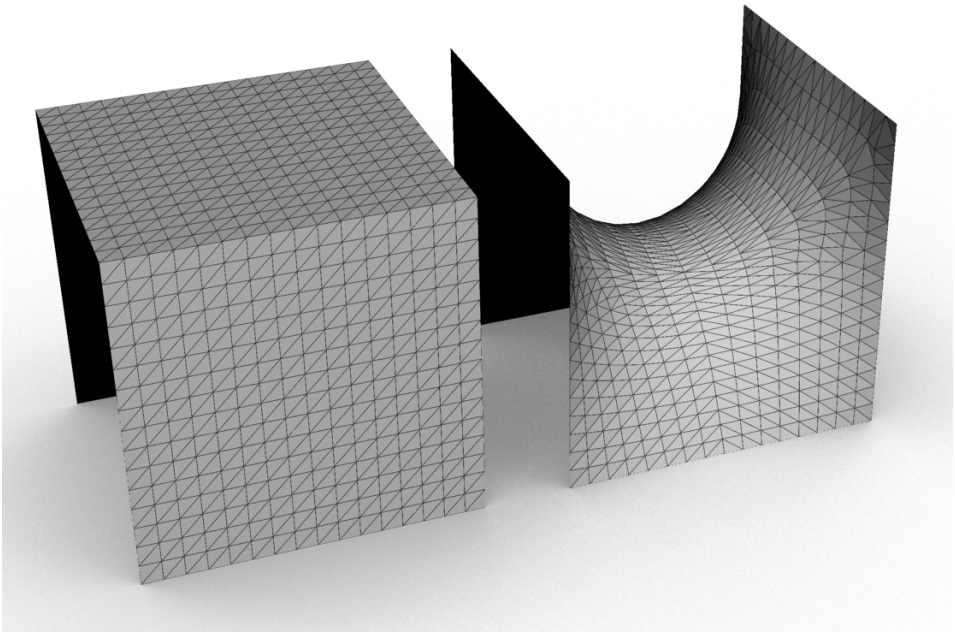

Figure 9.24. Simplicial minimal surface from Algorithm 9.23.

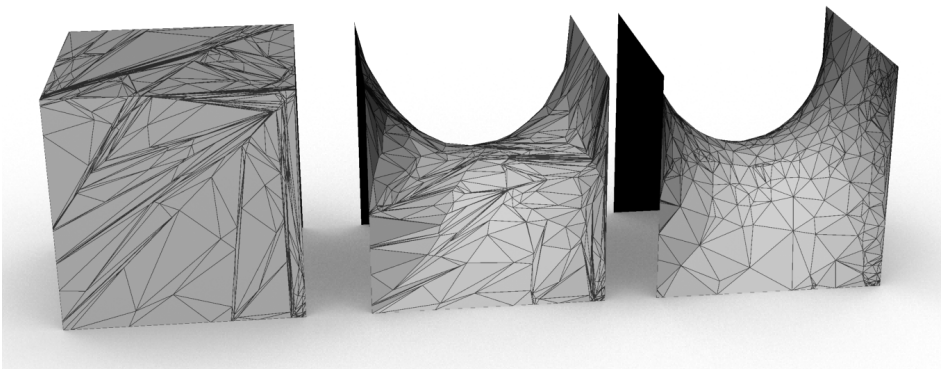

Figure 9.25. Using the intrinsic Laplace-Beltrami operator with and without change of combinatorics. Starting with a random triangulation the change becomes particularly eminent. (left) Random start triangulation. (middle) Result of Algorithm 9.23 without change of combinatorics. (right) Result of Algorithm 9.23 with change of combinatorics.

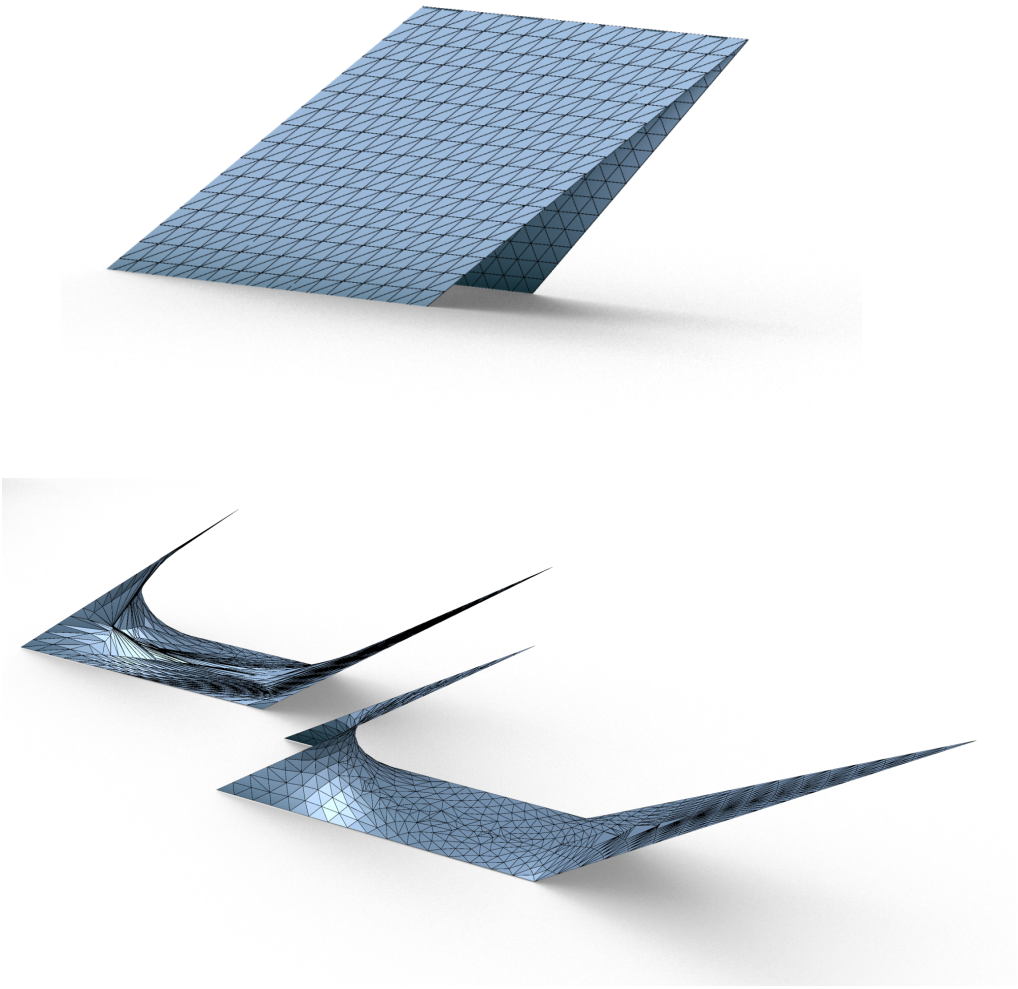

Figure 9.26. Comparing intrinsic and extrinsic Laplace-Beltrami operator. We start with a triangulation which is not suitable for the resulting minimal surface. (top) Start triangulation. (bottom left) Result of applying Algorithm 8.5 for some time. No convergence! (bottom right) Result of Algorithm 9.23.

10 Line congruences over simplicial surfaces

We develop a curvature theory for simplicial surfaces based on a discrete version of Steiner's formula.

10.1 Smooth line congruences

A *smooth line congruence* $\mathcal{L}$ is a smooth 2-dimensional manifold of lines described locally by lines $l(u,v)$ which connect corresponding points $a(u,v)$ and $b(u,v)$ of two parametrized surfaces. $e(u,v) \coloneqq b(u,v) - a(u,v)$ indicates the

Figure 10.1. Line congruence given by two parametrized surfaces.

direction of the line.
A *volume parametrization* of $\mathcal{L}$ is given by

$$x(u,v,\lambda) \coloneqq a(u,v) + \lambda e(u,v) = (1-\lambda)a(u,v) + \lambda b(u,v)$$

A *ruled surface* $\mathcal{R} \subset \mathcal{L}$ is described by two functions $u(t)$, $v(t)$ where the parametrization is given by

$$(t,\lambda) \mapsto x(u(t),v(t),\lambda)$$

$\mathcal{R}$ is called *developable* if $[e, e_t, a_t] = 0$ or equivalently $[e, b_t, a_t] = 0$, i.e. e, a_t, b_t are coplanar where $[\cdot,\cdot,\cdot]$ denotes the determinant. The corresponding equation for u_t and v_t is

$$u_t^2[e_u, a_u, e] + u_t v_t([e_u, a_v, e] + [e_v, a_u, e]) + v_t^2[e_v, a_v, e] = 0 \tag{10.1}$$

This quadratic equation has up to two solutions $\frac{u_t}{v_t}$ which are called *torsal directions*.

10.1.1 Normal line congruences

A line congruence formed by the lines orthogonal to a surface is called *normal line congruence*. $e(u,v)$ can be chosen unit.

$$(u,v) \mapsto a(u,v) \text{ curvature line parametrization } \Leftrightarrow\ e_u \parallel a_u,\ e_v \parallel a_v$$

The normals along a principal curvature line constitute a developable ruled surface. Thus the normal line congruences always have torsal directions. These directions are orthogonal and are called *principal directions*.

Remark 10.1. If $x(u,v,\lambda) = a(u,v) + \lambda e(u,v)$ is a volume parametrization of a normal line congruence, then any constant distance offset $a^d \coloneqq a + de$, $e^d \coloneqq e$ defines the same congruence $x^d(u,v,\lambda) = x(u,v,\lambda + d)$.

...

Figure 10.2. A normal shift of a surface constitutes the same normal congruence.

A general line congruence

$$x(u,v,\lambda) = a(u,v) + \lambda e(u,v)$$

might be a normal congruence of a yet unknown surface $a^*(u,v)$ with normal vectors $e(u,v)$. In order to find it we have to solve

$$a^*(u,v) = a(u,v) + \lambda(u,v)e(u,v)$$

for $\lambda(u,v)$. We restrict $e(u,v)$ to $|e| = 1$. Then the orthogonality conditions $\langle e, a^*_u\rangle = \langle e, a^*_v\rangle = 0$ are equivalent to

$$\lambda_u = -\langle a_u, e\rangle, \quad \lambda_v = -\langle a_v, e\rangle$$

This equation has a solution if and only if $\lambda_{uv} = \lambda_{vu}$, i.e.

$$\langle a_u, e_v\rangle = \langle a_v, e_u\rangle.$$

10.2 Line congruences defined over simplicial surfaces

Let A and B be two combinatorically equivalent simplicial surfaces with vertices $\{a_i\}$ and $\{b_i\}$. Via linear interpolation the correspondence $a_i \leftrightarrow b_i$ defines correspondences between faces $a_ia_ja_k$ and $b_ib_jb_k$. Connecting corresponding

...

Figure 10.3. Corresponding faces of two simplicial surfaces.

points we obtain a line congruence $\mathcal{L}$. Its volume parametrization for one face $a_ia_ja_k$ is given by

$$x(u,v,\lambda) = a(u,v) + \lambda e(u,v) \tag{10.2}$$

where

$$\begin{aligned} &a(u,v) = a_i + ua_{ij} + va_{ik}, \quad e(u,v) = e_i + ue_{ij} + ve_{ik}, \\ &e_i = b_i - a_i, \quad a_{ij} = a_j - a_i, \quad e_{ij} = e_j - e_i \end{aligned} \tag{10.3}$$

and $u,\ v,\ 1-u-v \geqslant 0$.
One can compute the torsal directions using (10.1). Assume that torsal directions exist for all (u,v). Then they can be integrated starting from any point. The corresponding integral curves are called *torsal lines*.

Proposition 10.1 (torsal lines on simplicial surfaces)**.** *Torsal lines on the linear interpolated line congruence (10.2), (10.3) are straight lines within each face.*

Proof. Let (α,β) be a torsal direction at (u_0,v_0), i.e. the vectors a_t, e_t, e are linear dependent at this point, where

$$(u,v)(t) = (u_0,v_0) + t(\alpha,\beta). \tag{10.4}$$

Computing the derivative using (10.3) on the line (10.4) we obtain that the vectors

$$a_{ij}\alpha + a_{ik}\beta, \quad e_{ij}\alpha + e_{ik}\beta, \quad e_i + e_{ij}u_0 + e_{ik}v_0 + t(e_{ij}\alpha + e_{ik}\beta) \tag{10.5}$$

are linearly dependent for all t if they are linearly dependent at the starting point $t = 0$. This implies that (10.4) is a torsal line. □

...

Figure 10.4. Torsal directions are straight lines within each face. Parsing over an edge from one triangle to another there are two torsal directions to continue. One chooses the one with minimal deviation.

Corollary 10.2 (torsal planes on simplicial surfaces)**.** *The developable surfaces in the linear interpolated line congruence (10.2), (10.3) corresponding to the straight torsal lines within a face are contained in a plane (which we call* torsal plane*).*

10.2.1 Discrete normal congruences over simplicial surfaces

Let us interprete $e : V(A) \to \mathbb{R}^3$ as a generalized Gauss map of the simplicial surface A with vertices $a : V(A) \to \mathbb{R}^3$.
This notion is however too generel, the Gauss map is neither unit nor orthogonal. To come closer to the smooth theory we introduce discrete normal congruences that are more special and have additional nice properties.

Definition 10.1 (normal line congruence of a simplicial surface)**.** A congruence $\mathcal{L}$ defined by a piecewise-linear correspondence of two simplicial line congruences A and B is called *normal*, if the torsal planes in the barycenter of corresponding faces are orthogonal.

We project a_i, b_i to the plane $\mathcal{O}$ orthogonal to the line connecting the barycenters. The resulting vertices are denoted by $\overline{a}_i$, $\overline{b}_i$, $\overline{e}_i = \overline{b}_i - \overline{a}_i$.

...

Figure 10.5. Two corresponding faces with the plane $\mathcal{O}$ orthogonal to the line connecting the barycenters.

Proposition 10.3 (normal congruence from two simplicial surfaces)**.** *Two simplicial surfaces A and B define a normal congruence if and only if for each pair of corresponding faces we have*

$$\langle \overline{a}_{ij}, \overline{b}_{ik} \rangle = \langle \overline{a}_{ik}, \overline{b}_{ij} \rangle$$

where $\overline{a}_{ij} \coloneqq \overline{a}_j - \overline{a}_i$, $\overline{b}_{ij} \coloneqq \overline{b}_j - \overline{b}_i$. This is equivalent to

$$\langle \overline{a}_{ij}, \overline{e}_{ik} \rangle = \langle \overline{a}_{ik}, \overline{e}_{ij} \rangle \tag{10.6}$$

where $\overline{e}_{ij} \coloneqq \overline{e}_j - \overline{e}_i$. It is sufficient that it holds for at least one choice of $i \neq j \neq k$.

Proof. Use the common image of barycenters as the origin of the coordinate system. There is a linear map α which maps $\overline{a}_i \mapsto \overline{b}_i$ $(i = 1, 2, 3)$. The torsal planes of the congruence intersect our auxiliary plane in the eigenspaces of α. So orthogonality of the torsial planes means α is symmetric

$$\langle x, \alpha(y) \rangle = \langle \alpha(x), y \rangle$$

which is exactly what is stated. □

10.2.2 Curvature via Steiner's formula

We compare the areas not of corresponding faces $\Delta = a_1 a_2 a_3$ and $\Delta' = b_1 b_2 b_3$ where $b_i = a_i + t e_i$ but their projections to the plane $\mathcal{O}$. The quotient for the corresponding areas is

$$\frac{[\overline{b}_{ij}, \overline{b}_{ik}]}{[\overline{a}_{ij}, \overline{a}_{ik}]} = 1 + t \frac{[\overline{a}_{ij}, \overline{e}_{ik}] + [\overline{e}_{ij}, \overline{a}_{ik}]}{[\overline{a}_{ij}, \overline{a}_{ik}]} + t^2 \frac{[\overline{e}_{ij}, \overline{e}_{ik}]}{[\overline{a}_{ij}, \overline{a}_{ij}]}.$$

Definition 10.2. Let A and B be two simplicial surfaces, combinatorically equivalent with vertices $\{a_i\}$, $\{b_i\}$, $e_i \coloneqq b_i - a_i$, defining a normal line congruence, i.e. (10.6) is satisfied. Let $\mathcal{O}$ be the plane orthogonal to the line connecting the barycenters of $\Delta a_i a_j a_k$ and $\Delta b_i b_j b_k$ and $e_0 \coloneqq \frac{1}{3}(b_i+b_j+b_k)-\frac{1}{3}(a_i+a_j+a_k)$ be a vector orthogonal to $\mathcal{O}$.
Then the *mean* and *Gaussian curvature* at the face $\Delta a_i a_j a_k$ are defined as

$$K \coloneqq \frac{[e_{ij}, e_{ik}, e_0]}{[a_{ij}, a_{ik}, e_0]}, \quad H \coloneqq -\frac{1}{2}\frac{[a_{ij}, e_{ik}, e_0] + [e_{ij}, a_{ik}, e_0]}{[a_{ij}, a_{ik}, e_0]} \tag{10.7}$$

Remark 10.2. $[\overline{a}, \overline{b}] = [a, b, e_0]$

Principal curvatures κ_1, κ_2 are defined through their symmetric functions

$$H = \frac{1}{2}(\kappa_1 + \kappa_2), \quad K = \kappa_1\kappa_2,$$

i.e. as reciprocal of the real zeros of the quadratic polynomial

$$1 - 2Ht + Kt^2 = (1 - \kappa_1 t)(1 - \kappa_2 t).$$

For normal congruences these zeros are always real. It is easy to check that the corresponding condition $H^2 > K$ is equivalent to the existence of torsal directions at the barycenter. The latter are defined as (orthogonal) *prinicipal directions*.

Let $(u, v) \mapsto a(u, v)$ be a smooth surface M in $\mathbb{R}^3$ with the Gauss map $e(u, v)$, i.e. $e \perp a_u, a_v$, $|e| = 1$. The map $\Lambda : \mathrm{T}_p M \to \mathrm{T}_p M$ of the tangent plane at $p \in M$ to itself defined via $\mathrm{d}a \mapsto^{\Lambda} -\mathrm{d}e$ is called the *shape operator*. In coordinates it is given by a 2×2 symmetric matrix. Its eigenvectors and eigenvalues define (orthogonal) principal directions and principal curvatures respectively.

In the setup of discrete normal congruences the shape operator is defined exactly in the same way. It is a linear map $\Lambda : \mathcal{O} \to \mathcal{O}$ (of the plane $\mathcal{O}$ orthogonal to e_0) which maps the edges of a to the reversed corresponding edges of e:

$$\Lambda(\overline{a}_{ij}) = -\overline{e}_{ij}.$$

Proposition 10.4. *Eigenvectors of the shape operator* Λ *indicate the (orthogonal) principal directions. The eigenvalues of* Λ *are the principal curvatures.*

Proof. By construction

$$\Lambda = -\frac{1}{t}(\alpha - \mathrm{id}),$$

where $\alpha : \mathcal{O} \to \mathcal{O}$ is the map from the proof of Proposition 10.3. The claim about eigenvectors follows.
To prove the claim about the eigenvalues use the formulas

$$\det\Lambda = \frac{\det(\Lambda(x), \Lambda(y))}{\det(x, y)}, \quad \mathrm{tr}\Lambda = \frac{\det(\Lambda(x), y) + \det(x, \Lambda(y))}{\det(x, y)},$$

where $x, y \in \mathbb{R}^2$ is an arbitrary basis of $\mathbb{R}^3$ and (x, y) is the matrix with colums x and y. Substituting $x = \overline{a}_{ij}$, $y = \overline{a}_{ik}$ we obtain formulas (10.7) for

$$H = \frac{1}{2}\mathrm{tr}\Lambda, \quad K = \det\Lambda.$$

□

Remark 10.3. In computer graphics applications one usually starts with a line congruence which is not far from normal. For example, one can take the normals at vertices that are area weighted averages of face normals. One can improve the corresponding line congruence making it "more normal" (or normal) by optimization of e (and of a).

11 Polyhedral surfaces with parallel Gauss map

We consider parallel polyhedral surfaces defined as discrete surfaces with parallel corresponding edges. Polyhedral surfaces parallel to a given surface build a vector space. Given two parallel surfaces f and f^+ , the formula $f_t = tf^+ + (1-t)f$ gives an interpolating family of parallel surfaces. The difference surface $n = f^+ - f$ is also parallel to both f^+ and f and the above-mentioned one-parameter family of parallel surfaces can be seen as built from the surface f and its generalized Gauss map n:

$$f_t = f + tn, \quad t \in \mathbb{R}.$$

The surface f^+ is called an *offset* of f or *Combescure transform* of f.

A special case of polyhedral surfaces are Q-nets.

Definition 11.1 (Q-net and torsal line congruence)**.** A *Q-net* is a quad-surface (i.e. a surface with quadrilateral faces) with planar faces.
A *torsal line congruence* is a map

$$l : V(D) \to \mathcal{L}$$

of vertices of a quad-graph D to the space of lines such that each two lines corresponding to an edge of D are coplanar.

A pair $f : V(D) \to \mathbb{R}^3$, $l : V(D) \to \mathcal{L}$ of a Q-net with a torsial line congruence such that the lines pass through the corresponding vertices $f(i) \in l(i)$ can be interpreted as a quad-surface with a generalized Gauss map.
The above mentioned one-parameter family of parallel discrete surfaces can be interpreted as a Q-net with a line congruence where the directions of the lines are given by the generalized Gauss map $n : V(D) \to \mathbb{R}^3$.

11.1 Polygons with parallel edges and mixed area

We start with a theory of polygons with parallel edges (recall that such polygons build faces of parallel surfaces). Let

$$v_1, \dots, v_k \in \mathbb{R}\mathrm{P}^1 = \mathbb{S}^1/\{\pm I\}$$

be a sequence of tangent directions of a k-gon $P = (p_1, \dots, p_k)$ in a plane; $p_{i+1} - p_i \parallel v_i$. Denote by $\mathcal{P}(v)$, $v = (v_1, \dots, v_k)$, the space of k-gons with edges parallel to $v_1, \dots, v_k$. The polygons are not supposed to be convex nor embedded. They may have degenerated edges. $\mathcal{P}(v)$ is a k-dimensional vector space. Factoring out translations (for example, normalizing $p_1 = 0$), we obtain a $(k-2)$-dimensional vector space $\tilde{\mathcal{P}}(v)$.

Let $A(P)$ be the oriented area of the polygon P. The oriented area of a k-gon with vertices $p_1, \dots, p_k$, $p_{k+1} = p_1$ is equal to

$$A(P) = \frac{1}{2} \sum_{i=1}^{k} [p_i, p_{i+1}],$$

where $[a, b] = \det(a, b)$ is the area form in the plane. For a quadrilateral $P = (p_1, p_2, p_3, p_4)$ with oriented edges $a = p_2 - p_1$, $b = p_3 - p_2$, $c = p_4 - p_3$, $d = p_1 - p_4$, we have

$$A(P) = \frac{1}{2}([a, b] + [c, d]).$$

The oriented area A is a quadratic form on the vector space $\tilde{\mathcal{P}}(v)$. Its corresponding bilinear symmetric form $A(\cdot,\cdot)$ is of central importance for the following theory.

Definition 11.2 (Mixed area)**.** Let P and Q be two k-gons with parallel corresponding (possibly degenerated) edges. Their mixed area is given by the bilinear symmetric form

$$A(P,Q) = \frac{1}{2}(A(P+Q) - A(P) - A(Q)).$$

The area of a linear combination of two polygons is given by the quadratic polynomial

$$A(P+tQ) = A(P) + 2tA(P,Q) + t^2A(Q). \tag{11.1}$$

We have a sort of scalar product $A(\cdot,\cdot)$ on the space of polygons with parallel edges.

We call the space $\tilde{\mathcal{P}}(v)$, $v = (v_1, v_2, v_3, v_4)$ (and all the quadrilaterals in this space) nondegenerate if every two of its consecutive tangent directions are different, $v_{i+1} \neq v_i$. The signature of the area form $A : \tilde{\mathcal{P}}(v) \to \mathbb{R}$ depends on the quadruple $v = (v_1, v_2, v_3, v_4) \in (\mathbb{R}\mathrm{P}^1)^4$ and can be also characterized in terms of the quadrilaterals in $\tilde{\mathcal{P}}(v)$.

Theorem 11.1 (Signature of the area form)**.** *Let $\tilde{\mathcal{P}}(v)$, $v = (v_1, v_2, v_3, v_4)$ be a nondegenerate space of quadrilaterals with consecutive edges parallel to the tangent directions v_1, v_2, v_3, $v_4 \in \mathbb{R}\mathrm{P}^1 = \mathbb{S}^1/\{\pm I\}$, and let $P \in \tilde{\mathcal{P}}(v)$ be a quadrilateral with nonvanishing edges. The area form $A : \tilde{\mathcal{P}}(v) \to \mathbb{R}$ is indefinite (resp. definite) if and only if all vertices of P are extremal points of their convex hull (resp. one of the vertices of P lies in the interior of the convex hull of the other three vertices).*

more cases: $A = 0$ and all concave vertices...
"proof" in caption

Figure 11.1. Left: The signature of the area form is indefinite; the vertices of the polygons lie on the boundary of their convex hull. Right: The signature of the area form is definite; for any quadrilateral of the family one vertex is in the interior of the convex hull of the other three.

11.2 Curvatures of a polyhedral surface with parallel Gauss map

Consider a polyhedral surface f equipped with a congruence of lines such that every vertex has a line passing through it and the lines assigned to adjacent vertices are coplanar. Our main example is a Q-net $f : V(D) \to \mathbb{R}^3$ with a line congruence $l : V(D) \to \mathcal{L}$ such that $f(u) \in l(u)$ for all $u \in V(D)$. Let $n : V(D) \to \mathbb{R}^3$ be the corresponding generalized Gauss map. If l is simply connected, then the net n is determined up to a constant factor and is fixed as soon as the length of the normal at one vertex is prescribed.

Theorem 11.2 (Parallel surface area)**.** *The area of the parallel surface* $f_t := f + tn$ *obeys the law*

$$A(f_t) = \sum_P (1 - 2tH_P + t^2 K_P) A(f(P)),$$

where

$$H_P = -\frac{A(f(P), n(P))}{A(f(P))}, \quad K_P = \frac{A(n(P))}{A(f(P))}. \tag{11.2}$$

Here the sum is taken over all (combinatorial) faces P*, and* $f(P)$ *and* $n(P)$ *are the corresponding faces of the surface* f *and its generalized Gauss map* n*.*

Proof. Since the corresponding faces and edges of discrete surfaces f and n are parallel, the claim follows from formula (11.1). □

Having in mind Steiners formula, we come to the following natural definition of the curvatures in the discrete case.

Definition 11.3 (Mean and Gaussian curvatures of polyhedral surfaces)**.** Let (f, n) be two parallel polyhedral surfaces. We consider n as the generalized Gauss map of f. The functions H_P and K_P on the faces given by (11.2) are the *mean* and the *Gaussian curvature* of the pair (f, n), i.e. of the polyhedral surface f with respect to the Gauss map n.

Note that, as in the smooth case, the Gaussian curvature is defined as the quotient of the areas of the Gauss image and of the original surface. Since for a given polyhedral surface with a line congruence the map n is defined up to a common factor, the curvatures at the faces are also defined up to multiplication by a constant.

The principal curvatures κ_1, κ_2 at the faces are naturally defined using the formulas $H = \frac{1}{2}(\kappa_1 + \kappa_2)$ and $K = \kappa_1\kappa_2$ as the zeros of the quadratic polynomial

$$A(f_t) = (1 - 2tH + t^2 K) A(f) = (1 - t\kappa_1)(1 - t\kappa_2) A(f).$$

Definition 11.4 (Principal curvatures of Q-nets)**.** Let $(f, n) : V(D) \to \mathbb{R}^3 \times \mathbb{R}^3$ be a Q-net with a generalized Gauss map. Assume that the area forms $A : \tilde{\mathcal{P}} \to \mathbb{R}$ are indefinite for all the faces $f(P)$. Then the functions κ_1, κ_2 of (11.2) are real-valued and are called the *principal curvatures* of the pair (f, n).

The results of the previous section imply that the principal curvatures exist for quadrilateral faces with vertices on the boundary of the convex hull. In particular, for a circular net, principal curvatures exist for any Gauss map.

11.3 Dual quadrilaterals

Investigating the minimal surface condition $H = 0$ in the case of quad-surfaces with parallel Gauss-map leads us to the notion of dual quadrilaterals.

Definition 11.5 (dual quadrilaterals)**.** Two quadrilaterals P, Q with parallel corresponding edges are called *dual* if their mixed area vanishes, i.e.

$$A(P, Q) = 0.$$

We write $Q = P^*$.

Proposition 11.3 (Dual quadrilaterals via mixed area)**.** *Two quadrilaterals $P = (p_1, p_2, p_3, p_4)$ and $Q = (q_1, q_2, q_3, q_4)$ with parallel corresponding edges are dual if and only if their non-corresponding diagonals are parallel, i.e.*

$$(p_1p_3) \parallel (q_2q_4) \quad \textit{and} \quad (p_2p_4) \parallel (q_1q_3).$$

Proof. Denote the edges of the quadrilaterals P and Q as in Figure 11.2. Formula (11.1) implies that the area of the quadrilateral $P + tQ$ is given by

$$A(P + tQ) = ([a + ta^*, b + tb^*] + [c + tc^*, d + td^*]).$$

Identifying the linear terms in t and using the identity $a + b + c + d = 0$, we get

...

Figure 11.2. Dual quadrilaterals.

$$\begin{aligned} 4A(P, Q) &= [a, b^*] + [a^*, b] + [c, d^*] + [c^*, d] \\ &= [a + b, b^*] + [a^*, a + b] + [c + d, d^*] + [c^*, c + d] \\ &= [a + b, b^* - a^* - d^* + c^*]. \end{aligned}$$

Vanishing of the last expression is equivalent to the parallelism of the non-corresponding diagonals, $(a + b) \parallel (b^* + c^*)$. □

Remark 11.1. If two non-corresponding diagonals of two quadrilaterals with parallel edges are parallel then the other non-corresponding diagonals are also parallel.

Proposition 11.4 (Existence and uniqueness of the dual quadrilateral)**.** *For any planar quadrilateral (A, B, C, D), a dual one exists and is unique up to scaling and translation.*

Remark 11.2. Let $\tilde{\mathcal{P}}$ be a non-degenerate vector space of quadrilaterals with edges parallel, factorized by translations such that $P = (A, B, C, D) \in \tilde{\mathcal{P}}$. Then $\dim \tilde{\mathcal{P}} = 2$ and $A(\cdot, \cdot)$ defines a non-degenerate bilinear form on $\tilde{\mathcal{P}}$. So $\dim\{P\}^\perp = 1$, i.e. there is $P^* \in \tilde{\mathcal{P}}$ with $A(P, P^*) = 0$, unique up to scaling. Despite this simple argument we proceed in a computational proof, since the obtained formulas will be useful later.

Proof. Uniqueness of the form of the dual quadrilateral can be argued as follows. Denote the intersection point of the diagonals of (A, B, C, D) by $M = (AC) \cap (BD)$. Take an arbitrary point M^* in the plane as the designated intersection point of the diagonals of the dual quadrilateral. Draw two lines l_1 and l_2 through M^* parallel to (AC) and (BD), respectively, and choose an arbitrary point on l_2 to be A^*. Then the rest of construction is unique: draw the line through A^* parallel to (AB); its intersection point with l_1 will be B^*; draw the line through B^* parallel to (BC); its intersection point with l_2 will be C^*; draw the line through C^* parallel to (CD); its intersection point with l_1 will be D^*. It remains to see that this construction closes, namely that the line through D^* parallel to (DA) intersects l_2 at A^*. Clearly, this property does not depend on the initial choice of A^* on l_2, since this choice only affects the scaling of the dual picture. Therefore, it is enough to demonstrate the closing property for some

...

Figure 11.3. Existence of the quadrilateral.

choice of A^*, or, in other words, to show the existence of one dual quadrilateral. This can be done as follows.

Denote by e_1 and e_2 some vectors along the diagonals, and introduce the coefficients $\alpha, \dots, \delta$ by

$$\overrightarrow{MA} = \alpha e_1, \quad \overrightarrow{MB} = \beta e_2, \quad \overrightarrow{MC} = \gamma e_1, \quad \overrightarrow{MD} = \delta e_2,$$

so that

$$\begin{aligned} \overrightarrow{AB} &= \beta e_2 - \alpha e_1, & \overrightarrow{BC} &= \gamma e_1 - \beta e_2, \\ \overrightarrow{CD} &= \delta e_2 - \gamma e_1, & \overrightarrow{DA} &= \alpha e_1 - \delta e_2. \end{aligned}$$

Construct a quadrilateral (A^*, B^*, C^*, D^*) by setting

$$\overrightarrow{M^*A^*} = -\frac{e_2}{\alpha}, \quad \overrightarrow{M^*B^*} = -\frac{e_1}{\beta}, \quad \overrightarrow{M^*C^*} = -\frac{e_2}{\gamma}, \quad \overrightarrow{M^*D^*} = -\frac{e_1}{\delta}.$$

Its diagonals are parallel to the noncorresponding diagonals of the original quadrilateral, by construction. The corresponding sides are parallel as well:

$$\begin{aligned} \overrightarrow{A^*B^*} &= -\frac{1}{\beta}e_1 + \frac{1}{\alpha}e_2 = \frac{1}{\alpha\beta}\overrightarrow{AB}, \\ \overrightarrow{B^*C^*} &= -\frac{1}{\gamma}e_2 + \frac{1}{\beta}e_1 = \frac{1}{\beta\gamma}\overrightarrow{BC}, \\ \overrightarrow{C^*D^*} &= -\frac{1}{\delta}e_1 + \frac{1}{\gamma}e_2 = \frac{1}{\gamma\delta}\overrightarrow{CD}, \\ \overrightarrow{D^*A^*} &= -\frac{1}{\alpha}e_2 + \frac{1}{\delta}e_1 = \frac{1}{\delta\alpha}\overrightarrow{DA}. \end{aligned}$$

Thus, the quadrilateral (A^*, B^*, C^*, D^*) is dual to (A, B, C, D). □

11.4 Koenigs nets

For a quad-surface $f : \mathcal{S} \to \mathbb{R}^N$ with quad-graph $\mathcal{S}$ and planar faces there exists a dual quad for every single quad of f, unique up to scaling and translation. Do they constitute a surface?
We characterize locally dualizable quad-surfaces.

Definition 11.6 (Koenigs net)**.** A quad-surface $f : \mathcal{S} \to \mathbb{R}^N$ with planar faces is called a discrete (local) *Koenigs net* if each vertex star of quadrilaterals admits a dual vertex star of quadrilaterals, i.e. corresponding quads are dual.

Remark 11.3.

- If $\mathcal{S}$ is simply-connected we can define a surface $f^* : \mathcal{S} \to \mathbb{R}^N$ such that all corresponding quads of f and f^* are dual. f^* is called the *Christoffel dual* of f.
- If $\mathcal{S}$ is not simply-connected the Christoffel dual f^* can be defined on the universal cover $\tilde{\mathcal{S}}$ of $\mathcal{S}$ such that all corresponding quads of $f : \tilde{\mathcal{S}} \to \mathbb{R}^N$ and $f^* : \tilde{\mathcal{S}} \to \mathbb{R}^N$ are dual.

Assume that the quad-graph $\mathcal{S}$ is bipartite (black and white vertices). On each quad (A, B, C, D) we have an oriented black diagonal (connecting the two black vertices), say $\overrightarrow{AC}$. Denoting the intersection point of the diagonals by M we introduce the quotient of oriented lengths

$$q\left(\overrightarrow{AC}\right) := \frac{l\left(\overrightarrow{MC}\right)}{l\left(\overrightarrow{MA}\right)}$$

where $l(\cdot)$ is the oriented length on the line (AC) with any chosen orientation.[40] Note that

$$q\left(\overrightarrow{CA}\right) = \frac{q\left(\overrightarrow{MA}\right)}{q\left(\overrightarrow{MC}\right)} = q\left(\overrightarrow{AC}\right).$$

We have introduced a multiplicative one-form

$$q : \overrightarrow{E}_b \to \mathbb{R}$$

on the black oriented diagonals and define it in the same way on the white oriented diagonals

$$q : \overrightarrow{E}_w \to \mathbb{R}.$$

Theorem 11.5 (Algebraic characterization of discrete Koenigs nets)**.** *A quad-surface $f : \mathcal{S} \to \mathbb{R}^N$ with planar faces is a discrete Koenigs net if and only if the multiplicative one-forms $q : \overrightarrow{E}_b \to \mathbb{R}$ and $q : \overrightarrow{E}_w \to \mathbb{R}$ are closed, i.e. for any elementary cycle γ of oriented diagonals (black or white) surrounding one vertex the product of all quantities q along this cycle is equal to one:*

$$\prod_{\vec{e} \in \gamma} q\left(\vec{e}\right) = 1$$

Proof. Consider a vertex star of n quadrilaterals and suppose that there is exists a corresponding piece of a dual surface.
For $i = 1, \ldots, n$ denote the oriented lengths of the diagonal segments of the i-th quad by $\alpha_i, \beta_i, \gamma_i, \delta_i$ as depicted in Figure 11.4.

...

Figure 11.4. Closeness of the multiplicative one-form q on a Koenigs net.

The dual quadrilaterals are uniquely determined up to scaling factors $\lambda_1, \ldots, \lambda_n$. We recall from the proof of Proposition 11.4 that

$$\overrightarrow{O^* X_i^*} = \frac{\lambda_i}{\alpha_i \delta_i} \overrightarrow{OX_i}$$

which comes from dualizing the i-th quad and

$$\overrightarrow{O^* X_i^*} = \frac{\lambda_{i+1}}{\alpha_{i+1} \beta_{i+1}} \overrightarrow{OX_i}$$

[40] Note that the quotient of oriented lengths does not depend on the choice of the orientation on the line.

which comes from dualizing the $(i+1)$-th quad, where all indices are to be take modulo n.
So f Koenigs (locally around the given vertex) if and only if

$$\frac{\lambda_{i+1}}{\lambda_i} = \frac{\alpha_{i+1}\beta_{i+1}}{\alpha_i\delta_i} \tag{11.3}$$

holds for all $i = 1, \dots, n$
Suppose f is Koenings. Then for the product over all quadrilaterals we obtain.

$$1 = \prod_{i=1}^{n} \frac{\lambda_{i+1}}{\lambda_i} = \prod_{i=1}^{n} \frac{\beta_i}{\delta_i} = \prod_{i=1}^{n} q\left(\overrightarrow{X_i X_{i+1}}\right)$$

Conversely suppose

$$\prod_{i=1}^{n} q\left(\overrightarrow{X_i X_{i+1}}\right) = \prod_{i=1}^{n} \frac{\beta_i}{\delta_i} = 1 \tag{11.4}$$

We fix λ_1 arbitrarily and define $\lambda_2, \dots, \lambda_n$ by using (11.3) for $i = 1, \dots, n-1$. Then (11.4) ensures that (11.3) holds cyclicaly, i.e. also for $i = n$. □

Remark 11.4. $n = 3$ neighboring quadrilaterals are Koenigs if

$$q(\overrightarrow{AB})q(\overrightarrow{BC})q(\overrightarrow{CA}) = 1$$

...

Figure 11.5. Three neighboring quads with $\prod q = -1$. Can they be dualized together?

In a configuration like Figure 11.5 (convex non-overlapping quads) we can only achieve

$$q(\overrightarrow{AB})q(\overrightarrow{BC})q(\overrightarrow{CA}) = -1$$

In this case the vertex star can still be dualized considering a double covering.

Theorem 11.6 (Geometric characterization of Koenigs nets in terms of intersection points of diagonals)**.** *Let $f : \mathcal{S} \to \mathbb{R}^N$ be a quad-surface with planar faces. For a vertex f denote its neighbors by $f_1, \dots, f_n$ and the intersection points of the diagonals by $M_1, \dots, M_n$. If $f_1, \dots, f_n$ are in general position, then f is Koenigs if and only if $M_1, \dots, M_n$ lie in an $(n-2)$-dimensional affine subspace.*

Proof. Generalized Menelaus theorem. □

Remark 11.5.

- We see that Koenigs nets belong to projective geometry, i.e. the property of being Koenigs is preserved by projective transformations.
- $n = 3$ neighboring quads are Koenigs if M_1, M_2, M_3 are colinear.
- $n = 4$ neighboring quads are Koenigs if M_1, M_2, M_3, M_4 are coplanar.
- Note that for n points to be in general position the dimension of the ambient space has to satisfy $N \geqslant n - 1$.
  So for the standard case of $\mathcal{S} = \mathbb{Z}^2$ we are fine with $N = 3$.

Theorem 11.7 (Geometric characterization of Koenigs nets in terms of vertices)**.** *Let $f : \to \mathbb{R}^N$ be a quad-surface with planar faces and vertex-stars of full dimension (i.e. $f_i - f$, $i = 1, \dots, n$ are linear independent).*
Then f is a discrete Koenigs net if and only if any vertex f and its n next-neighbors $f_{i,i+1}$ lie in a $(n-1)$-dimensional affine subspace $V \subset \mathbb{R}^N$, not containing some (and then any) of the vertices $f_1, \dots, f_n$.

Proof.

($\Rightarrow$) Let f be Koenigs. Then

$$V \coloneqq f + \operatorname{span}\left\{\overrightarrow{ff_{i,i+1}} \mid i = 1, \dots, n\right\} = f + \operatorname{span}\left\{\overrightarrow{fM_i} \mid i = 1, \dots, n\right\}$$

is $(n-1)$-dimensional as follows from Theorem 11.6.
Suppose $f_1 \in V$. Then $f_{12} \in V$ implies $f_2 \in V$. So eventually $f_1, \dots, f_n \in V$. Since also $f \in V$ this contradicts that the vertex star has full dimension.

($\Leftarrow$) Let V be $(n-1)$-dimensional. The affine space W spanned by $f_1, \dots, f_n$ is also $(n-1)$-dimensional. They both lie in the n-dimensional space spanned by the vertex star. The intersection of two $(n-1)$-dimensional spaces in a n-dimensional space is generically $(n-2)$-dimensional. So

$$M_i \in V \cap W$$

lie in an $(n-2)$-dimensional. So Theorem 11.6 implies that f is Koenigs.

□

Remark 11.6.

- Note that the restriction on the ambient dimension is even higher for this characterization. We need n linear independent vectors, so $N \geqslant n$.
  In the standard case of $\mathcal{S} = \mathbb{Z}^2$ this means $N \geqslant 4$.
- For the case of high valence and low ambient dimension one has to develop special "projected" conditions.

Remark 11.7. One can generalize Koenigs nets $f : \mathbb{Z}^2 \to \mathbb{R}^N$ to $f : \mathbb{Z}^m \to \mathbb{R}^N$ such that all $\mathbb{Z}^2$ sublattices are Koenigs to obtain a discrete intgrable system.

11.5 Minimal and CMC quad-surfaces with parallel Gauss-map

For a pair (f, n) of a quad-surface $f : \mathcal{S} \to \mathbb{R}^N$ with planar quads and parallel Gauss map $n : \mathcal{S} \to \mathbb{R}^N$ we had defined its mean and Gaussian curvature by

$$K = \frac{A(n)}{A(f)} \qquad H = -\frac{A(f,n)}{A(f,f)}$$

as functions on the faces.
We use this to define minimal and constant mean curvature surfaces by

$$\begin{aligned}(f,n) \text{ minimal} &:\Leftrightarrow H = 0\\ (f,n) \text{ CMC} &:\Leftrightarrow H = const.\end{aligned}$$

and are now in a position two characterize these in the case of quad-surfaces.

Theorem 11.8. *Let $f : \mathcal{S} \to \mathbb{R}^N$ be a quad-surface with planar quads and parallel Gauss map $n : \mathcal{S} \to \mathbb{R}^N$. Then*

$$(f, n) \text{ minimal } \Leftrightarrow \text{ } f \text{ Koenigs and } n = f^*$$
$$(f, n) \text{ CMC with } H = H_0 \neq 0 \Leftrightarrow \text{ } f \text{ Koenigs and } n = (f^* - f)H_0$$

Proof. The statement about minimal surfaces follows immediately from our definitions.
Let $H_0 \neq 0$. Then

$$\begin{aligned} H = H_0 &\Leftrightarrow A(f, n) + H_0 A(f, f) \\ &\Leftrightarrow A(f, n + H_0 f) = 0 \\ &\Leftrightarrow A(f, f + \frac{1}{H_0} n) = 0 \\ &\Leftrightarrow f^* = f + \frac{1}{H_0} n \\ &\Leftrightarrow n = H_0(f^* - f). \end{aligned}$$

□

Corollary 11.9. *Let (f, n) be a quad-surface with planar quads and parallel Gauss map and constant mean curvature $H_0 \neq 0$.*
Then the parallel surface $f + \frac{1}{H_0} n$ is dual to f and the parallel surface $f + \frac{1}{2H_0} n$ has constant Gaussian curvature $K = 4H_0^2$.

Proof. It only remains to show that the mid-surface $f + \frac{1}{2H_0} n$ with Gauss map n satisfies $K = 4H_0^2 = const.$

$$\begin{aligned} A\left(f + \frac{1}{2H_0} n\right) &= A\left(f + \frac{1}{2H_0}, f\right) + A\left(f + \frac{1}{2H_0}, \frac{1}{2H_0} n\right) \\ &= A\left(f + \frac{1}{2H_0}, f\right) + A\left(f, \frac{1}{2H_0}\right) + \frac{1}{4H_0^2} A(n) \\ &= A\left(f + \frac{1}{H_0}, f\right) + \frac{1}{4H_0^2} A(n) = \frac{1}{4H_0^2} A(n) \end{aligned}$$

So

$$K = \frac{A(n)}{A\left(f + \frac{1}{2H_0} n\right)} = 4H_0^2.$$

□

We see that any discrete Koenigs net f can be extended to a minimal or to a constant mean curvature Q-net by an appropriate choice of the Gauss map n. Indeed,

(f, n) is minimal for $n = f^*$;
(f, n) has constant mean curvature for $n = f^* - f$.

However, n defined in such generality can lead us too far away from the smooth theory. It is natural to look for additional requirements which bring it closer to the Gauss map of a surface. In the smooth case, n is a map to the unit sphere. The following three discrete versions of this fact are natural to consider:

(1) n is a polyhedral surface with all vertices on the unit sphere $\mathbb{S}^2$. This implies that all faces of the Q-net n are circular. This condition holds also for any parallel surface. In particular, f is also a circular net.

(2) n is a polyhedral surface with all faces touching the unit sphere $\mathbb{S}^2$. This implies that for any vertex p there is a cone of revolution with the tip p touching all faces of n incident to p. This property holds true for any parallel surface. In particular, f is also a conical net.

(3) n is a polyhedral surface with all edges touching the unit sphere $\mathbb{S}^2$. Polyhedra with this property are called *Koebe polyhedra*. For any vertex p, all edges incident to p lie on a cone of revolution with the tip p. Also this property holds true for any parallel surface, in particular for f. Such nets are called nets of *Koebe type*.

The implementation of these additional requirements into the theory makes it more intriguing.

11.6 Koebe polyhedra

combinatorics → geometry

Theorem 11.10 (Strong Steinitz, existence of Koebe polyhedra)**.** *For every strongly regular cell-decomposition (polytopal cell-decomposition) of the sphere, there is a combinatorial equivalent polyhedron with edges tangent to a sphere. This polyhedron is unique up to projective transformations that fix the sphere. There is a simultaneous realization of the dual polyhedron such that corresponding edges of the dual and the original polyhedron touch the sphere at the same points and intersect orthogonally.*

...

Figure 11.6. From combinatorics to a geometric realization of a Koebe polyhedron

- Is the Koebe polyhedron dualizable?

Combining the Koebe polyhedron and its dual we obtain a quad-graph with faces touching the sphere.

...

Figure 11.7. Combining a Koebe polyhedron and its dual to obtain a quad-graph.

The touching points are the intersection points of the diagonals. These intersection points lie on circle, so in particular they are coplanar.
We obtain a quad-surface n which is conical and Koenigs. So the dual surface $f \coloneqq n^*$ is a discrete minimal surface of conical type.

11.6.1 Koebe polyhedra and circle patterns

A Koebe polyhedron constitutes a *circle packing* on the corresponding sphere.

...

Figure 11.8. Circle packing of a Koebe polyhedron.

Remark 11.8. We can map this circle pattern conformally to the plane by stereographic projection (circles are mapped to circles while tangency is preserved).

Connecting the centers of touching circles by edges we obtain the *tangency graph* Σ of the circle packing.

...

Figure 11.9. Tangency graph of a circle packing.

The circle packing of the dual Koebe polyhedron is orthogonal to the first at intersection points.
Together we obtain an orthogonal *circle pattern*.

Theorem 11.11 (Strong Steinitz, circle pattern formulation)**.** *For any strongly regular cell-decomposition Σ of $\mathbb{S}^2$ there exists a pair of circle packings (or equivalently an orthogonal circle pattern), such that Σ is the tangency graph of the first circle packing, the dual cell-decomposition is the tangency graph of the second circle packing and the circles of both circle packings intersect orthogonally in their common tangency points.*
This pair of circle packings is unique up to Möbius transformations.

For a circle packing with the tangency graph Σ being a triangulation there always is an orthogonal circle pattern.
So it is unique up to Möbius transformation on its own.

...

Figure 11.10. Three touching circles. The circle through the touching point is orthogonal to all three circles: Map one touching point to infinity by a Möbius transformation.

Theorem 11.12 (Strong Steinitz, triangulation)**.** *For any triangulation Σ of $\mathbb{S}^2$ there is a circle packing such that Σ is its tangency graph.*
This circle packing is unique up to Möbius transformations.

Mapping an inner point of one of the circles on $\mathbb{S}^2$ to infinity[41] all the other circles get mapped inside the image of this circle.
We obtain a circle packing inside a disc.

...

Figure 11.11. Circle pattern on $\mathbb{S}^2 \to$ circle pattern in a disc.

Theorem 11.13 (Strong Steinitz, triangulation, disc version)**.** *For any triangulation Σ of the disc there is a circle packing in the unit disc D^1 such that*

[41] Or applying a stereographic projection with north-pole in an inner point of a circle.

circles correspond to vertices, two circles touch if and only if the corresponding vertices are adjacent and the circles corresponding to the boundary vertices touch $\mathbb{S}^1 = \partial D^1$.
This circle packing is unique up to Möbius transformations of D^1.

12 Willmore energy

12.1 Smooth Willmore energy

Let M be a surface in $\mathbb{R}^3$ without boundary. Its *Willmore energy* is defined to be

$$W(M) \coloneqq \frac{1}{4}\int_M (\kappa_1 - \kappa_2)^2 \mathrm{d}A$$

where $\mathrm{d}A$ is the area element of M and κ_1, κ_2 are the principal curvatures.
We list some important properties of the Willmore energy of a closed surface.

(i) $W \geqslant 0$ and $W = 0 \Leftrightarrow M$ is a sphere

(ii) $(\kappa_1 - \kappa_2)^2 \mathrm{d}A$ is Möbius invariant.

(iii) $(\kappa_1-\kappa_2)^2 = (\kappa_1+\kappa_2)-4K = \kappa_1^2+\kappa_2^2-2K$ where $K = \kappa_1\kappa_2$ is the Gaussian curvature. Since the total Gaussian curvature $\int_M K\mathrm{d}A = 2\pi\chi(M)$ is a topological invariant for closed surfaces the following functionals are equivalent.

$$\int_M (\kappa_1 - \kappa_2)^2 \mathrm{d}A \;\sim\; \int_M (\kappa_1 + \kappa_2)^2 \mathrm{d}A \;\sim\; \int_M (\kappa_1^2 - \kappa_2^2)\mathrm{d}A$$

But the geometric meaning of minimizing each of them is different.

- $\int_M (\kappa_1 - \kappa_2)^2 \mathrm{d}A \rightsquigarrow$ as round as possible
- $\int_M (\kappa_1 + \kappa_2)^2 \mathrm{d}A = 4\int_M H^2 \mathrm{d}A \rightsquigarrow$ as minimal as possible
- $\int_M (\kappa_1^2 - \kappa_2^2)\mathrm{d}A \rightsquigarrow$ as planar as possible

(iv) Consider the Willmore energy $W(r, R)$ of all tori of revolution with radii $0 < r < R$. Then Willmore energy depends only on the quotient $\frac{R}{r}$ and is minimal if and only if $\frac{R}{r} = \sqrt{2}$. The resulting torus is called the *Clifford torus*.

We are going to discretize the first two properties.

12.2 Discrete Willmore energy

Definition 12.1 (discrete Willmore energy)**.** Let S be a simplicial surface in $\mathbb{R}^3$. Then we define the *discrete Willmore energy* of S at the vertex $v \in V$ to be

$$W(v) \coloneqq \sum_{e \sim v} \beta(e) - 2\pi$$

where $\beta(e)$ is the intersection angle of the circumcircles of the two triangles adjacent to e as depicted in Figure 12.1.
If S is closed we define

$$W(S) \coloneqq \frac{1}{2}\sum_{v \in V} W(v) = \sum_{e \in E} \beta(e) - \pi\,|V|$$

Remark 12.1.

- Note that the triangles do not get unfolded and the angle β between the circumcircle is measured in space.

- The definition of the discrete Willmore energy is obviously Möbius invariant.

...

Figure 12.1. Intersection angle of circumcircles from the definition of discrete Willmore energy.

Consider a vertex $v \in V$ of valence n with angles $\beta_1, \dots, \beta_n$ between the adjacent circumcircles. We want to investigate whether the sum of these angles $\sum_{i=1}^{n} \beta_i$ can be less than 2π.
Consider a Möbius transformation that maps $v \mapsto \infty$. Then the circumcircles become lines outlining which constitute a (not necessarily planar) n-gon in $\mathbb{R}^3$ with exterior angles β_i.[42]

...

Figure 12.2. Mapping the circumcircles around a vertex v to a (not necessarily planar) polygon.

Lemma 12.1. *Let $\mathcal{P}$ be a (not necessarily planar) n-gon in $\mathbb{R}^3$ with exterior angles $\beta_1, \dots, \beta_n$. Choose any point $P \in \mathbb{R}^3$ and connect it to all vertices of $\mathcal{P}$. Let $\alpha_1, \dots, \alpha_n$ be the angles of the triangles at the tip of the resulting pyramid. Then*

$$\sum_{i=1}^{n} \beta_i \geqslant \sum_{i=1}^{n} \alpha_i$$

and the equality holds if and only if $\mathcal{P}$ is planar and convex and P lies inside of $\mathcal{P}$.

...

Figure 12.3. Pyramid with tip P build on top of a (not necessarily planar) n-gon in $\mathbb{R}^3$.

Proof. For the enumeration of the angles $\alpha_1, \dots, \alpha_n$ we refer to Figure 12.3 while introducing the additional angles $\gamma_1, \dots, \gamma_n$ and $\delta_1, \dots, \delta_n$ at the sides of the pyramid. So for all i we have $\alpha_i + \gamma_i + \delta_i = \pi$ from which we get

$$\sum_{i=1}^{n} (\gamma_i + \delta_i) = n\pi - \sum_{i=1}^{n} \alpha_i$$

and $\delta_i + \gamma_{i+1} + \beta_{i+1} \geqslant \pi$ from which we get

$$\sum_{i=1}^{n} (\gamma_i + \delta_i) = n\pi - \sum_{i=1}^{n} \beta_i$$

Together we obtain the desired inequality.
Additionally $\delta_i + \gamma_{i+1} + \beta_{i+1} = \pi$ if and only if the corresponding vertex star is planar and the angles do not overlap. In the sum this means planarity and P lying inside of $\mathcal{P}$. □

[42] We note that if the circumcircles lie on a sphere we can choose the Möbius transformation in such a way that the resulting n-gon is planar and hence $W(v) = 0$.

Corollary 12.2. *At each vertex $v \in V$ the discrete Willmore energy satisfies*

$$W(v) \geqslant 0$$

Proof. Consider the corresponding n-gon $\mathcal{P}$ as obtained from a Möbius transformation.
If $\mathcal{P}$ is a planar, convex polygon, choose P inside $\mathcal{P}$. We obtain

$$\sum_{i=1}^{n} \beta_i = \sum_{i=1}^{n} \alpha_i = 2\pi$$

If $\mathcal{P}$ is non-planar, choose P in the convex hull of the vertices of $\mathcal{P}$. Then we have

$$\sum_{i=1}^{n} \beta_i \geqslant \sum_{i=1}^{n} \alpha_i < 2\pi$$

since the "pyramid" with tip P constitutes a vertex star of a polyhedral surface with negative Gaussian curvature. □

Remark 12.2. So $W(S) = 0 \Leftrightarrow W(v) = 0$ for all $v \in V$.

We are now prepared to proof the discrete analog of property (i) of the smooth Willmore energy.

Theorem 12.3. *Let S be a closed simplicial surface. Then*

$$W(S) \geqslant 0$$

and equality holds if and only if S is a convex polyhedron inscribed in a sphere, i.e. a Delaunay triangulation of $\mathbb{S}^2$.

Proof. From our previous considerations we immediately get

$$W(S) = \frac{1}{2} \sum_{v \in V} W(v) \geqslant 0$$

So only the claim about the equality remains to show.

($\Leftarrow$) Let S be a Delaunay triangulation of $\mathbb{S}^2$.
In particular each vertex star lies on a sphere. Then $W(v) = 0$ at every vertex $v \in V$.

($\Rightarrow$) Let $W(S) = 0$.
Then $W(v) = 0$ at every vertex $v \in V$. So the star of each vertex v lies on a sphere S_v and is Delaunay.
Consider two adjacent vertices v_1 and v_2. Then the corresponding spheres S_{v_1} and S_{v_2} share two circles (the circumcircles of adjacent to the edge $(v_1 v_2)$) and therefore coincide.
So all spheres S_v coincide and all edges are Delaunay.

...

Figure 12.4. If two neighboring vertex stars have $W(v_1) = W(v_2) = 0$ they lie on the same sphere.

□

12.3 Inscribable and non-inscribable simplicial spheres

Part III
Appendix

A The Heisenberg magnet model

We have seen the Heisenberg flow playing an important role in the characterization of elastica (in the smooth and in the discrete case, see Section 4).
The Heisenberg flow (3.4) as it acts on the tangent vectors

$$\partial_t T = (\partial_t \gamma)' = (\gamma'' \times \gamma')' = \gamma''' \times \gamma' = T'' \times T \tag{A.1}$$

is also obtained as the equation of motion in the continuous *Heisenberg magnet model* also known as the continuous *Heisenberg chain*.

Although later seen to be a rather naive discretization the following discrete model might motivate the continuous Heisenberg chain. Consider a system of N classical spins $S_k = (S_k^1, S_k^2, S_k^3) \in \mathbb{S}^2$ on a (closed) chain, i.e. $S : \mathbb{Z}_N \to \mathbb{S}^2$. We introduce isotropic nearest neighbor interactions by defining the Hamilton function

$$H(S_1, \ldots, S_N) = -J \sum_{i=1}^{N} \langle S_i, S_{i+1} \rangle,$$

with interaction coefficient $J \neq 0$.[43] So a configuration with many aligned neighboring spins has low energy while a configuration with many anti-parallel next neighbors has high energy. To make each spin behave like a magnetic momentum we introduce an angular momentum-like Poisson structure by the following relations:

$$\{S_i^\alpha, S_j^\beta\} = \sum_\gamma \varepsilon^{\alpha\beta\gamma} \delta_{ij} S_j^\gamma$$

for $\alpha, \beta = 1, 2, 3$, $i, j = 1, \ldots, N$, where $\varepsilon_\gamma^{\alpha\beta}$ and δ_{ij} are the Levi-Civita and Kronecker symbols.
Let us compute the time flow of this Hamiltonian system.

$$\partial_t S_i^\alpha = \{S_i^\alpha, H\} = -J \sum_{j,\beta} \{S_i^\alpha, S_j^\beta S_{j+1}^\beta\}.$$

With

$$\begin{aligned} \{S_i^\alpha, S_j^\beta S_{j+1}^\beta\} &= \{S_i^\alpha, S_j^\beta\} S_{j+1}^\beta + S_j^\beta \{S_i^\alpha, S_{j+1}^\beta\} \\ &= \sum_\gamma (\varepsilon^{\alpha\beta\gamma} \delta_{ij} S_i^\gamma S_{j+1}^\beta + \varepsilon^{\alpha\beta\gamma} \delta_{i,j+1} S_i^\gamma S_j^\beta) \end{aligned}$$

we obtain

$$\partial_t S_i^\alpha = -J \sum_{\beta,\gamma} \varepsilon^{\alpha\beta\gamma} S_i^\gamma (S_{i+1}^\beta + S_{i-1}^\beta),$$

so for the spin vectors S_i

$$\partial_t S_i = \{S_i, H\} = J S_i \times (S_{i+1} + S_{i-1}). \tag{A.2}$$

[43] Notice that we introduced periodic boundary conditions when setting $N + 1 = 1$.

Uniformly refining the chain on the interval $[0, N]$ while keeping the length of the spins unit, the smooth limit is a continuous chain of spins $S : [0, N] \to \mathbb{S}^2$ with periodicity $S(x + N) = S(x)$.
Introducing appropriate scaling the smooth limit of the equations of motion (A.2) is

$$\partial_t S = JS \times S'', \tag{A.3}$$

which is the Heisenberg flow as seen in (A.1) with $J = -1$. A corresponding Hamilton function is

$$H[S] = \frac{J}{2} \int_0^L \left\|S'(x)\right\|^2 \mathrm{d}x,$$

with Poisson structure given by

$$\{S^\alpha(x), S^\beta(y)\} = \sum_\gamma \varepsilon^{\alpha\beta\gamma} \delta(x - y) S^\gamma(x),$$

where δ denotes the delta-distribution.

These all are smooth limits of the discrete equations above.
Indeed, let us start with the Hamilton function. Taking $x = \varepsilon i$ we get

$$\begin{aligned}\langle S_i, S_{i+1}\rangle &= \langle S(x), S(x + \varepsilon)\rangle \\ &= \langle S(x), S(x), \varepsilon S'(x) + \frac{1}{2}\varepsilon^2 S''(x) + o(\varepsilon^2)\rangle \\ &= 1 + \frac{1}{2}\varepsilon^2 \langle S(x), S''(x)\rangle + o(\varepsilon^2).\end{aligned}$$

From the orthogonality of $S(x)$ and $S'(x)$ we get

$$0 = \frac{\mathrm{d}}{\mathrm{d}x}\langle S(x), S'(x)\rangle = \left\|S'(x)\right\|^2 + \langle S(x), S''(x)\rangle.$$

Altogether while replacing H by $H + N$ we obtain[44]

$$\begin{aligned}H &= \frac{J}{2}\varepsilon^2 \sum \left\|S'(x)\right\|^2 + o(\varepsilon^2) \\ &= \frac{J}{2}\varepsilon \int \left\|S'(x)\right\|^2 \mathrm{d}x + o(\varepsilon).\end{aligned}$$

So we have to scale the Hamilton function by $\frac{1}{\varepsilon}$ upon taking the limit.
The scaling of the Hamilton function corresponds to replacing the equations of motion (A.2) by

$$\partial_t S_i = \left\{S_i, \frac{1}{\varepsilon} H\right\} = \frac{J}{\varepsilon} S_i \times (S_{i+1} + S_{i-1}).$$

So we get

$$\begin{aligned}\partial_t S(x) &= \frac{J}{\varepsilon} S(x) \times (S(x + \varepsilon) + S(x - \varepsilon)) \\ &= \frac{J}{\varepsilon} S(x) \times (2S(x) + \varepsilon^2 S''(x) + o(\varepsilon^2)) \\ &= J\varepsilon S(x) \times S''(x) + o(\varepsilon),\end{aligned}$$

[44] Already knowing the result we might get this immediately from observing

$$1 - \langle S_i, S_{i+1}\rangle = \frac{1}{2}\langle S_{i+1} - S_i, S_{i+1} - S_i\rangle = \frac{1}{2}\varepsilon^2 \left\|S'(x)\right\|^2 + o(\varepsilon^2).$$

which still needs rescaling to get a non-trivial limit. Since the Hamilton function is already fixed this can be achieved by rescaling the time. Replacing t by εt we obtain (A.3).
The limit of the Poisson structure can be obtained similarly.

Remark A.1. The continuous Heisenberg chain is integrable, see e.g. [**hamiltonian-methods-solitons**]. In Proposition 3.2 we see that the discrete flow (A.2) does not commute with the tangent flow which indicates that the naive discrete model we used to motivate the continuous Heisenberg chain might actually not be an appropriate discretization rather than (3.14) which is discrete integrable.
With the notation from this chapter this is

$$\partial_t S_i = 2JS_i \times \left(\frac{S_{k+1}}{1 + \langle S_{k+1}, S_k \rangle} + \frac{S_{k-1}}{1 + \langle S_k, S_{k-1} \rangle} \right),$$

which is associated with the Hamilton function

$$H = -2 \sum_i \log \left(\frac{1 + \langle S_i, S_{i+1} \rangle}{2} \right).$$

B Exercises

B.1 Curves and Curvature

Exercise B.1 (Planar curves)**.** Let $\gamma : I \to \mathbb{R}^2$ be a smooth regular curve. Prove the following statements:

1. If $\varphi : J \to I$ is a monotone increasing diffeomorphism, then the curve $\tilde{\gamma} = \gamma \circ \varphi$ has curvature $\tilde{\kappa} = \kappa \circ \varphi$.

2. Let (T_0, N_0) be the orthonormal frame of the arc-length parametrized curve γ at t_0. Then the curve can locally be written as a graph in the following form:

$$\gamma(t_0 + h) = \gamma(t_0) + hT_0 + \frac{1}{2}\kappa(t_0)h^2 N_0 + r(h),$$

   with $\lim_{h\to 0} r(h)/h^2 = 0$.

3. Consider the family of circles C_λ, $(\lambda \neq 0)$ tangent to (the tangent of) the curve γ at a point $\gamma(t_0)$ given by

$$C_\lambda = \{x \in \mathbb{R}^2 \mid \|x - (\gamma(t_0) + \lambda N_0)\|^2 = \lambda^2\},$$

   where N_0 is the normal to the curve at $\gamma(t_0)$. Let $\kappa : I \to \mathbb{R}$ be the curvature function of γ and t_0 such that $\kappa'(t_0) \neq 0$. Show that for there exists a neighborhood of $\gamma(t_0)$ in $\mathbb{R}^2$ such that the circle C_λ lies on one side of the curve *if and only if* $\lambda \neq 1/\kappa(t_0)$.

Exercise B.2 (Curvature of an ellipse)**.** Consider an ellipse in $\mathbb{R}^2$ given by the equation $\frac{x^2}{a^2} + \frac{y^2}{b^2} = 1$ with $a, b > 0$. Let l be the line connecting the points $(a, 0)$ and $(0, b)$. Then the line through (a, b) perpendicular to l intersects the x- and the y-axis in the points P_x and P_y, respectively. Show that the curvature of the ellipse at $(a, 0)$ is $1/(a - P_x)$ and at $(0, b)$ is $1/(b - P_y)$, i.e. the P_x and P_y are the centers of the osculating circles at $(a, 0)$ and $(0, b)$, respectively.

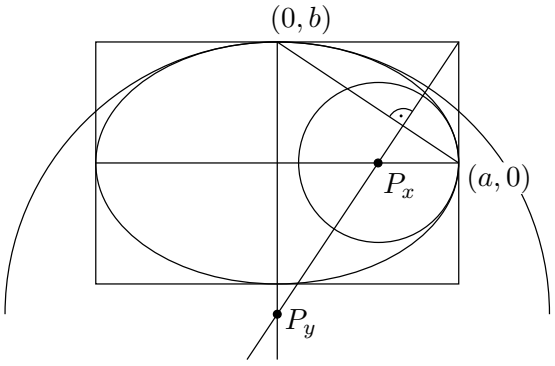

Exercise B.3 (Oriented area of a bounded region)**.** Let A be a simply connected bounded region in $\mathbb{R}^2$ with boundary curve $\gamma : [0, L] \to \mathbb{R}^2$. Show

$$\text{area}(A) = \frac{1}{2}\int_0^L \det(\gamma(t), \gamma'(t))\text{dt}.$$

Exercise B.4 (Lagrange multipliers and calculus of variations)**.** For plane curves γ consider the integral

$$A(\gamma) = \frac{1}{2}\int_{s_0}^{s_1} \det(\gamma, \gamma')ds.$$

1. Calculate the variation equation of A for variations γ_t of an arclength parametrized γ.
2. Show $\frac{\partial}{\partial t}|_{t=0} A(\gamma_t) = 0$ for all variations with fixed endpoints and fixed length if and only if γ has constant curvature $\kappa \neq 0$.

Exercise B.5 (Hyperbolic geodesics in the halfplane model)**.** For curves $\gamma : [s_0, s_1] \to H^2_+ = \{\binom{x_1}{x_2} : x_2 > 0\}$ consider the hyperbolic length:

$$L_H(\gamma) = \int_{s_0}^{s_1} \frac{1}{\langle \gamma, e_2\rangle}\sqrt{\langle \gamma', \gamma'\rangle}ds.$$

Show for an arclength parametrized curve γ that

$$\frac{d}{dt}|_{t=0} L_H(\gamma_t) = 0$$

for all variations γ_t of γ with fixed endpoints, if and only if

$$\langle \gamma, e_2\rangle \kappa N - \langle T, e_2\rangle T + e_2 = 0.$$

Deduce that $\kappa' = 0$. (Hint: Scalar multiply the previous equation with N.) Show further:

1. If $\kappa = 0$, then γ lies on a vertical line.
2. If $\kappa \neq 0$, then γ is an arc of a circle with center on the e_1-axis.

Exercise B.6 (Schwarzian derivative and reparametrization)**.** Let $\gamma : I \to \mathbb{C}$ be a plane curve.

1. Let $\phi : \tilde{I} \to I$ be a diffeomorphism. Show

$$S_{\gamma\circ\phi} = (S_\gamma \circ \phi) \cdot {\phi'}^2 + S_\phi.$$

2. Show that S_γ is real if and only if γ is a parametrization of a circle or a line.
(Hint: What is the Schwarzian derivative for curves parametrized by arclength?)

Exercise B.7 (Schwarzian derivative and Moebius transformations.)**.** 1. Show that if $[c] : I \to \mathbb{C}\mathrm{P}^1$ is a curve of the form $c(s) = \binom{as+b}{cs+d}$ with $ad - bc = 1$, then $S_c = 0$.

2. Show that if $S_c = 0$ for a normalized lift c of a curve $[c] : I \to \mathbb{C}\mathrm{P}^1$, then $c(s) = \binom{as+b}{cs+d}$ with $ad - bc = 1$.

Exercise B.8 (Discrete cycloid)**.** Suppose a regular n-gon in $\mathbb{R}^2$ rolls in one direction on the x-axis. Let $\ldots < t_{-1} < t_0 < t_1 < \ldots$ be the sequence of times when an edge of the polygon lies flat with one edge on the x-axis. A *discrete cycloid* is a discrete curve $\gamma : \mathbb{Z} \to \mathbb{R}^2$ such that γ_j is the position of a particular vertex at time t_j.

1. Find a formula for the discrete cycloids (preferably using complex numbers).
2. Draw a picture for $n = 3, 5, 6$.
3. Are they regular discrete curves by the definition from the lecture?

Exercise B.9 (Evolute of the discrete cycloid)**.** Now let n be odd and consider the osculating edge circles defined in the lecture, i.e. circles touching three consecutive edges. The *discrete (edge) evolute* is the curve consisting of these centers.

1. Show that the discrete (edge) evolute of the discrete cycloid is a translate of the original curve – another discrete cycloid. How do you deal with the singular points?

This is a beautiful analog of the smooth fact that the evolute of a smooth cycloid is a cycloid as well.

B.2 Flows on curves

Exercise B.10 (Conserved quantities of mKdV-Flow)**.** Let $\gamma : [0, L] \to \mathbb{C}$ be a closed curve parametrized by arclength with unit tangent vector T and normal N.

Show that the mKdV-flow $\dot{\gamma} = \frac{1}{2}\kappa^2 T + \kappa' N$ preserves the total squared curvature $\frac{1}{2}\int_0^L \kappa^2(s)ds$.

Exercise B.11.

1. Show that for $I = [1, \ldots, n]$ and $I = \mathbb{Z}_n$ the set $\mathcal{C}_I^{\mathrm{reg}}$ is open and dense in $(\mathbb{R}^N)^n$. In particular $\mathcal{C}_I^{\mathrm{reg}}$ is a nN-dimensional sub-manifold.
   Hint: Express the regularity condition in terms of a continuous map on $(\mathbb{R}^N)^n$.
2. Show that $\mathcal{C}^{\mathrm{arc}}_{[0,\ldots,n]}$ is an $N+n(N-1)$-dimensional and $\mathcal{C}^{\mathrm{arc}}_{\mathbb{Z}_n}$ an $(n+1)(N-1)$-dimensional sub-manifold of $(\mathbb{R}^N)^n$.
3. How about $\mathcal{C}_I^{\mathrm{reg,arc}}$?

Exercise B.12 (Tangent flow)**.** Which arc-length parametrized discrete curves in the plane are just translated by the tangent flow? Which are rotated?

Which arc-length parametrized discrete curves in $\mathbb{R}^3$ are translated by the Heisenberg flow given by

$$\frac{\partial}{\partial x}\gamma = \frac{T_k \times T_{k-1}}{1 + \langle T_k, T_{k-1}\rangle} \, ?$$

Exercise B.13 (Commuting flows)**.** Consider the discrete Heisenberg and the discrete tangent flow given by:

$$\partial_x \gamma_k = \frac{T_k \times T_{k-1}}{1 + \langle T_k, T_{k-1} \rangle} \quad \text{and} \quad \partial_t \gamma_k = \frac{T_k + T_{k-1}}{1 + \langle T_k, T_{k-1} \rangle}.$$

Show that these flows commute, i.e.,

$$\partial_x \partial_t \gamma_k = \partial_t \partial_x \gamma_k,$$

where x and t are the flow parameters of the Heisenberg and the tangent flow respectively.

B.3 Elastica

Exercise B.14 (Equivalent functionals on discrete curves)**.** For an arc-length parametrized discrete curve $\gamma : \{0, \dots, n\} \to \mathbb{R}^3$ let

$$\begin{aligned} S_1(\gamma) &= \sum_{i=0}^{n-1} \log(1 + \frac{\kappa_i^2}{4}), \\ S_2(\gamma) &= \sum_{i=0}^{n-1} \log(1 + \langle T_i, T_{i-1} \rangle), \\ S_3(\gamma) &= \sum_{i=0}^{n-1} \log \|T_i + T_{i-1}\|, \end{aligned}$$

where $T_i = \gamma_{i+1} - \gamma_i$ is the tangent vector and $\kappa_i = 2 \tan \frac{\varphi_i}{2}$ (with φ_i the bending angle at vertex γ_i) is the discrete curvature. Show that these functionals have the same critical curves (regardless which variations are allowed).

Exercise B.15 (Discrete rods)**.** A *discrete rod* can be characterize through the property that evolves by an Euclidean motion under a linear combination of Heisenberg and tangent flow.

Write down the corresponding equation.

Exercise B.16 (Quaternionic calculations)**.** Show that for $p, q \in \mathbb{H}$ the conjugation and absolute value fulfill

$$\overline{pq} = \overline{q} \cdot \overline{p} \quad \text{and} \quad |pq| = |p|\,|q|\,.$$

Let $x, y \in \mathrm{Im}\mathbb{H} \cong \mathbb{R}^3$. Show

1. $xx = -|x|^2 = -\|x\|^2$
2. $\langle x, y \rangle = -\frac{1}{2}(xy + yx)$
3. $x \times y = \frac{1}{2}(xy - yx)$
4. $x || y \Leftrightarrow xy = yx$ $x \perp y \Leftrightarrow xy = -yx$.

Suppose $v \in \mathrm{Im}\mathbb{H} \cong \mathbb{R}^3$ and $|v| = 1$. Show that for $s, t \in \mathbb{R}$,

1. $e^{tv} = \cos t + (\sin t)\, v$

2. $e^{tv}e^{sv} = e^{(t+s)v}$
3. $\frac{d}{dt}\, e^{tv} = ve^{tv} = e^{tv}v$

where e^q is defined (as usual) by the power series $e^q = \sum_{n=0}^{\infty} \frac{1}{n!}\, q^n$.

Exercise B.17 (Flow of Euclidean motions)**.** Let Φ_t be the flow induced by the smooth time dependent vector field

$$v(t, x) = a(t) \times x + b(t)$$

on $\mathbb{R}^3$. This means that for each t, Φ_t is a map $\mathbb{R}^3 \to \mathbb{R}^3$, Φ_0 is the identity, and for all x and t

$$\frac{d}{dt}\, \Phi_t(x) = a(t) \times \Phi_t(x) + b(t).$$

Show that for each t, the map Φ_t is an Euclidean motion (i.e. Φ_t is an isometry of $\mathbb{R}^3$ with respect to the standard Euclidean scalar product).

Exercise B.18 (Quaternions and Möbius Transformations)**.** *Sphere inversion:* Consider a sphere with center $c \in \mathbb{R}^3$ and radius $R > 0$ given by

$$S_{c,r} = \{x \in \mathbb{R}^3 \mid \|x - c\| = R\}.$$

The inversion in $S_{c,r}$ maps $x \in \mathbb{R}^3 \cup \{\infty\}$ to $x' \in \mathbb{R}^3 \cup \{\infty\}$ such that:

- $c \mapsto \infty$ and $\infty \mapsto c$,
- x and x' lie on the same ray emanating from c, and
- $\|x - c\|\|x' - c\| = R^2$.

The group of Möbius transformations of $\mathbb{R}^3$ is generated by reflections in hyperplanes and inversions in spheres. $\mathbb{R}^3$ may be identified with the imaginary quaternions $\mathrm{Im}\mathbb{H}$.

1. Describe reflection in a hyperplane and inversion in a sphere using quaternions.
2. Let $q_1, q_2, q_3, q_4 \in \mathrm{Im}\mathbb{H}$. The quaternionic cross ratio is defined as follows:

   $$\mathrm{cr}(q_1, q_2, q_3, q_4) = (q_1 - q_2)(q_2 - q_3)^{-1}(q_3 - q_4)(q_4 - q_1)^{-1}.$$

   Show that the absolute value of the cross ratio is invariant with respect to Möbius transformations.

Exercise B.19 (Characterization of commuting rotations in $\mathbb{R}^3$)**.** Show that two rotations of $\mathbb{R}^3$ (which fix the origin and are not the identity) commute if and only if either their axes are the same or they are 180° rotations around orthogonal axes.

B.4 Darboux transforms

Exercise B.20 (mKdV-Flow of the Darboux Transform of the straight line)**.** Consider the Darboux transform $\gamma(t) = (t - 2\tanh(t), \frac{2}{\cosh(t)})$ of the straight line given by $t \mapsto (t, 0)$.

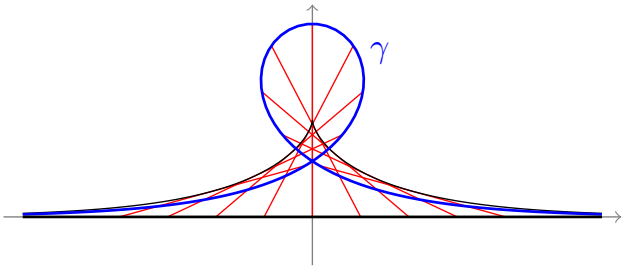

1. Calculate the curvature κ of γ.
2. Show that $\frac{1}{2}\kappa^2 T + \kappa' N = T - \binom{1}{0}$.
3. Show that if $\gamma(t, s)$ is the curve evolving according to the mKdV-flow $\dot{\gamma} = \frac{1}{2}\kappa^2 T + \kappa' N$ with initial values $\gamma(0, s) = \gamma(s)$, then

$$\gamma(t, s) = \gamma(s + t) - t\binom{1}{0}.$$

   Deduce that γ is an elastic curve.

Exercise B.21 (Tractrix)**.** Consider a triangle $\triangle(A_1A_2A_3)$ in $\mathbb{R}^2$, and let P_{12}, P_{23}, P_{31} be some points on the lines (A_1A_2), (A_2A_3), (A_3A_1), different from the vertices A_i of the triangle. Denote by Q_{12} the intersection point of the line (A_1A_2) with $(P_{23}P_{31})$.

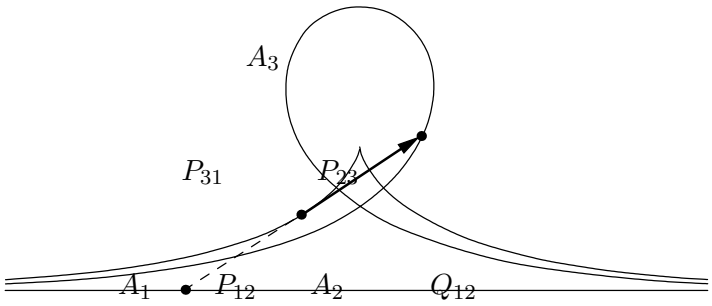

Show that

$$\frac{l(A_1, P_{12})}{l(P_{12}, A_2)} \cdot \frac{l(A_2, P_{23})}{l(P_{23}, A_3)} \cdot \frac{l(A_3, P_{31})}{l(P_{31}, A_1)} = -cr(A_1, P_{12}, A_2, Q_{12}).$$

Exercise B.22 (Möbius Transformations)**.** Let $f : \mathbb{C}\mathrm{P}^1 \to \mathbb{C}\mathrm{P}^1$ be an orientation preserving Möbius transformation, i.e., a map of the form

$$f(z) = \frac{az + b}{cz + d}$$

with $a, b, c, d \in \mathbb{C}$ and $ad - bc \neq 0$. Then the following are equivalent

- f maps the unit disc to the unit disc.
- $a = \bar{d}$ and $b = \bar{c}$.
- $\left(\begin{smallmatrix} a & b \\ c & d \end{smallmatrix}\right) \in SU(1,1)$, the group of special unitary matrices for the Hermitian scalar product $\mathbb{C}^2 \times \mathbb{C}^2 \to \mathbb{C}$ with signature $(1,1)$

$$\langle v, w \rangle = \bar{v}_1 w_1 - \bar{v}_2 w_2 \quad \text{for } v, w \in \mathbb{C}^2.$$

Exercise B.23 (Types of Möbius transformations)**.** Let $f : \mathbb{C}\mathrm{P}^1 \to \mathbb{C}\mathrm{P}^1$ with $f(z) = \frac{az+b}{cz+d}$ with $a, b, c, d \in \mathbb{C}$ and $ad - bc = 1$ that maps the unit disc to the unit disc. In how far do the fixed points of the Möbius transformation depend on the trace $a + d$ of f? Show

1. If $|a + d| = 2$ then f is either the identity or has one fixed point on the boundary of the disc (parabolic motion).
2. If $|a + d| > 2$ then f has two fixed points on the boundary of the unit disc (hyperbolic case).
3. If $|a + d| < 2$ then f has one fixed point outside and one inside the unit disc (elliptic case).

Exercise B.24 (Darboux transformation and tractrix)**.** Let $\gamma : I \to \mathbb{R}^2$ be a smooth curve. Show that the following two statements are equivalent:

1. $\tilde{\gamma}$ is a Darboux transform of γ.
2. $\widehat{\gamma} := \frac{1}{2}(\gamma + \tilde{\gamma})$ is a tractrix of γ.

Exercise B.25 (Darboux transforms)**.** Let $\gamma : I \to \mathbb{C}$ and $\tilde{\gamma} : I \to \mathbb{C}$ be two regular curves with $|\gamma - \tilde{\gamma}| = 2r > 0$.

Show: $\tilde{\gamma}$ is a Darboux transform of γ if $T\tilde{T} = S^2$, where $T = \gamma/|\gamma|$, $\tilde{T} = \tilde{\gamma}/|\tilde{\gamma}|$, and $S = (\tilde{\gamma} - \gamma)/2r$.

Exercise B.26 (Permutability: parallelogram case)**.** Let $\gamma : I \to \mathbb{C}$ be a regular curve and $\gamma_1 = \gamma + 2r_1 S_1$ and $\gamma_2 = \gamma + 2r_2 S_2$ ($S_1 \neq \pm S_2$) be two Darboux transforms of γ at distance $2r_1$ in direction S_1 and at distance $2r_2$ in direction S_2, respectively.

Show: $\tilde{\gamma} = \gamma_1 + 2r_2 S_2 = \gamma_2 + 2r_1 S_1$ is a Darboux transform of γ_1 and γ_2 if and only if γ has constant curvature. The curvature of γ is

$$\kappa_0 = \frac{1}{r_1} \sin(\alpha_1) = \frac{1}{r_2} \sin(\alpha_2),$$

where α_1 and α_2 are the angles between $T(t_0)$, and $S_1(t_0)$ and $S_2(t_0)$, respectively. (γ lies on a circle with radius $1/\kappa_0$).

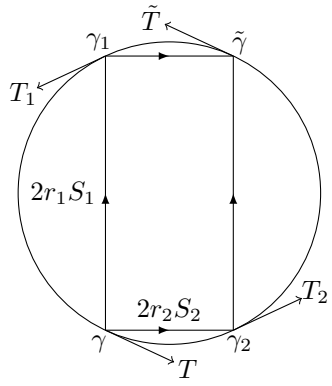

Exercise B.27 (Darboux transforms and signed area)**.** Let $\gamma : \{0, \dots n\} \to \mathbb{R}^2$ be a discrete planar curve and let $p \in \mathbb{R}^2$ be any point. The total signed area of the triangles $(p, \gamma_k, \gamma_{k+1})$ is

$$A(p, \gamma) = \frac{1}{2} \sum_{k=0}^{n-1} \det \begin{pmatrix} \gamma_k - p & \gamma_{k+1} - p \end{pmatrix}.$$

Suppose $\tilde{\gamma}$ is a Euclidean Darboux transform of γ and both are closed discrete curves. Show that $A(p, \gamma) = A(p, \tilde{\gamma})$.

Exercise B.28 (Permutability of Darboux transforms)**.** For $z_1, z_2 \in \mathbb{C}$ with $z_1 \neq z_2$ and $q \in \mathbb{C} \backslash \{0, 1\}$ let

$$L_{z_1, z_2, q} = \begin{pmatrix} 1 & -(z_2 - z_1) \\ -\frac{q}{(z_2 - z_1)} & 1 \end{pmatrix}.$$

Show that

$$L_{z_1, z_{12}, q_1} L_{z, z_1, q_2} = L_{z_2, z_{12}, q_2} L_{z, z_2, q_1}$$

if and only if

$$\mathrm{cr}(z, z_1, z_{12}, z_2) = \frac{q_2}{q_1},$$

where the cross ratio is defined by $\mathrm{cr}(a, b, c, d) = \frac{(a-b)(c-d)}{(b-c)(d-a)}$.

Exercise B.29 (Permutability theorem and circles)**.** Consider seven points $z, z_1, z_2, z_3, z_{12}, z_{13}, z_{23}$ in $\mathbb{C}$ such that z, z_i, z_j, z_{ij} for $i \neq j$ and $\{i, j\} \subset \{1, 2, 3\}$ lie on a circle. Show that the three circles through z_i, z_{ij}, z_{ik} with $\{i, j, k\} = \{1, 2, 3\}$ intersect in one point.

Exercise B.30 (Closed Möbius Darboux transforms)**.** Discuss closed Darboux transforms $\tilde{\gamma}$ of a regular discrete curve γ of period three with constant cross-ratio q, i.e.,

$$\mathrm{cr}(\gamma_k, \gamma_{k+1}, \tilde{\gamma}_{k+1}, \tilde{\gamma}_k) = q.$$

Is it possible to restrict to a equilateral triangle?

B.5 Abstract discrete surfaces

Exercise B.31 (Gluing a torus)**.** It is easy to cut up a torus to get a quadrilateral with opposite edges identified (see figure below, left).

1. A torus can also be cut up so that one gets a hexagon with opposite edges identified. How? (Draw a picture.)
   Hint: The six vertices of the hexagon corrspond to how many vertices on the torus?

2. A genus 2 surface can be cut up so that one obtains an octagon with opposite edges identified. How? (Draw a picture.)
   Hint: Try to visualize how you get a genus 2 surface by glueing opposite sides of an octagon. Start with the top and bottom edges, then glue the left and right edges.

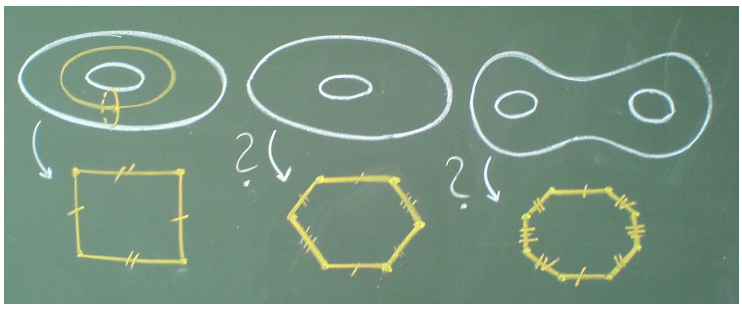

Exercise B.32 (Strongly regular cell decompositions)**.** A 3-dimensional convex polytope is the bounded intersection of finitely many half-spaces or the convex hull of finitely many points. If P is full dimensional, then it is a topological 3-ball and its boundary ∂P is homeomorphic to a 2-sphere.

1. Show that the vertices, edges, and 2-faces of (the boundary of) a convex polytope P always determine a *strongly* regular cell decomposition of the boundary of P.

2. Give an example of a discrete sphere, i.e., a discrete surface homeomorphic to a 2-sphere, such that the corresponding cell decomposition is regular, but not strongly regular.

B.6 Polyhedral surfaces and piecewise flat surfaces

Exercise B.33 (Discrete Gauss curvature)**.** 1. Show that a convex polyhedron has positive Gauss curvature at every vertex.

2. Give an example of a non-convex polyhedron with positive Gauss curvature at every vertex to show that the converse is not true.

Exercise B.34 (Straight curves on a polyhedral surface)**.** Let S be a polyhedral surface with vertices V. For each point $P \in S \backslash V$, there is a neighbourhood which is isometric to an open disc in $\mathbb{R}^2$. (For points in the interior of a 2-face this is trivial, for points in the interior of an edge one just has to "unfold" along the edge). Let γ be a curve in $S \backslash V$. The curve γ is called *straight*, if all images of γ under the above described isometries are straight line segments.

1. Express in terms of angles how γ crosses the edges of S.

2. Find a polyhedral surface S which contains two points P and Q, such that there are infinitely many straight lines between P and Q.

Exercise B.35 (Simplical faces and simple vertices of a convex polyhedron)**.** Show that every convex polyhedron has a triangle face or a vertex of degree 3 (or both). Even stronger: Show that the number of triangle faces plus the number of vertices of degree 3 is at least eight, so there are at least four triangle faces or four vertices of degree 3.

Hint: Use Euler's polyhedron formula and double counting of the edges.

Exercise B.36 (Normal shifts of smooth surfaces)**.** Let $f : \mathbb{R}^2 \supseteq U \to \mathbb{R}^3$, $(x, y) \mapsto f(x, y)$ be a parametrized surface patch with Gauss map $N : U \to S^2$. Suppose that f is parametrized by curvature lines. This means that

$$\partial_x N = -\kappa_1 \, \partial_x f, \qquad \partial_y N = -\kappa_2 \, \partial_y f,$$

where κ_1 and κ_2 are the principal curvature functions. Show that the parallel surfaces

$$f_\rho(x, y) = f(x, y) + \rho N(x, y)$$

(with $\rho \in \mathbb{R}$ small enough)

1. have the same Gauss map,
2. are also parametrized by curvature lines, and
3. their principal curvatures $\kappa_{1\rho}$, $\kappa_{2\rho}$ satisfy

$$\frac{1}{\kappa_{i\rho}} = \frac{1}{\kappa_i} - \rho.$$

Exercise B.37 (Triangle inequality for face areas)**.** Let $P \subset \mathbb{R}^3$ be a compact convex 3–dimensional polyhedron with n faces $F_1, \ldots, F_n$. Show that

$$\operatorname{area}(F_1) < \sum_{i=2}^{n} \operatorname{area}(F_i).$$

Exercise B.38 (Minkowski's theorem in dimension 2)**.** Let $\nu_1, \ldots, \nu_n$ be pairwise different unit vectors in $\mathbb{R}^2$ such that $\operatorname{span}\{\nu_1, \ldots, \nu_n\} = \mathbb{R}^2$ and let $c_1, \ldots, c_n \in (0, +\infty)$ be such that $\sum_{i=1}^n c_i \nu_i = 0$. Show that there exists a unique convex n–gon with edge lengths $c_1, \ldots, c_n$ and corresponding outward unit normals $\nu_1, \ldots, \nu_n$.

Exercise B.39 (Minkowski's formula for smooth surfaces)**.** Let $M \subset \mathbb{R}^3$ be a closed smooth surface, and let ν be the field of outward unit normals to M. Show that

$$\int_M \nu \, \mathrm{darea} = 0.$$

(*Hint:* apply the divergence theorem to a constant vector field.)

Exercise B.40 (Monotonicity of the total mean curvature wrt edge lengths)**.** Let $S(t)$ be a smooth family of compact convex 3–dimensional polyhedra with

the same combinatorics. Assume that the length of each edge is a monotone increasing function in t. Show that

$$t_1 > t_2 \quad \Rightarrow \quad TM(S(t_1)) > TM(S(t_2)),$$

where TM is the total mean curvature. How can the assumption on the monotonicity of edge lengths be modified in the case of non-convex polyhedral surfaces, so that the same conclusion holds?

B.7 Discrete cotan Laplace operator

Exercise B.41 (Geometric interpretation of cotan Laplacian)**.** Let $f : G \to \mathbb{R}^2$ be a planar simplical surface. Consider two triangles sharing the edge $[x_i, x_j]$ as shown in the picture below.

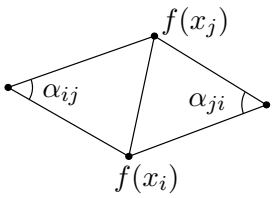

Give a geometric intepretation of the vector

$$\frac{1}{2}(\cot \alpha_{ij} + \cot \alpha_{ji})(f(x_i) - f(x_j)).$$

Hint: Consider circumcircle centers.

Exercise B.42 (Cotan Laplacian of planar immersions)**.** Let $f : G \to \mathbb{R}^2$ be a planar simplical surface. Show that the discrete Laplace operator

$$(\Delta f)(x) = \sum_{\text{edges } [x,x_j]} w([x, x_j])(f(x) - f(x_j))$$

with cotan weights $w([x_i, x_j]) = \frac{1}{2}(\cot \alpha_{ij} + \cot \alpha_{ji})$ vanishes at internal vertices of f (notation see above).

Exercise B.43 (Negative cotan–Laplace)**.** Are there triangulations of a compact polyhedral surfaces without boundary, such that all cotan-weights are negative?

Exercise B.44 (Area Gradient)**.** Let S be a simplicial surface with an embedding $f : S \to \mathbb{R}^n$. Consider a vertex x and the triangles T_i containing vertex x labeled in cyclic order. Denote the edge opposite to x in T_i by a_i.

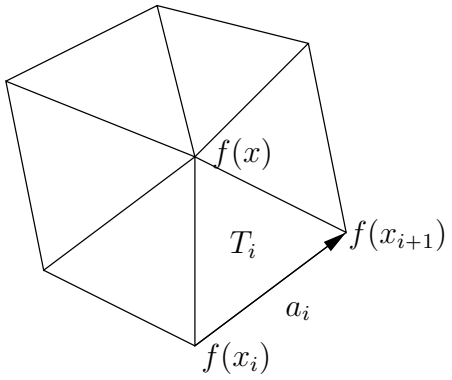

Further let J_i be the rotation in the plane containing T_i by $\frac{\pi}{2}$. Then the gradient of the area functional A defined in the lecture is

$$\nabla A(x) = \frac{1}{2} \sum_{i=1}^{n} J_i a_i,$$

where $a_i = f(x_{i+1}) - f(x_i)$.

Exercise B.45 (Area minimal surfaces.)**.** Consider the simplicial surface shown in the picture below with coordinates:

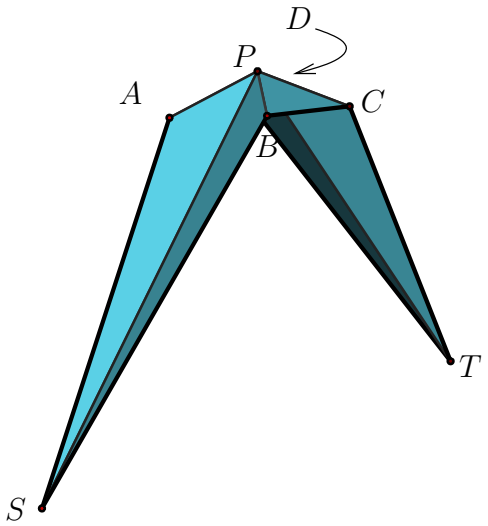

$P = (0, 0, h)$,
$A = (-1, -1, 0)$,
$B = (-1, 1, 0)$,
$C = (1, 1, 0)$,
$D = (1, -1, 0)$,
$S = (-u, 0, -v)$,
$T = (u, 0, -v)$.

Show that there exist positive $u, v, h \in \mathbb{R}$ such that the surface is minimal with respect to the area functional.

Hint: It suffices to analyze the gradient of the area functional for suitable h. You may use your favorite computer algebra tool for tedious computations.

B.8 Delaunay tessellations

Exercise B.46 (Delaunay edges I)**.** Let ABD and DBC be two adjacent triangles in the plane as in the figure below. Let α and γ be the angles opposite the common edge BD. Show that C lies outside the circumcircle of triangle ABD if and only if $\cot \alpha + \cot \gamma > 0$.

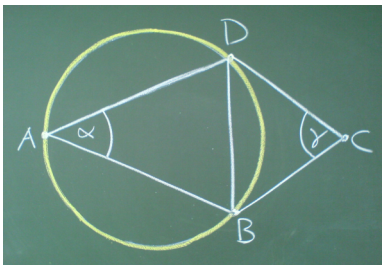

Exercise B.47 (Delaunay edges II)**.** Are there triangulations of a compact polyhedral surface without boundary, such that all edges of the triangulation are not Delaunay edges?

Exercise B.48 (Delaunay edges III)**.** Consider the Delaunay tesselation of the vertices of a convex quadrilateral $(1, 2, 3, 4)$. Show that the diagonal (1,3) is a Delaunay edge if and only if $r_1 r_3 < r_2 r_4$, where r_i is the distance from the vertex i to the intersection point of diagonals.

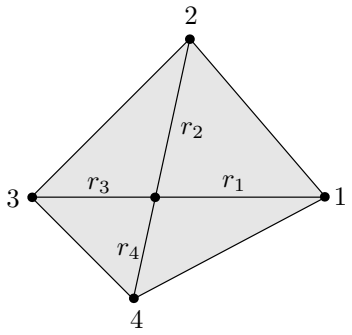

Exercise B.49 (Delaunay-Voronoi quad tessellation)**.** Consider a finite point set in the plane and its Voronoi and the Delaunay tesselation. *Show* that both are strongly regular cell decompositions.

Further consider the Delaunay-Voronoi quad tessellation, where the quad-cells are defined by joining the corresponding edges of Voronoi (dotted) and Delaunay (dashed) tesselation:

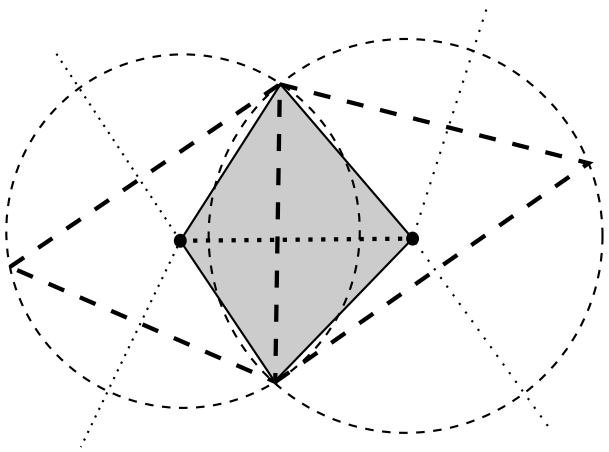

Show that these quadrilaterals together with the edges and vertices define a strongly regular cell decomposition.

Exercise B.50 (Edge flipping algorithm)**.** Given a geodesic triangulation of the vertices of a polyhedral surface, by flipping an edge one obtains another geodesic triangulation with the same number of vertices, edges, and faces. Succesive flipping of non-Delaunay edges produces a Delaunay triangulation of the polyhedral surface. Show that every non-Delaunay edge can be flipped. (Note that on a polyhedral surface edges and/or vertices of adjacent triangles in a geodesic triangulation may coincide.)

Exercise B.51 (Delaunay property)**.** Consider the functional $\alpha(T)$ that assigns to a triangulation T its minimal angle. Show that the Delaunay triangulation maximizes this functional.

Exercise B.52 (Harmonic index)**.** Show that equilateral triangles minimize the harmonic index.

Exercise B.53 (Infinitely many triangulations)**.** Give an example of a polyhedral surface with infinitely many triangulations with the same combinatorics.

B.9 Line congruences over simplicial surfaces

Exercise B.54 (Torsal directions of line congruences)**.** Consider two triangles $\{a_i\}$ and $\{b_i\}$ for $i = 1, 2, 3$ in $\mathbb{R}^3$. Via linear interpolation on the two triangles we obtain a line congruence $\mathcal{L}$. Show that if torsal direction curves exist, they are straight lines on each triangle, i.e., if you consider a line through a point in the triangle in direction of a torsal direction, then the there exists a torsal direction which is constant along this line.

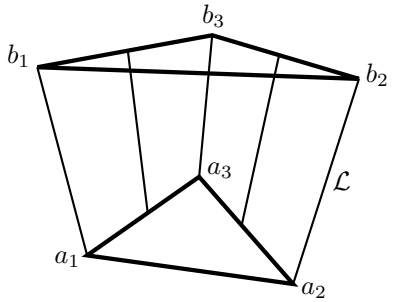

Exercise B.55 (Trivial line congruence)**.** Consider two combinatorially equivalent triangulated surfaces $\{a_i\}$ and $\{b_i\}$ and the line congruence $\mathcal{L}$ obtained by linear interpolation. Show that if all the edges of the mesh $\{a_i\}$ are torsal directions, then all lines at the vertices of the congruence $\mathcal{L}$ pass through one point or are parallel.

Under which additional assumption on the meshes $\{a_i\}$ and $\{b_i\}$, do *all* the lines of the congruence $\mathcal{L}$ satisfy the above condition?

B.10 Polyhedral surfaces with parallel Gauss map

Exercise B.56 (Oriented area of a k-gon)**.** Consider directions $V = \{[v_1], \ldots, [v_k]\}$ in $\mathbb{R}\mathrm{P}^1$ and the corresponding $(k-2)$-dimensional vector space $\tilde{\mathcal{P}}(V)$ of k-gons

with parallel edges factored by translation. Show that the oriented area

$$A(P) = \frac{1}{2}\sum_{i=1}^{k} \det(p_i, p_{i+1}),$$

for is a quadratic form on $\tilde{\mathcal{P}}(V)$.

Exercise B.57 (Area form of quadrilaterals)**.** Consider the two dimensional vector space of quadrilaterals $\tilde{\mathcal{P}}(V)$ with directions $V = \{[v_1], \dots, [v_4]\}$ in $\mathbb{R}\mathrm{P}^1$, such that $[v_i] \neq [v_{(i+1) \mod 4}]$ for $i = 1, \dots, 4$. Let $P \in \tilde{\mathcal{P}}(V)$ be a quadrilateral with nonvanishing edges.

1. Show that $\mathrm{cr}([v_1], [v_2], [v_3], [v_4]) < 0$ if and only if one of the vertices of P lies in the interior of the convex hull of the other three. Show further that this is equivalent to the oriented area form A being definite (positive or negative).

2. Show that $\mathrm{cr}([v_1], [v_2], [v_3], [v_4]) > 0$ if and only if the vertices of the quadrilateral lie on the boundary of the convex hull of the vertices. Show further that this is equivalent to the oriented area form A being indefinite.

Exercise B.58 (Area form of quadrilaterals)**.** Show that the area form $A : \tilde{\mathcal{P}}(v) \to \mathbb{R}$ is indefinite (resp. definite) if and only if the cross-ratio $q(v_1, v_2, v_3, v_4) > 0$ (resp. $q < 0$).

Exercise B.59 (Area form of quadrilaterals)**.** Show that if a crossed quadrilateral $ABCD$ has signed area 0, then the diagonals AC and BD are parallel.

Exercise B.60 (Dual quadrilaterals)**.** Let Q and Q^* be two quadrilaterals in the complex plane $\mathbb{C}$ which is identified with $\mathbb{R}^2$. Denote the directed edges of Q by $a, b, c, d \in \mathbb{C}$ in cyclic order and assume that they are parallel to the corresponding edges of Q^*, so that $a^* = \alpha a$, $b^* = \beta b$, $c^* = \gamma c$, and $d^* = \delta d$ for some $\alpha, \beta, \gamma, \delta \in \mathbb{R}$.

1. Show that $(\alpha - \delta)a + (\beta - \delta)b + (\gamma - \delta)c = 0$ and calculate $(\delta - \alpha)(a + b)$ in terms of b and c.

2. Show that the two quadrilaterals are dual to each other if and only if $\alpha\gamma = \beta\delta$.

3. Deduce that two quadrilaterals with parallel edges are dual in $\mathbb{C}$ if their complex cross-ratio

$$\mathrm{cr}(z_1, z_2, z_3, z_4) = \frac{(z_1 - z_2)(z_3 - z_4)}{(z_2 - z_3)(z_4 - z_1)}$$

with $z_i \in \mathbb{C}$ is the same.